Quantifying the breeding distribution and habitat use of the snow petrel (Pagodroma nivea), the world's most southerly breeding vertebrate

JOSIE FRANCIS

Josie Francis

Quantifying the breeding distribution and habitat use of the snow petrel (*Pagodroma nivea*), the world's most southerly breeding vertebrate

Abstract

Seabirds in the Southern Ocean serve as important ecological indicators of ecosystem status, responding to environmental conditions at both local and regional scales. However, knowledge of the spatial distribution of many polar seabird species is incomplete due to logistical difficulties of accessing remote breeding locations. A prime example is the snow petrel *Pagodroma nivea*, the most southerly breeding vertebrate in the world, whose breeding distribution has not been assessed in almost three decades. This thesis aims to quantify this species' breeding distribution, characterise breeding habitat, and test whether remote sensing can detect known breeding sites. To do so, records of breeding locations, including population estimates when available, were collected from previously published work. Local scale environmental conditions at breeding sites (lithology, temperature, precipitation and wind speed), distance to the coast and regional sea-ice conditions accessible within defined foraging ranges were characterised. Two large breeding sites were subsequently selected for remote sensing, with image enhancement and unsupervised classification performed. The results provide the first updated version of the circumpolar breeding distribution, in which 456 breeding sites are now known, 158 more than the previous inventory. Most known breeding sites are biased towards the location of research stations, indicating more remote breeding sites remain undiscovered. As a cavity-nesting species, the distribution is partly controlled by cavity availability, and results suggest preferential use of cavities in intrusive igneous and high-grade metamorphic lithologies, with the majority of the known breeding population located on the latter. Breeding snow petrels face a central-place foraging constraint, needing to repeatedly return to their nests, and it has been hypothesised therefore that the breeding distribution is limited by distance to pack-ice, where they forage. Characterising regional sea-ice conditions in areas accessible from breeding sites (foraging habitat) supports this, with a median distance from breeding sites to the November ice edge of 430 km. However, the most remote sites are > 1000 km from this foraging habitat. The lack of accessible foraging habitat, due to the year-round persistence of high concentration sea ice in the Weddell Sea, likely explains the absence of breeding sites on the eastern Antarctic Peninsula. However, other gaps in the breeding distribution remain unexplained. The results of remote sensing indicate that if we are to detect breeding sites remotely, better spectral and spatial resolution imagery will be needed, as well as ground truthing data recorded at breeding sites. As ~70% of known breeding sites were recorded before 2000, more consistent and detailed data on breeding sites and breeding populations are also needed to better understand the distribution. Similarly, more widespread long-term studies of snow petrel populations are needed in order to predict the response of this species to climate change.

Quantifying the breeding distribution and habitat use of the snow petrel (*Pagodroma nivea*), the world's most southerly breeding vertebrate.

Josie Francis

Thesis submitted for the degree of Geography MSc by Research

Department of Geography
Durham University

2024

Contents

Abstract i
Title Page ii
Contents iii
List of figures v
List of tables v
List of equations v
Statement of Copyright vi
Declaration vi
Acknowledgements vii

Chapter 1 1
1.1 Introduction 1
1.1.1. Background and rationale 1
1.1.2. Aims and objectives 3

Chapter 2 4
2.1 Literature Review 4
2.1.1 Present understanding of snow petrel breeding distribution 4
2.1.2 Methods of snow petrel observation 6
2.1.3 Foraging habitat use 6
2.1.4 Breeding habitat use 8
2.1.5 Remote sensing of Antarctic seabirds 9
2.1.6 Summary 11

Chapter 3: The breeding distribution and habitat use of the snow petrel 13
3.1 Methods 13
3.1.1 Database compilation 13
3.1.2 Local environmental conditions 14
3.1.3 Regional sea-ice conditions 15
3.2 Results 16
3.2.1 Spatial distribution and size of breeding sites 16
3.2.2 Local environmental conditions 19
3.2.3 Regional sea-ice conditions 22

3.3 Discussion 25
3.3.1 Geographic distribution 25
3.3.2 Regional absences 25
3.3.3 Potential environmental limits on the breeding distribution 27
3.3.4 Past and future breeding distribution 29

Chapter 4: Can snow petrels be detected from space? 32
4.1 Methods 32
4.1.1 Selecting areas of interest 32
4.1.2 Selecting satellite imagery 32
4.1.3 Pre-processing 35
4.1.4 Image enhancement 36
4.1.5 Unsupervised classification 37
4.2 Results 38
4.2.1 Medium resolution imagery 38
4.2.2 Very high resolution imagery 42
4.2.3 Unsupervised classification 45
4.3 Discussion 50
4.3.1 Can known breeding sites be detected from space? 50

Chapter 5 53
5.1 Discussion 53
5.1.1 Knowledge of breeding sites and populations 53
5.1.2 Gaps in the breeding distribution 54
5.1.3 Long-term monitoring 54

Chapter 6: Conclusions 56

References 58

Appendix 72
Appendix A: Snow petrel database 72
Appendix B: Snow petrel paper 163

List of figures:

Figure 1.	Nesting adult snow petrel …….	3
Figure 2.	Circumpolar breeding distribution of snow petrels ……...	5
Figure 3.	Foraging distribution of snow petrels from Pointe Géologie ……..	7
Figure 4.	Nesting cavity pictures …….	9
Figure 5.	Spectral profile of Adélie penguin guano ……...	10
Figure 6.	Updated circumpolar breeding distribution of snow petrels ……	17
Figure 7.	Distance to the coast, and number of breeding pairs ……..	18
Figure 8.	Distance of breeding sites and bedrock to the nearest station ……..	19
Figure 9.	Mean seasonal climate variables ……	20
Figure 10.	Breeding site lithology ……..	22
Figure 11.	November and February sea-ice extent and concentration ……...	23
Figure 12.	Distance to sea-ice concentrations and foraging area ……	24
Figure 13.	Medium resolution imagery for Svarthamaren …….	39-40
Figure 14.	Medium resolution imagery for Mount Henderson ……...	41
Figure 15.	Very high resolution imagery for Svarthamaren ……...	42
Figure 16.	Very high resolution imagery for Mount Henderson ……	43
Figure 17.	Spectral index ratio and ratioing of Mount Henderson ……	44
Figure 18.	*K*-means classification of Svarthamaren ……...	45
Figure 19.	*K*-means classification of NE Svarthamaren ……	47
Figure 20.	*K*-means classification of Mount Henderson ……	49

List of tables:

Table 1.	Local climate variables ……..	21
Table 2.	Spectral band wavelengths for Landsat and Sentinel ……..	33
Table 3.	Image details of Landsat 8, Landsat 9, and Sentinel 2 ……	34
Table 4.	Spectral band wavelengths for Worldview 3 ……..	34
Table 5.	Image details of Worldview 3 ……	35

List of equations:

Equation 1.	Radiometric calibration for Worldview 3 ……..	35
Equation 2.	Spectral index ratio for guano ……..	37
Equation 3.	Band ratio for guano ……	37

Declaration

I confirm that no part of the material presented in this thesis has been previously submitted for a degree in this or any other university. In all cases the work of others, where relevant, has been fully acknowledged.

Acknowledgements

Firstly, I would like to express my thanks to my supervisors Professor Stewart Jamieson, Dr Ewan Wakefield, and Professor Erin McClymont for their encouragement and expertise throughout the whole year. I have learnt a lot this year and I have really enjoyed working with them. I would also like to thank the other members of the ANTSIE research team (Reconstructing Antarctic sea-ice evolution using a novel biological archive) who have all been so welcoming and made the year interesting and enjoyable. Thanks also to Ieuan Hopkins and Alysa Fisher who facilitated access to the British Antarctic Survey archives, and to Dominic Hodgson, Richard Phillips and Peter Fretwell from the British Antarctic Survey who provided advice throughout the year. Furthermore, I would like to thank Colin Southwell and Louise Emmerson at the Australian Antarctic Division for providing unpublished records of breeding locations and their advice on the project, and to Sébastien Descamps at the Norwegian Polar Institute who also provided unpublished observations of breeding locations.

To my friends and family, thank you for your support during this year.

This research has been supported by the European Research Council H2020 (ANTSIE (grant no. 864637)), and the Leverhulme Trust (Research Leadership Award RL-2019-023). Finally, I would like to thank the donor of the Durham Inspired Climate Change and Polar Research scholarship who made the degree possible.

CHAPTER 1

1.1 Introduction

1.1.1 Background and rationale

Globally, seabirds are one of the most threatened marine taxonomic groups (Sydeman et al., 2012; Dias et al., 2019). However, knowledge of the spatial distribution and population sizes of many seabird species are incomplete (Rodríguez et al., 2019). This gap is exacerbated in polar regions where many seabird breeding sites are poorly quantified, particularly in remote and inaccessible locations. Yet in the Southern Ocean, seabird distributions serve as important indicators of ecosystem health (Durant et al., 2009; González-Zevallos et al., 2013; Pande & Sivakumar, 2022; Gonzalez et al., 2023). Satellite remote sensing in Antarctica has enabled the discovery and estimation population sizes for colonies of several surface-nesting species, including Adélie penguins *Pygoscelis adeliae*, emperor penguins *Aptenodytes forsteri*, chinstrap penguins *P. antarcticus* and Antarctic petrels *Thalassoica antarctica* (Schwaller et al., 1989; Fretwell & Trathan, 2009; Fretwell et al., 2012; Schwaller et al., 2013; LaRue et al., 2014; Lynch & LaRue, 2014; Fretwell et al., 2015; Schwaller et al., 2018). However, knowledge of the circumpolar distributions of smaller cavity-nesting or burrowing seabirds remains reliant on direct observations (Southwell et al., 2011; Barbraud et al., 2018). The focus of this thesis is the breeding distribution of the most southerly breeding seabird, the snow petrel *Pagodroma nivea*, which has not been investigated at a continent-wide scale since the identification of 298 colonies almost three decades ago (Croxall et al., 1995). Since then, scientific research has intensified on the continent, and several targeted surveys have been undertaken (Barbraud et al., 1999; Convey et al., 1999; Olivier et al., 2004; Pande et al., 2020). As a result, it is now timely to provide an updated review of the circumpolar breeding distribution of this species.

Snow petrels are a high-trophic-level seabird endemic to Antarctica with a northern breeding limit in South Georgia (Croxall & Prince, 1980; Clarke et al., 2012). They have one of the highest affinities for pack-ice of all Antarctic seabirds, feeding predominantly on fish, krill, and squid in proportions that vary dependent on foraging location (Ainley & Jacobs, 1981; Ainley et al., 1984; Ridoux & Offredo, 1989). When foraging at sea, snow petrels are largely confined to the Marginal Ice Zone [MIZ], in particular to intermediate sea ice concentrations between 12.5 – 50% (estimated from 1 – 4 oktas) (Zink, 1981; Ainley et al., 1984; Ainley et al., 1998). Foraging habitat use during the breeding season is localised due to the central-place constraint. As a central-place forager, snow petrels are required to return to the nest

site after foraging trips; they thus face a distance-dependent cost of accessing their prey, and must nest within reach of suitable foraging habitat (Wakefield et al., 2014). Variability in the sea ice conditions within areas used by foraging snow petrels, both prior to and during the breeding season, affects annual adult survival, colony size, and breeding phenology (Barbraud et al., 2000; Barbraud & Weimerskirch, 2001; Jenouvrier et al., 2005; Sauser et al., 2021b). Despite this understanding, the relationship between foraging habitat use and the circumpolar breeding distribution has not yet been quantified.

Snow petrels are a cavity-nesting species, requiring ice-free areas for breeding (Walton, 1984). The lithology and geomorphology at breeding sites is thus important in determining cavity presence. Nest cavities occur both on cliff faces, on scree slopes, and under boulders on flat and sloping ground (Figure 1). Specific characteristics including slope, aspect, number of entrances, and nest bowl slope are variable. However, nests with single, narrow entrances are more frequently used, and hatching success and chick survival are greatest when cavities have flat nest bowls (Jouventin & Bried, 2001; Einoder et al., 2014). Local meteorological conditions at breeding sites can affect access to nests and cause breeding failure (Sydeman et al., 2012), and it has been suggested that the interplay between nest aspect and local wind direction is critical in providing suitable snow-free cavities (Olivier & Wotherspoon, 2006). However, the relationship is not consistent. For example, in the Windmill Islands (East Antarctica), most snow petrel nesting cavities are oriented towards strong prevailing winds (Cowan, 1981), whilst nesting cavities in the Bunger Hills and Dronning Maud Land are typically oriented to be protected from strong katabatic winds (Gibson, 2000; Wand & Hermichen, 2005). Variability in local climatic conditions during the breeding season, including the timing, intensity and duration of precipitation; wind speed, direction and duration; and local air temperatures, impact the breeding phenology and demographics of local snow petrel populations (Chastel et al., 1993; Sauser et al., 2021a; 2021b). As snow petrel populations are responding to marine and terrestrial environmental changes, updated knowledge of their breeding distribution at a continental scale, as well as baseline knowledge of environmental conditions in their foraging and breeding habitats during the breeding season, is therefore required for predicting how populations are likely to respond to future environmental changes at sea and on land.

Figure 1. Nesting adult snow petrel depicting a deep nesting cavity under boulders. Photo from Ewan Wakefield (Durham University).

1.1.2 Aims and objectives

The primary aim of this study is to quantify the known global breeding distribution and breeding habitat use of snow petrels. Breeding location and cavity selection by snow petrels is hypothesised to be driven by a hierarchy of local and regional environmental conditions. Constrained by their central-place foraging behaviour, breeding site selection is most importantly limited by the availability of suitable breeding substrate (bare rock) within sustainable distance of suitable foraging habitat (the Marginal Ice Zone). At locations within range of suitable foraging habitat, snow petrels may then select specific cavities based on local conditions, such as cavity size (for predation protection) and aspect.

This aim will be achieved in Chapter 3 by addressing the following research objectives:

1) Produce a map and detailed attribute table of all known snow petrel breeding locations, including where possible colony sizes.
2) Characterise breeding habitat according to local scale environmental conditions (specifically substrate and climate) at breeding sites themselves.
3) Characterise breeding habitat according to regional scale sea ice conditions within waters accessible from breeding sites (foraging habitat).

The capability of remote sensing to detect cavity-nesting seabirds such as snow petrels has never been tested. Therefore, guided by remote sensing studies on other Antarctic seabirds, the final aim is to test whether snow petrel breeding sites can be sensed remotely in satellite imagery. This is focused on in Chapter 4, and addressed by the final research objective:

4) Using multiple techniques, test whether snow petrel breeding sites can be identified in satellite imagery with different spatial and spectral resolutions.

CHAPTER 2

2.1 Literature Review

2.1.1 Present understanding of snow petrel breeding distribution

Snow petrels nest exclusively on ice-free terrain between their northern breeding limit on South Georgia (36°7'S, 54°W) and as far south as 80°44'S (Genghis Hills, Transantarctic Mountains) (Croxall & Prince, 1980; Walton, 1984; Croxall et al., 1995). Although some sites such as the Petermann Range and Untersee Oasis (Dronning Maud Land) may have been continuously/repeatedly occupied by snow petrels for up to 58,000 years (Berg et al., 2019; McClymont et al., 2022), it is suggested that sites newly exposed since the Last Glacial Maximum are still being colonised by an expanding population (Jouventin & Viot, 1985). Therefore, it is pertinent to investigate the distribution of snow petrels at a continental scale as well as to make observations of individual colonies. However, at and above a regional scale, snow petrel distribution data are extremely rare (Olivier & Wotherspoon, 2006). Population monitoring at a continental scale is limited to a single inventory compiled almost three decades ago (Croxall et al., 1995), which has not been updated since, despite the intensification of scientific research on the continent.

The latter, which reviewed both published and unpublished snow petrel breeding locations, found 298 records of breeding presence across Antarctica and adjacent islands (Figure 2), with breeding confirmed at 195 of these sites, and suggested at the other 103 (Croxall et al., 1995). From the available population data, this yielded a minimum total breeding population of 63,000 pairs (Croxall et al., 1995). Typically, a large proportion (> 50%) of petrel populations is represented by non-breeders (juveniles, immatures, and non-breeding adults) (Phillips et al., 2017; Carneiro et al., 2020), and based on regional at-sea counts (Ainley et al., 1984; Cooper & Woehler, 1994), a total population size of several million birds was estimated (Croxall et al., 1995). However, known regional snow petrel breeding populations are often much smaller than regional at-sea densities of snow petrels would suggest. For example, at-sea estimations suggest that there are 1.97 million snow petrels in the Ross Sea area, but this is a region where only 14 breeding sites were recorded, totalling ~ 5300 breeding pairs (Ainley et al., 1984; Croxall et al., 1995), suggesting that many breeding sites may have been unknown at the time of the previous study.

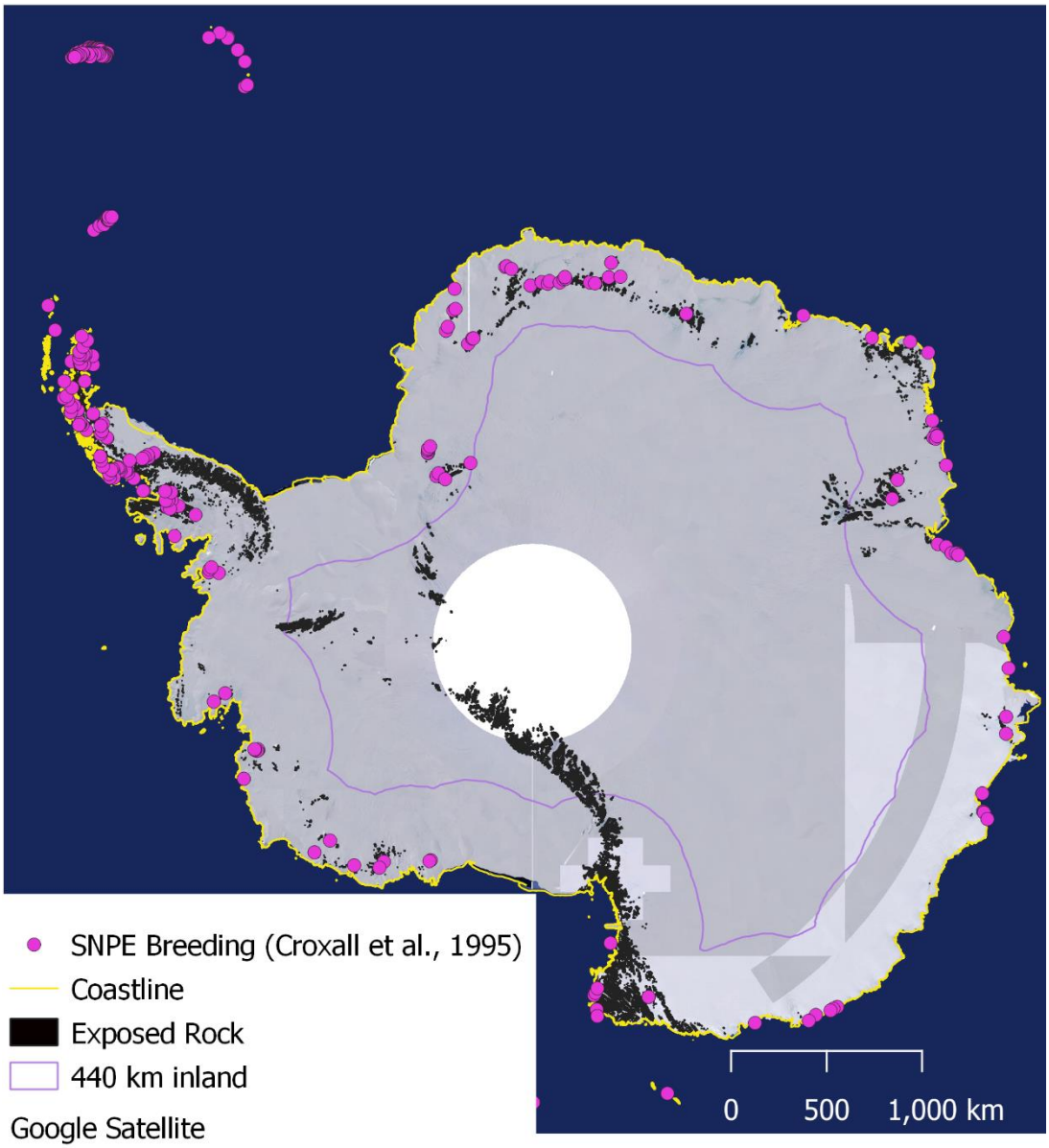

Figure 2. 298 snow petrel nesting sites as recorded in Croxall *et al*., 1995. There is an evident circumpolar distribution, however, there is much exposed rock where snow petrels have not been reported. Exposed bedrock is sourced from Burton-Johnson et al. (2016) in Quantarctica (https://www.npolar.no/quantarctica), and underlying imagery is Google Satellite.

Critically, the previous inventory of breeding locations provides presence-only data. This means that other sites are assumed not to have snow petrels, whether or not those sites have been visited for confirmation. To conduct any spatial analysis on snow petrel breeding and foraging habitats, it is vital to update this inventory, and consider any available absence data that could potentially explain gaps in the known breeding distribution. Within the current known distribution, the majority of breeding sites are evenly distributed along the Antarctic coast and adjacent islands, with fewer than 40 breeding sites (13%) located > 100 km inland (Croxall et al., 1995). More recent observations have extended the location of the furthest inland breeding site from over 300 km from open water at Tottanfjella (Bowra et al., 1966) to

440 km at Greenall Glacier in the Prince Charles Mountains, implying a foraging trip of up to 1000 km during the breeding season (Goldsworthy & Thomson, 2000). Evidently, with the discovery of new breeding sites, characterising the breeding and foraging habitats of all known sites could yield important information for the prediction of undiscovered breeding locations.

2.1.2 Methods of snow petrel observation

Field observations of snow petrel breeding sites consist of both incidental/opportunistic observations and dedicated surveys. Although records from observations are much more numerous and therefore have contributed significantly to the known distribution of snow petrels, their descriptions of local breeding habitats are often limited, providing little more information than snow petrel presence and an estimate of colony size (e.g., Greenfield & Smellie, 1992). Alternatively, local surveys offer better quantitative descriptions of breeding habitat (e,g., cavity altitude and aspect) and colony characteristics including nest densities and population counts (e.g., Convey et al., 1999; Olivier et al., 2004; Olivier & Wotherspoon, 2008). Local surveys can also be a rare but valuable source of absence data (e.g., Pande et al., 2020). However, local surveys are limited in number due to the costs and logistical difficulties of conducting them in Antarctica, thus the information known about each breeding site is varied. Systematic characterisation of all known snow petrel breeding habitats, which would help future prediction of undiscovered breeding locations, is therefore needed to further the understanding of the breeding distribution of snow petrels.

2.1.3 Foraging habitat use

During the pre-breeding period, snow petrels are estimated to have a mean foraging range of 2648 ± 1054 km, and a maximal range of 4978 km (Delord et al., 2016). However, during the breeding period the highest densities of snow petrels tend to be within 700 km of breeding sites due to the central-place foraging constraint (Figure 3; Delord et al., 2016). Recent tracking data from two sites in Dronning Maud Land indicate a maximal foraging range of 1500 km during the breeding season (McClymont, Wakefield & Honan, pers. comms). Within these foraging ranges, the most important component of the snow petrel's foraging habitat is the regional sea ice conditions (Ainley et al., 1984). Regional at-sea distributions of snow petrels suggest that the most suitable foraging habitat is between sea ice concentrations [SICs] of 12.5 – 50% (1 – 4 oktas; Zink, 1981). Regionally, there is slight variability in this range, reported as 10 – 30% SIC in the Weddell Sea (Cline et al., 1969). In the Ross Sea, at-sea densities of snow petrels are highest within 20 km of the pack edge

(Ainley et al., 1984). When estimated from satellite imagery, the sea ice edge is typically defined when SIC is 15% (Olivier et al., 2005). Therefore, 15 - 50% SIC encompasses the important foraging habitat for snow petrels (Zink, 1981).

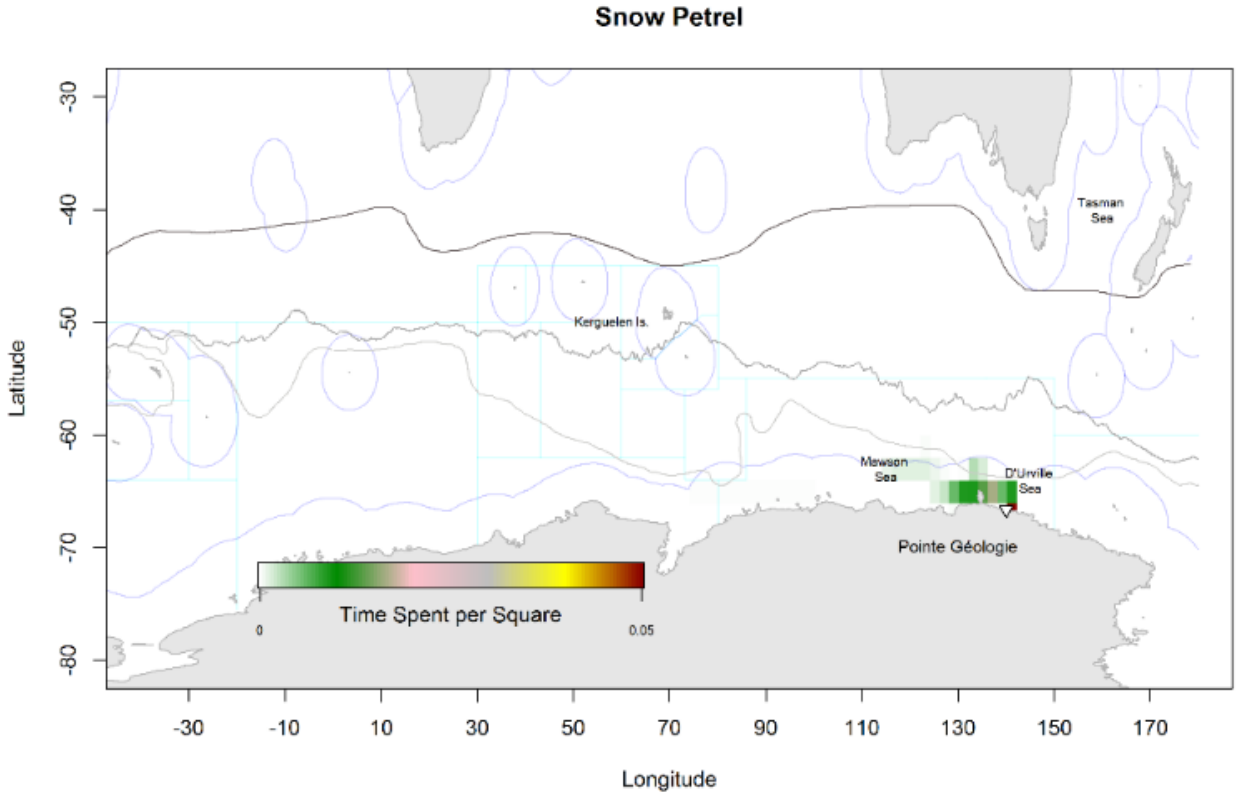

Figure 3. Distribution of snow petrels from Pointe Géologie tracked using geolocators (per cent of time of residence spent in each cell) during the post-brood chick-rearing period (late January - February), sourced from Figure S2 in Delord et al. (2016).

Investigations of the relationship between sea ice dynamics and snow petrels (both during the austral winter / non-breeding season, and austral summer / breeding season) are multiple (e.g., Barbraud et al., 2000; Barbraud & Weimerskirch, 2001; Jenouvrier et al., 2005; Olivier et al., 2005; Sauser et al., 2021b). Predominantly, these studies focus on how sea-ice conditions affect the breeding phenology and demographics of local populations, with results showing for example that breeding starts later and hatching is delayed when SIC is high during the breeding season (Sauser et al., 2021b), and adult annual survival is better (3 – 4% higher) when the sea-ice edge is closer than average to the continent in May – July and October (Barbraud et al., 2000). However, the spatial extent of these studies are limited: most are conducted at the scale of individual colonies on either Île des Pétrels in the Pointe Géologie Archipelago (Adélie Land), or Reeve Hill by Casey Station in East Antarctica, the

only two sites where long-term monitoring of snow petrel populations occur. Therefore, investigating the relationship between sea ice and snow petrels at a continent-wide scale , and focusing on sea ice and breeding site distribution, rather than on population demographics and phenology will provide a different view of the species.

Fundamentally, all trophic levels of snow petrel prey rely on Southern Ocean primary production, which peaks during the austral summer, generated by springtime ice retreat (Smith & Nelson, 1985; Smith & Comiso, 2008) and is greater at the sea ice edge (Ainley et al., 1984). Within their foraging range, the dependence of snow petrels on low concentration sea ice for foraging is so critical that the distribution of breeding sites is hypothesised to be affected by the existence of accessible pack ice during the breeding season (Ainley et al., 1984). However, this hypothesis has not been tested. Primarily, quantifying the distance distribution from breeding sites to their foraging habitat during the breeding season, and quantifying the area of suitable foraging habitat accessible within their foraging ranges, would allow exploration of the relationship between sea ice dynamics and the selection of breeding sites.

2.1.4 Breeding habitat use

Locally to their breeding sites, snow petrel breeding habitat encompasses cavity type, topography, substrate, and local climate conditions. As a cavity-nesting species, field observation and detection of active nests can be difficult, and detection probability is higher for larger cavities (Southwell et al., 2011). From direct observations, cavities are variously reported as in vertical cliff faces (e.g., Heatwole et al., 1991), on scree slopes (e.g., Goldsworthy & Thomson, 2000), between rocks (e.g., Lawther & Macallister, 1973), and on ledges (Brook & Beck, 1972) (Figure 4). Within a sustainable range of suitable foraging habitat, cavity selection is an important part of breeding site selection. Generally, nest density is constrained by the structure of exposed bedrock and availability of cavities (Ryan & Watkins, 1989; Olivier & Wotherspoon, 2006), suggesting the importance of local lithology for cavity availability. However, data on the lithology of nesting sites are rare (Brook & Beck, 1972; Starck, 1980; Heatwole et al., 1991; Melick et al., 1996; Rankin et al., 1999; Goldsworthy & Thomson, 2000), meaning any relationship between relative use versus availability of different lithologies has yet to be identified.

Figure 4. Photos from Heimefrontfjella, Dronning Maud Land, showing examples of snow petrel nesting cavities in high grade metamorphic lithologies. Cavities have narrow entrances and are deep, can be between large slabs on a wall or scree slope. Photos from Mike Bentley (Durham University). Stomach-oil deposits (mumiyo) are indicated by the red arrows.

In the process of habitat selection, microhabitat quality is very important (Olivier & Wotherspoon, 2006), therefore, individuals may also select cavities based on cavity characteristics and the interplay between local climate conditions. On Béchervaise Island (East Antarctica), cavity selection by breeding snow petrels is dependent on both of these conditions: disproportionately higher use of cavities with a flat nest bowl improves the success of laying and chick survival, and a single, narrow entrance is likely to increase shelter by reducing air flow (Einoder et al., 2014). Though these cavity characteristics provide better quality nests, there is simultaneously a trade-off between how sheltered a cavity is, and how prone the cavity is to ice accumulation when snowfall is high; on Béchervaise Island, sheltered cavities more commonly experienced breeding failure due to ice accumulation (Einoder et al., 2014). Fundamental aspects of the terrestrial breeding habitat, such as local lithology, and average local climatic conditions, are rarely recorded when observations of snow petrel breeding sites are made. As potentially important controls on snow petrel breeding distributions, these variables require systematic investigation across the whole known breeding distribution.

2.1.5 Remote sensing of Antarctic seabirds

Remote sensing is increasingly use to detect and survey Antarctic seabird colonies, and has become an efficient method of distinguishing birds / their nesting areas from other parts of the ecosystem (such as rock, vegetation, and snow), and quantifying the total population sizes of numerous surface nesting species. The remote sensing technique is underlain by the unique spectral characteristics of seabird guano and nesting sites, which reflect distinct parts of the electromagnetic spectrum (e.g., Figure 5) (Fretwell et al., 2015). For example, the spectral profile of Adélie penguin guano increases in reflection at wavelengths from 700

nm to maximum reflectance at 1300 nm, and is high between 1100 – 1300 nm. Two secondary local maxima occur at 1650 and 2200 nm, whilst local minima occur at 400, 1450, 1920, and 2500 nm (Figure 5). Thus the wavelengths of maximum Adélie penguin guano reflectance correspond to various bands in the short-wave infrared [SWIR] region, depending on the satellite used (Fretwell et al., 2015). Critically, penguin guano reflectance is distinct from other surface components of the Antarctic ecosystem: ice/snow is typically most reflective in the visible region (Winther, 1994), Antarctic vegetation is highly reflective in the near-infrared [NIR] relative to the visible red region (Fretwell et al., 2011), and most types of geology have a different spectral signature to guano (Fretwell et al., 2015).

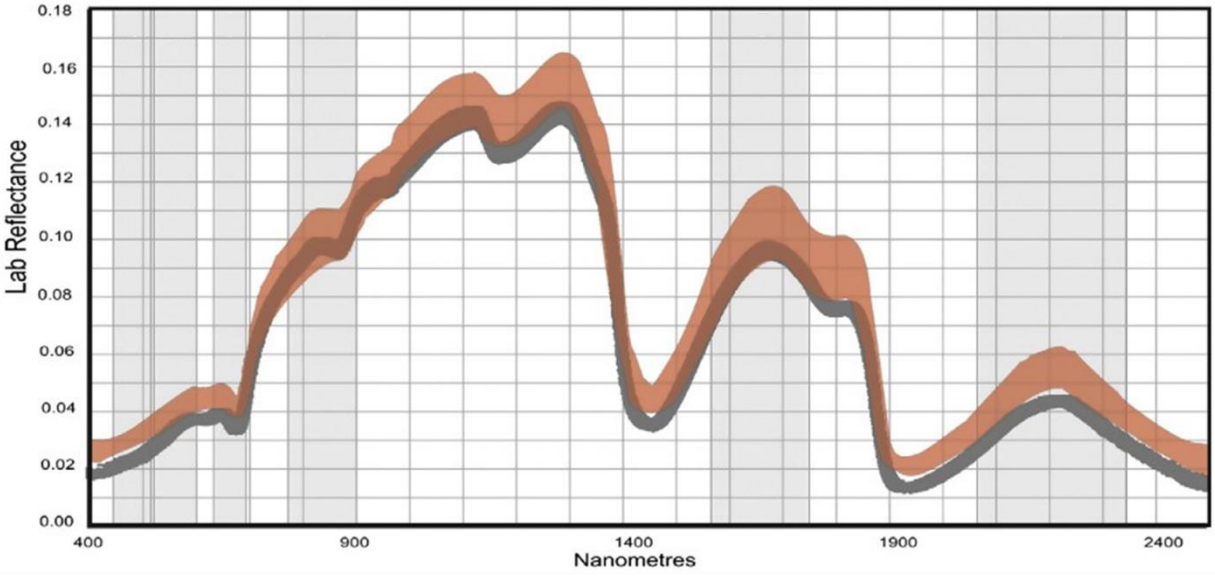

Figure 5. Laboratory derived spectral profile of Adélie penguin guano from Fretwell et al. (2015). The two lines (pink and grey) denote the two sample pieces, and variation indicated by the line width denotes the range of the 20 scans from various angles of each piece. Wavelength of reflected energy is recorded in nanometres.

The first application of this technique was to assess the extent of Adélie penguin rookeries on Beaufort Island and Ross Island based on measurements of both laboratory and field reflectance (Schwaller et al., 1984; 1989). Since then, medium resolution Landsat imagery has been used to survey the continental-scale breeding distribution of Adélie penguin colonies, in which six previously unreported colonies were discovered (Schwaller et al., 2013), as well as conduct a global census of the Adélie breeding population (LaRue et al., 2014; Lynch & LaRue, 2014). Similarly, the location of emperor penguin colonies (including the discovery of new colonies and the repositioning of poorly recorded colonies) and an estimate of their global population size have been conducted from Landsat imagery (Fretwell & Trathan, 2009; Fretwell et al., 2012). More recently, colonial surface nesting seabirds within Marguerite Bay (Antarctic Peninsula) and Antarctic petrel colonies across the whole

of Antarctica have also been detected (Fretwell et al., 2015; Schwaller et al., 2018). In a largely inaccessible area such as Antarctica, the use of remote sensing to identify colonies and quantify populations of seabirds, that are otherwise difficult to monitor and census, provides valuable information and facilitates the analysis of population structures and long-term research. For example, geographic structuring of penguin populations (both emperor and Adélie), driven by intraspecific trophic competition and associations with habitat availability, has been identified based on the data of their circumpolar breeding distributions (Santora et al., 2020). The capability of remote sensing to detect known and unknown seabird colonies should thus be tested on more species.

To date, remote sensing has not been applied to investigate the distribution or habitats of snow petrels. Obvious challenges arise from the low density of snow petrel colonies, and their cavity nesting nature (Olivier & Wotherspoon, 2006). Despite the latter, breeding sites with large numbers of snow petrels do produce obvious guano-staining of rocks (Greenfield and Smellie, 1992), which is the typical target for remote sensing of seabird colonies. Furthermore, the production of nutrient enriched soils surrounding snow petrel nests deriving from concentrations of guano, carcasses, feathers, and eggshells (Cocks et al., 1999) may further distinguish snow petrel habitats from surrounding bare rock. Similarly, the long-term accumulation and preservation of snow petrel stomach-oil deposits (Antarctic mumiyo) around snow petrel nests (Hiller et al., 1995) provides another substance that could have a unique spectral signature specific to snow petrel breeding sites (Figure 4). Therefore, it is justifiable to test whether known snow petrel breeding sites have a distinct spectral signature that could be used to detect unknown colonies. The majority of previous remote sensing investigations of Antarctic seabirds utilise medium/high resolution Landsat imagery (Schwaller et al., 2013; 2018), occasionally supplemented by very high resolution images (QuickBird, Worldview-2; Fretwell et al., 2012; 2015), or very high resolution Unmanned Aerial Vehicle [UAV] imagery (Román et al., 2022). Any potential detection of snow petrel colonies is likely to be more successful in imagery with higher spatial resolution, due to the relatively low density of nests in comparison to colonial surface-nesting species. Therefore, to investigate whether known snow petrel colonies can be detected in satellite imagery, using not just freely available medium-high resolution, but very high resolution imagery will be more informative.

2.1.6 Summary

From this review, a number of key themes have been identified which together will allow the breeding distribution and breeding habitat use of the snow petrel to be quantified. Firstly, the

breeding distribution must be inventoried at a continent-wide scale and population data, where available, collected. Secondly, lithology and local meteorological conditions influence both nest site availability and microhabitat quality for this cavity-nesting species (Ryan & Watkins, 1989; Einoder et al., 2014). Therefore, systematic characterisation of these local environmental conditions, which are rarely and inconsistently reported in observational records, would allow breeding habitat to be described across the whole breeding distribution. During the breeding season, snow petrels depend on low concentration sea-ice (15 – 50 % SIC) accessible within their foraging range for foraging (Zink, 1981). The availability and proximity of low concentration sea ice is hypothesised to limit the breeding distribution (Ainley et al., 1984), but this hypothesis requires further testing, and quantifying the distance from breeding sites to this foraging habitat, as well as the area of available foraging habitat would improve the state of knowledge of how sea-ice conditions affect the breeding distribution of snow petrels. Finally, the accumulation of guano and stomach-oil deposits at breeding sites with large populations indicates that it is justifiable to test whether known breeding sites are identifiable in satellite imagery.

CHAPTER 3: The breeding distribution and habitat use of the snow petrel

The focus of this chapter is on the primary aim of quantifying the known global breeding distribution and breeding habitat use of snow petrels. To achieve this, the first three research objectives are addressed: an updated map and detailed attribute table of all known snow petrel breeding locations are produced, and the attribute table is attached in Appendix A. Breeding habitat is also characterised according to local scale environmental conditions at breeding sites themselves, and regional sea-ice conditions in waters accessible from breeding sites (foraging habitat). This chapter also forms part of a paper, the full version of which is attached in Appendix B. The project was conceived by E. McClymont, S. Jamieson, E. Wakefield, M. Bentley. All data collection, analysis, paper drafting and writing was completed by myself. Other co-authors commented on a paper draft.

3.1 Methods

3.1.1 Database compilation

To determine the known breeding distribution of snow petrels, an intensive search of the published literature was conducted and records of snow petrel breeding sites were identified. Based on the qualitative and quantitative data available in the literature, a database was constructed in which the relevant information was collated. This included spatial data (breeding site name and decimal coordinates), as well as all information relating to breeding site or colony characteristics. This typically included breeding site aspect, elevation and local lithology, and when survey data were available, nest density. Snow petrel nest densities range from highly dispersed (0.3 nests per ha) to relatively dense aggregations (24.1 nests per ha) (Olivier et al., 2004; Olivier & Wotherspoon, 2008), and uncalculated densities may be higher. However, even the maximum densities do not reach the high densities of colonies of closely related colonial breeders such as the Antarctic petrel (Mehlum et al., 1988; Schwaller et al., 2018). Therefore, it is difficult to define the spatial extent of a snow petrel colony, and to avoid ambiguity, the term ‘breeding site’ is used instead of ‘colony’, where a breeding site is defined as a locality with individual coordinates where snow petrel breeding is likely or confirmed (based on observations). No grouping of sites was conducted in this analysis. Sites were differentiated depending on being recorded as a site by original authors in observational papers. Sites in these papers may have been grouped, though this is often unclear; as such, there is inherent variability but no specific criteria for a site (other than records of breeding) have been imposed here.

Where quantitative data (e.g., coordinates, estimates of population size) had been reported in multiple papers for a specific breeding site, the most recent data were recorded. Additional fields included breeding site identifications [IDs] and Antarctic Conservation Biogeographic Regions / Benthic Biogeographic Regions (Terauds & Lee, 2016; Convey et al., 2014). For breeding sites between 30 °E and 150 °E, fields of 'Spatial sub-group' and 'Site_ID(s)' were added to conform with the spatial reference system of Southwell et al. (2021). At each locality, it was also distinguished whether breeding was confirmed or unconfirmed. For nesting and breeding to be confirmed, observations of active nests and the presence of eggs or chicks had to be reported. Otherwise, where nests were suspected but not found (e.g., Moss Island (González-Zevallos et al., 2013)), or breeding was either not mentioned or reported to be likely or possible (e.g., Stinear Peninsula (Pande et al., 2020)), breeding was recorded as unconfirmed. Sites where snow petrel breeding was checked for (i.e., during dedicated surveys) but did not occur, were recorded separately as absences.

The abundance of snow petrel breeding sites cited from unpublished data and personal communications within Croxall et al. (1995) indicated that archival data (e.g., field reports, field maps) would substantially expand the distribution known from published literature alone. Therefore, guided by Croxall et al. (1995), archived field reports, field notebooks, and maps from 1945 onwards at the British Antarctic Survey were searched to extract relevant spatial data, including from locations provided by Croxall et al. (1995). To further expand the updated breeding distribution database, we contacted seabird biologists with field knowledge of the Antarctic region, and additional data were included (Descamps, pers. com., 2023; Southwell & Emmerson, pers. com., 2023).

3.1.2 Local environmental conditions

To describe breeding habitat use at the local scale, climate and lithology at the terrestrial breeding sites were quantified. All analyses were carried out in QGIS and Rstudio.

Climate reanalysis data for the years 1992 – 2021 were obtained from the ERA5-Land monthly averaged dataset, Copernicus (Muñoz Sabater, 2019), including: 2 m surface temperature, total precipitation, and 10m wind speed and direction. The spatial/temporal resolution and continuity of this monthly, gridded data were best suited to the analysis of seasonal climatic conditions at specific breeding sites, compared to the discontinuous monthly data at point locations available from observational Antarctic Weather Station data (Wang et al., 2023), and the discontinuous annual gridded data from RACMO modelling (Melchior Van Wessem et al., 2018). The breeding season was defined as November –

March, and seasonal 30-year averages of each variable were calculated for each breeding site to provide a baseline for future studies. Based on these averages, summary statistics of each variable (mean, standard deviation, median, interquartile range, range) were also calculated.

Lithological data were extracted and appended to snow petrel breeding sites from the SCAR GeoMAP shapefile, comprising the known geology of all Antarctic bedrock and surficial deposits (Cox et al., 2023a). Breeding site lithologies were subsequently grouped into 8 categories for analysis, according to the simple lithological description in Cox et al. (2023b). In order to determine if habitat use reflected availability, the relative frequency distribution of lithology at breeding sites was compared to that within all exposed rock polygons.

3.1.3 Regional sea-ice conditions

To characterise the foraging habitat available to snow petrels at each breeding site, the assessment was focused on sea ice conditions within the mean and maximum snow petrel foraging ranges during the breeding season. While a range of foraging ranges have been identified, a mean and maximum foraging range of 700 and 1500 km respectively are used here (Delord et al., 2016; McClymont, Wakefield & Honan, pers. comms).

Passive microwave sea ice data for the austral summer and snow petrel breeding season for the years 1992 – 2021 were acquired from the National Snow and Ice Data Centre (NSIDC). Sea-ice conditions were based on 30-year averages in November and February – chosen as the points in the breeding season when sea-ice extent [SIE] is at its maximum and minimum, respectively. In November, most breeding snow petrels return to breeding sites and eggs are laid, and most remain at the breeding sites in February during the post-brood chick-rearing period.

To describe breeding habitat use at a regional scale, analysis is focused on the low sea ice concentration [SIC] MIZ most commonly used by snow petrels for foraging. For November and February, the contours at the outer ice edge with 15% SIC (Olivier et al., 2005) were calculated for each year between 1992 and 2021. The contours at 50% SIC for these months were also calculated, as at-sea densities of snow petrels have been recorded to be highest within the sea ice edge and with SICs of up to 50% (Zink, 1981). The associated rasters of SIC were also generated.

The distance from breeding sites to the contours of 15 and 50% SIC in November and February for each year between 1992 – 2021 were calculated, then averaged over the 30

years. A final calculation of foraging area within the mean and maximum foraging ranges of each breeding site was conducted, to estimate the area of sea ice between 15 – 50% concentration available to snow petrels during their breeding season. Using buffers of 700 and 1500 km from breeding sites (representing the mean and maximum foraging ranges, respectively), the number of pixels between 15 – 50% SIC for both months in each year were counted. Each count was then transformed to an area by multiplying the number of pixels by the area of a single pixel (625 km^2), and averaged over the 30 years to indicate the longer-term average conditions. For all sea ice metrics, results were plotted by frequency, and summarised by calculating the median, inter-quartile range [IQR], and range.

3.2 Results

3.2.1 Spatial distribution and size of breeding sites

The updated database represents a considerable expansion in knowledge of the global breeding distribution of snow petrels (Figure 6) since Croxall et al. (1995). We list a total of 456 confirmed and suspected (snow petrels observed but breeding unconfirmed) breeding sites. Of these, 158 are newly identified, principally in Dronning Maud Land (28 new sites), the Prince Charles Mountains (11 new inland, 43 new coastal sites), and Adélie Land (19 new sites). Additionally, surveys in localities such as the Larsemann Hills (Pande et al., 2020) have enabled the separation of a single breeding locality in Croxall et al. (1995) into multiple localities in the new database. Of the 456 known sites, breeding is confirmed at 267 (59%), and unconfirmed (but suspected, based on observations) at the remaining 189. Most breeding sites (n = 336, 74%) are located on the continent, and 120 (26%) on islands (Bouvet Island, Balleny Islands, South Orkney Islands, South Sandwich Islands, South Georgia). However, when considering the total populations of birds, just 51% of known breeding pairs are located on the continent – noting that population estimates are only available for 55% of continental breeding sites, and that the estimate of 20,000 breeding pairs on Laurie Island (South Orkney Islands) constitutes a large proportion of the known breeding population.

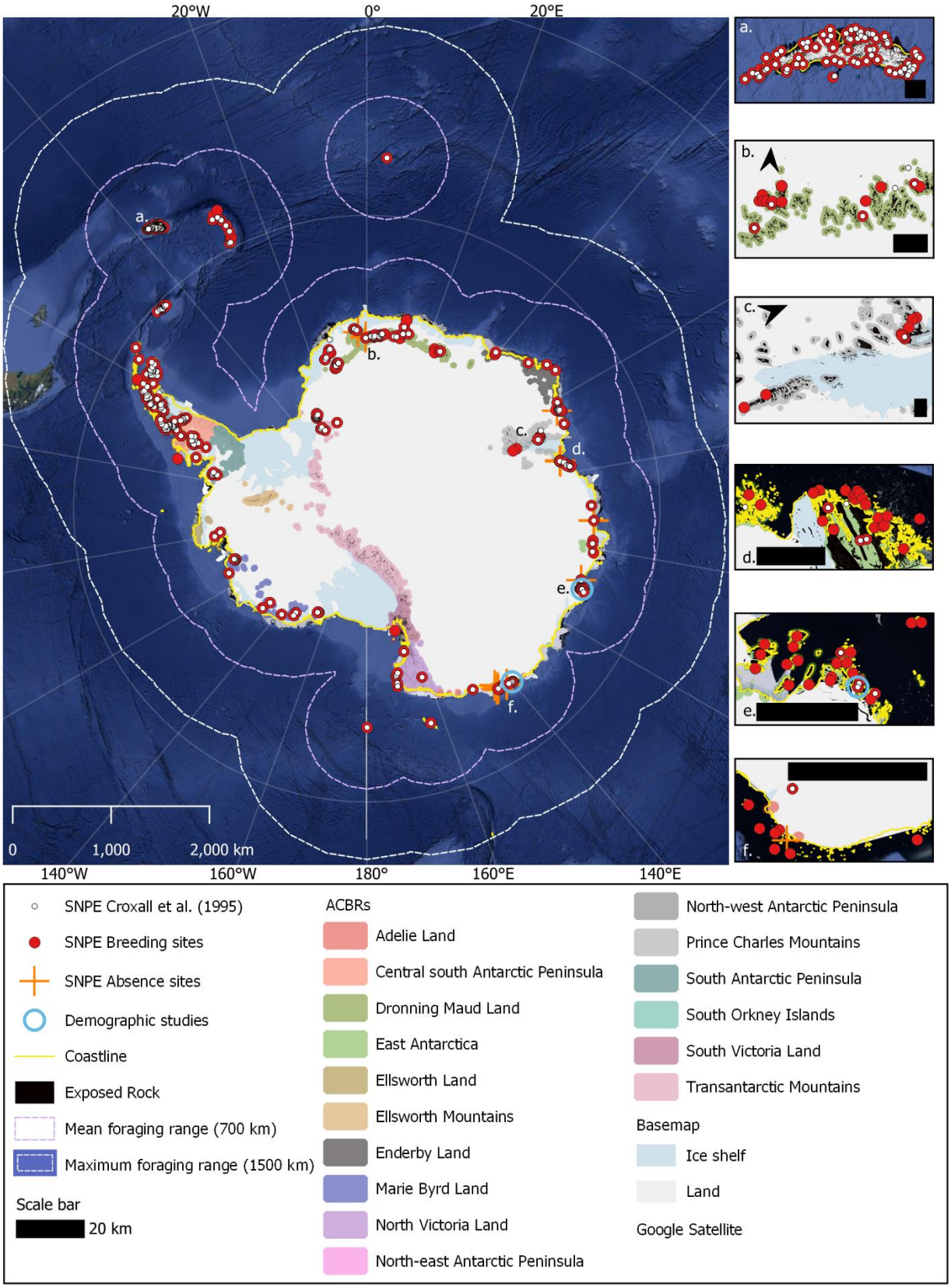

Figure 6. The updated breeding distribution of snow petrels (SNPE), with each dot representing one breeding site. The 298 breeding sites as recorded in Croxall et al. (1995) are shown in white, and the updated breeding distribution shown in red (456 breeding sites). Regional insets for **a.** South Georgia, **b.** Dronning Maud Land, **c.** Inland Prince Charles Mountains, **d. & e.** East Antarctica**,** and **f.** Adélie Land, show new breeding sites. Known absence sites shown by orange crosses. Coastline is combined data from the SCAR Antarctic Digital

Database (accessed 2023, Gerrish et al., 2022), and Thematic Mapping World Borders (accessed 2023). Exposed rock is sourced from Cox et al. (2023a); Antarctic Conservation Biogeographic Regions (ACBRs) are sourced from Terauds & Lee (2016); basemap from NPI/Quantarctica, and underlying imagery is Google Satellite. Map projection is Antarctic Polar Stereographic.

The median distance of breeding sites from the coastline (Gerrish et al., 2023) was 1.15 km (IQR = 0.23 to 42.75 km, range = 0.00 to 471.27 km, n = 456). Prior to 1995, the furthest known inland breeding sites were in the Tottanfjella, Dronning Maud Land, over 300 km from the coast (Bowra et al., 1966). Whilst most snow petrel breeding sites are very close to the coast (Figure 7a), a small breeding colony has been discovered 440 km inland at Greenall Glacier, Mawson Escarpment, and a nearby unconfirmed nesting site at Rimington Bluff (470 km inland) in the inland Prince Charles Mountains (Goldsworthy & Thomson, 2000). The site at Greenall Glacier increases the distance inland at which snow petrels are known to breed by 140 km.

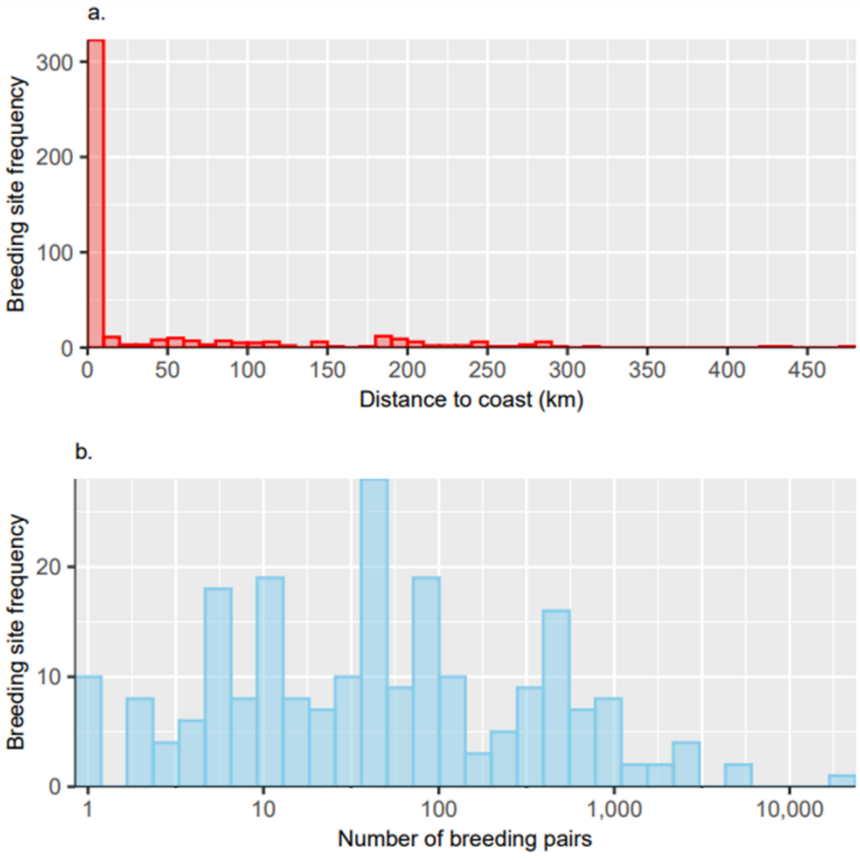

Figure 7. (a) Frequency distribution of breeding site distance to the coast, and **(b)** frequency distribution of the number of birds at breeding sites on a logarithmic scale.

The number of breeding pairs is extremely variable between breeding sites (median = 50, IQR = 10 to 171, range = 1 to 20,000, n = 222; Figure 7b). At some sites, single pairs were recorded (e.g., Orvinfjella region, Dronning Maud Land; Dragons Teeth Cliffs, Prince Charles Mountains; Mount Haskel, north-west Antarctic Peninsula). In contrast, 4,575 breeding pairs were estimated on Browning Peninsula in the South Windmill Islands (Olivier et al., 2004),

and 20,000 breeding pairs on Laurie Island, South Orkney Islands (Clarke, 1906; Croxall et al., 1995). However, the number of breeding pairs is only known (from either counts or estimates) at 222 sites (49%). These data give a minimum total breeding population estimate of ~77,400 breeding pairs. Where population data are known, 69% of breeding sites contain ≤ 100 breeding pairs.

Most known snow petrel breeding sites are relatively close to research stations (median distance = 25.96 km, IQR = 8.53 to 81.76 km, range = 0.32 to 875.38 km; Figure 8), with 406 breeding sites (86%) < 200 km from the nearest station, and 297 (65%) < 50 km from the nearest station. However, much exposed rock (a requirement for snow petrel nesting) is available beyond 50 km from stations where considerably fewer breeding sites are reported, and unknown breeding sites may exist.

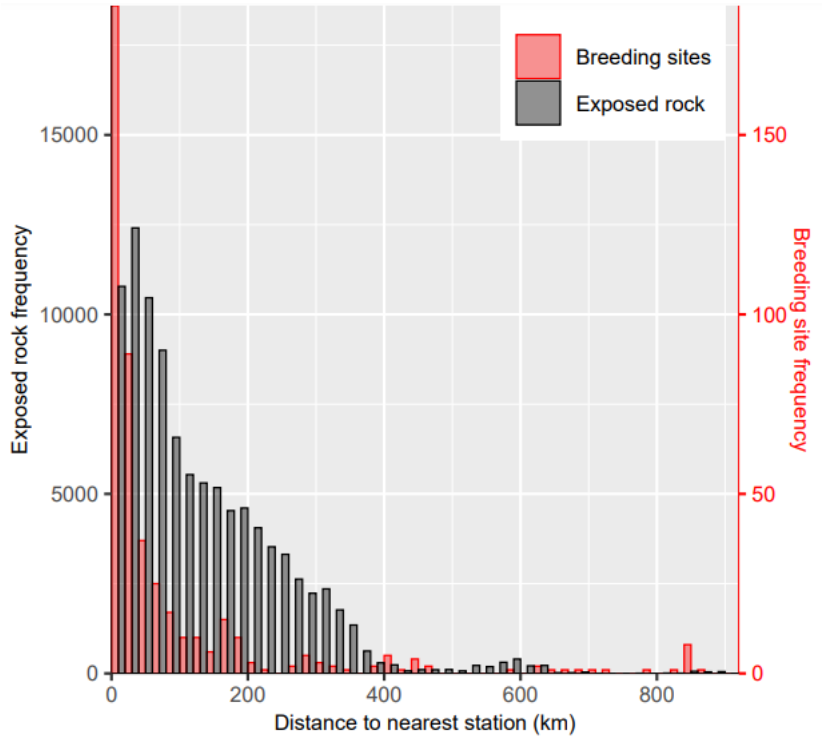

Figure 8. Frequency distribution of the distance between exposed rock polygons (grey) and the nearest station, and frequency distribution of the distance between breeding sites (red) and the nearest station plotted on a secondary axis. Stations represent scientific research stations / facilities, sourced from CONMAP 2017, Quantarctica. Exposed rock polygons sourced from Cox et al. (2023).

3.2.2 Local environmental conditions

There was extensive variation in environmental conditions at breeding sites (Figure 9; Table 1), with a median of the average summer temperatures of -6.9°C (IQR = -12.8 to -4.2°C, range = -23.8 to 2.9°C, n = 247), median total precipitation of 1.0 mm (IQR = 0.7 to 3.1 mm, range = 0.1 to 6.9 mm) and median seasonal wind speed of 3.5 ms^{-1} (IQR = 2.5 to 4.9 ms^{-1}, range = 0.5 to 10.0 ms^{-1}). The mildest climatic conditions are experienced at South Georgia (the northern breeding limit), where mean seasonal temperatures and total precipitation were > 0°C and > 3.0 mm, respectively, but mean wind speeds were similar to

the median for all sites. On the Antarctic Peninsula, mean seasonal surface temperatures vary between -10 and 0°C, and total precipitation between 0.5 and 7.0 mm, with warmer and wetter conditions closer to the west coast. The lowest, most extreme mean seasonal temperatures are experienced at inland Antarctic breeding sites, varying between -23.8 and -4.0°C, whereas mean seasonal wind speeds are highest at sites in coastal East Antarctica.

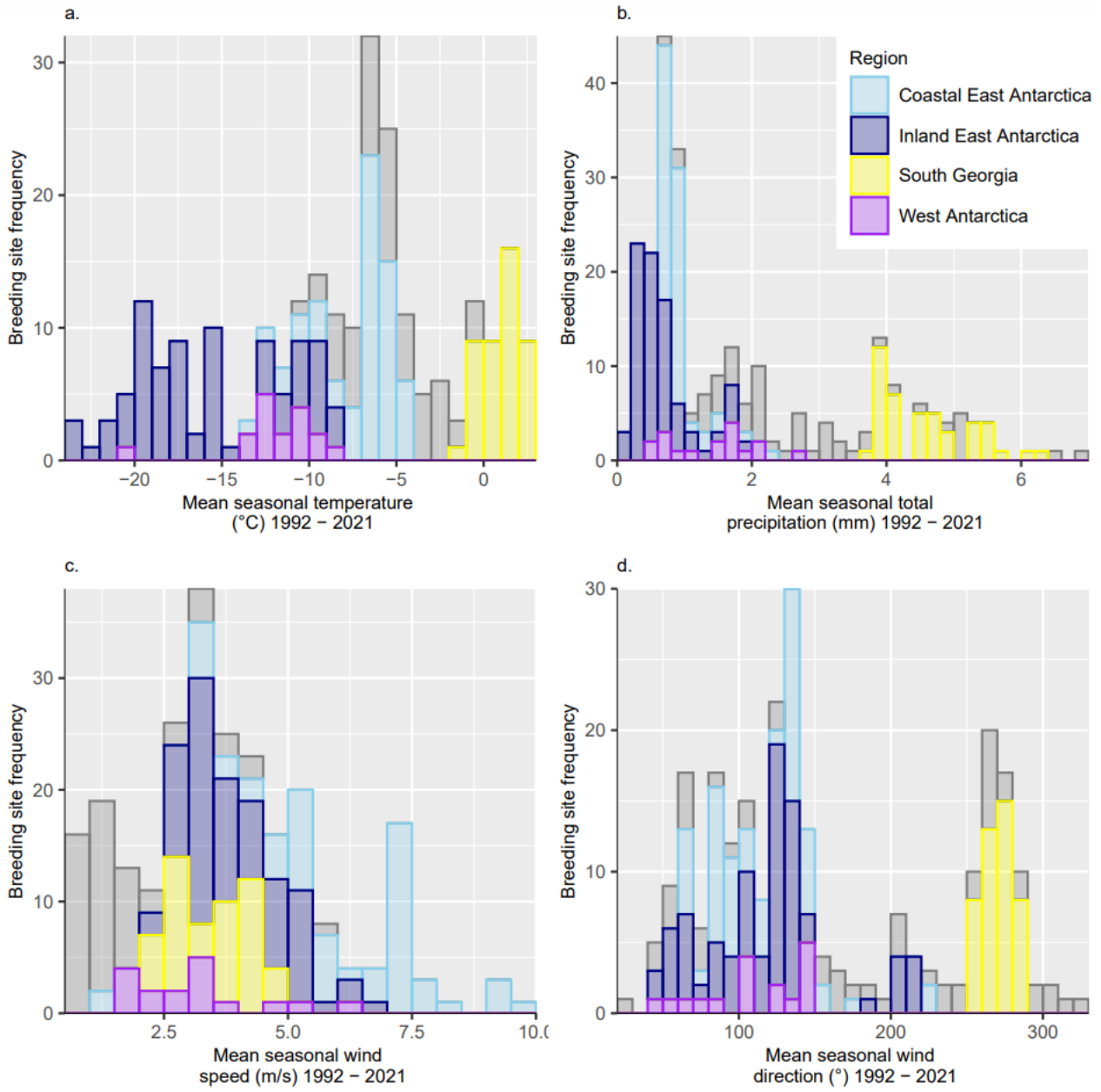

Figure 9. Frequency distributions of mean seasonal climate variables at snow petrel breeding sites between 1992 – 2021, displayed by region. **(a)** 2 m surface temperature (°C), **(b)** total precipitation (mm), **(c)** wind speed (m/s), **(d)** wind direction (°). Climate data sourced from Muñoz Sabater (2019), accessed January 2023.

Table 1. Descriptive characteristics of local climate variables within snow petrel breeding habitats during the austral summers (November - February) between 1992 – 2021. For all breeding sites n = 247, Antarctic continent (West Antarctica and inland/coastal East Antarctica) n = 150, Antarctic Peninsula n = 54, and South Georgia n = 43.

	Mean	Standard deviation	Range (Minimum to Maximum)	Median	Interquartile range
All Breeding Sites					
Mean seasonal air temperature (°C)	-8.3	6.7	-23.8 – 2.9	-6.9	-12.8 - -4.2
Mean seasonal total precipitation (mm)	1.9	1.7	0.1 – 6.9	1.0	0.7 – 3.1
Mean seasonal wind speed (m/s)	3.8	2.0	0.5 – 10.0	3.5	2.5 – 4.9
Antarctic Continent					
Mean seasonal air temperature (°C)	-12.0	5.5	-23.8 - -4.1	-10.8	-17.2 - -6.7
Mean seasonal total precipitation (mm)	0.8	0.5	0.1 – 2.6	0.8	0.50 – 1.0
Mean seasonal wind speed (m/s)	4.6	1.8	1.1 – 10.0	4.3	3.2 – 5.7
Antarctic Peninsula					
Mean seasonal air temperature (°C)	-5.4	2.4	-11.0 – -0.6	-5.4	-7.1 – -3.5
Mean seasonal total precipitation (mm)	2.8	1.5	0.8 – 6.9	2.3	1.8 – 3.5
Mean seasonal wind speed (m/s)	1.7	1.1	0.5 – 5.9	1.3	0.9 – 1.9
South Georgia					
Mean seasonal air temperature (°C)	1.0	1.1	-1.5 – 2.9	1.1	0.2 – 1.7
Mean seasonal total precipitation (mm)	4.5	0.7	3.8 – 6.2	4.4	4.0 – 4.8
Mean seasonal wind speed (m/s)	3.5	0.8	2.4 – 4.8	3.7	2.7 – 4.3

As a rock-cavity nesting species, snow petrel breeding habitat use at the local scale must also consider the lithology at breeding sites. The most available lithology by frequency in Antarctica is intrusive igneous (27%), followed by sedimentary (21%) and high-grade metamorphic rock (18%) (Figure 10a). Snow petrel breeding sites are found most often on intrusive igneous rock (28%), and high grade metamorphic rock (26%). Comparatively, fewer breeding sites occur on sedimentary rock (17%) despite its relatively high availability. For the 222 breeding sites with population estimates, the number of breeding pairs on high-

grade metamorphic rock (> 45,000 pairs) outnumbers the number of pairs on intrusive igneous rock (< 17,000 pairs) or any other lithology.

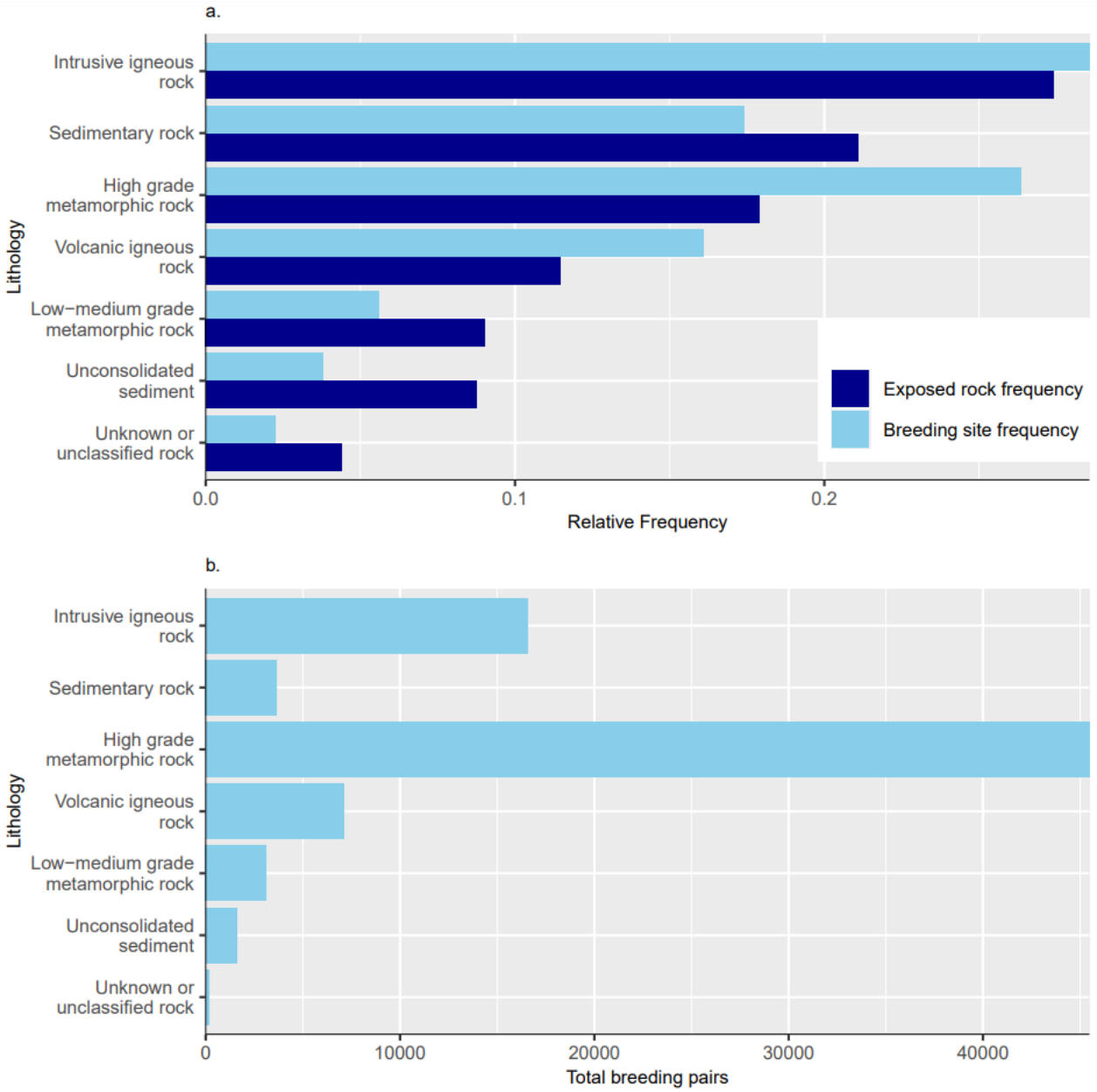

Figure 10. (a) Relative frequency distribution of lithology at snow petrel breeding sites (light blue), compared to the relative frequency distribution of the lithology of exposed rock polygons across the Antarctic (dark blue). **(b)** Total number of breeding pairs of snow petrels on each lithology. Lithological data from Cox et al. (2023a).

3.2.3 Regional sea-ice conditions

Sea-ice conditions in waters accessible to snow petrels from breeding sites differed between regions and throughout the breeding season (Figure 11). Breeding sites on Bouvet Island, the South Shetland Islands, South Orkney Islands, South Sandwich Islands, and South Georgia, are at or beyond the 30-year average November ice edge contour (Figure 11a). Therefore, the likely foraging habitat is very different to sites with accessible foraging areas

within the MIZ, and quantified descriptions of foraging habitat use are given only for breeding sites where the birds likely feed within the MIZ (n = 333).

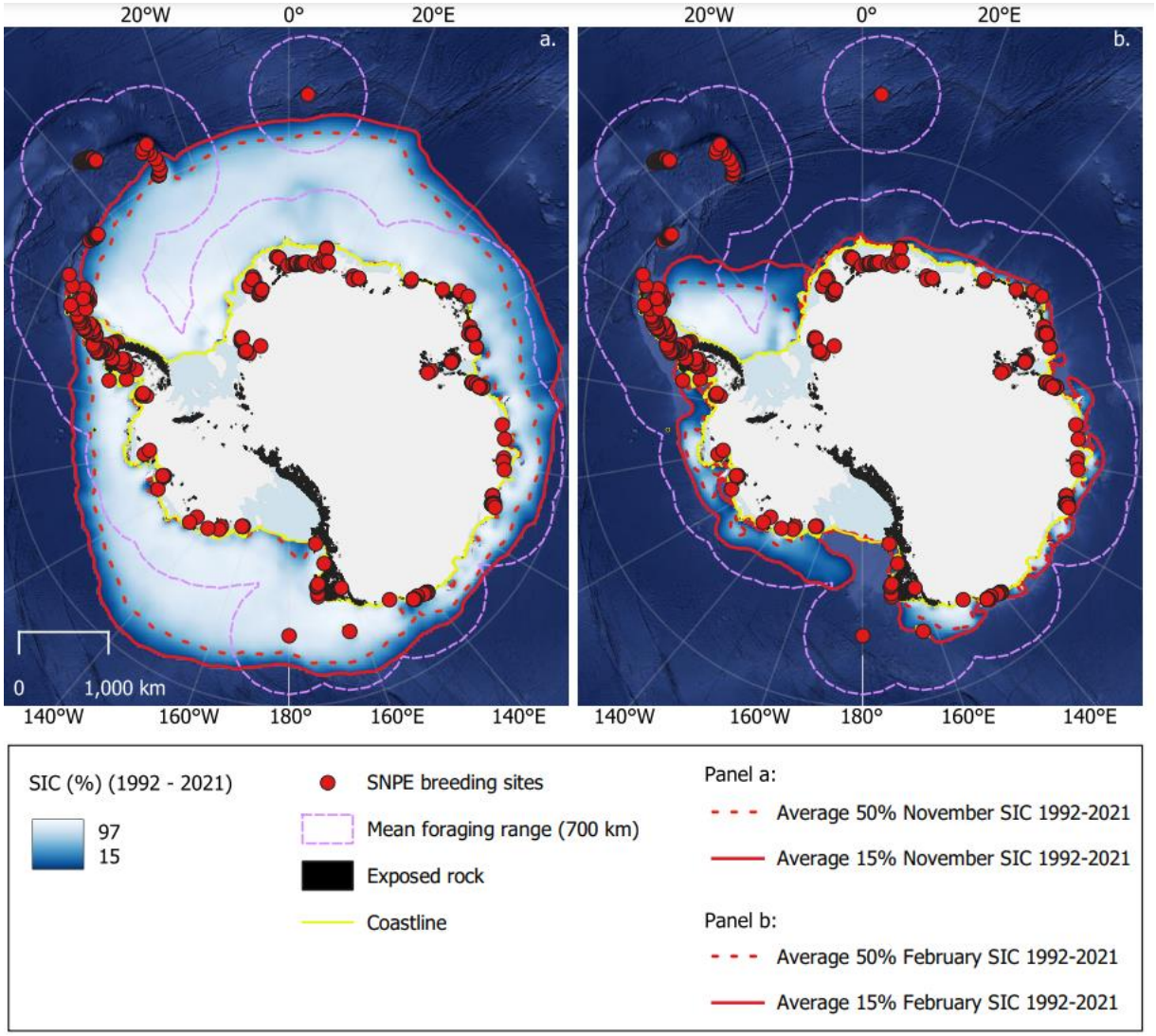

Figure 11. (a) Mean November sea-ice concentration [SIC] in 1992 – 2021 within foraging ranges of known snow petrel breeding sites. **(b)** Mean February SIC for 1992 – 2021 surrounding breeding sites.

In November, when sea ice extent is at its maximum during the breeding season, the median distance from breeding sites to the ice edge is 430 km (IQR = 295 to 694 km, range = 6 to 1682 km), whilst the median distance to the 50% SIC contour is 136 km (IQR = 30 to 282 km, range = 1 to 737 km) (Figure 12a, 12b). These distances generally lie within the mean foraging range (~700 km) and are well within the maximum foraging range (1500 km). The 15 – 50% SIC zone lies beyond the mean foraging range only for inland breeding sites in Dronning Maud Land, the Transantarctic Mountains, and Marie Byrd Land. The November 50% SIC contour only reached the coast adjacent to coastal breeding sites east and west of Amery Ice Shelf, Adélie Land, and north of the Ross Ice Shelf (Figure 11a). Within the assumed mean snow petrel foraging range, the median area of sea ice between 15 – 50%

SIC in November is 113,000 km^2 (IQR = 42,400 to 167,000 km^2, range = 4,520 to 237,000 km^2). Within the maximum foraging range, the median foraging area is 396,000 km^2 (IQR = 325,000 to 762,000 km^2, range = 19,500 to 841,000 km^2).

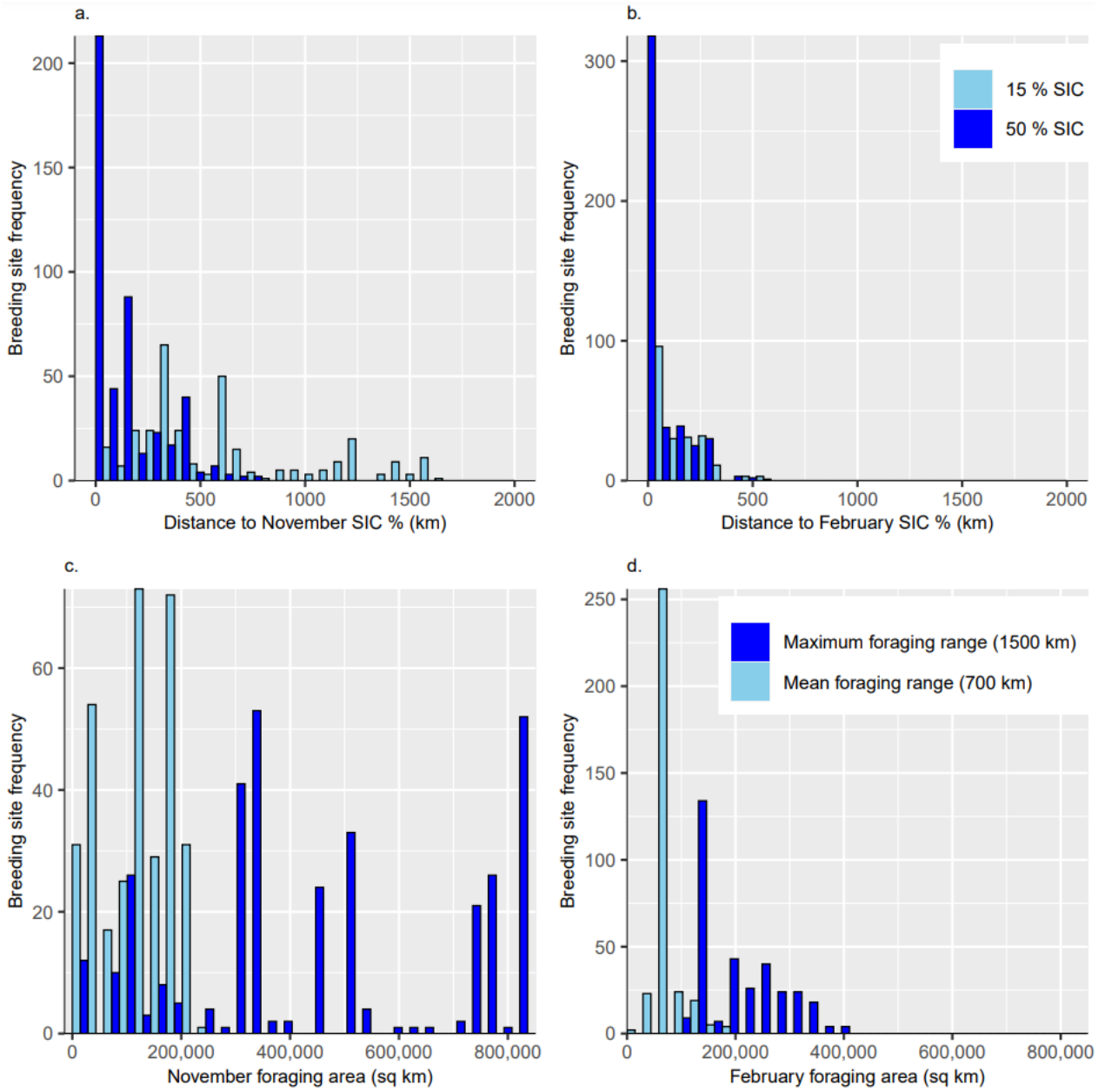

Figure 12. Frequency distributions describing snow petrel foraging habitat at key points in the breeding season (November and February) between 1992 – 2021. **(a)** Frequency distribution of distance from breeding sites to contours of 50% SIC (dark blue) and 15% SIC (light blue) in November, **(b)** and in February. **(c)** Frequency distribution of foraging area in November within the mean (light blue) and maximum (dark blue) foraging ranges of breeding sites, **(d)** and in February. Foraging area is calculated as the total area of sea ice between 15 – 50% concentration.

Between November and February, the ice edge retreats towards the continent by hundreds of km (mean = 472 km, standard deviation = 344 km, range = -8 to 1248 km). The greatest distance of ice edge retreat is recorded north of Dronning Maud Land (> 1000 km). By

February, the most extensive and highest concentration remaining sea ice (> 90% SIC) is in the Weddell and Bellingshausen Seas, and adjacent to the coast of North Victoria Land; these are all areas with no or relatively few known snow petrel breeding sites (Figure 11b). The median distance from breeding sites to the February ice edge is 47 km (IQR = 21 to 163 km, range = 0.3 to 564 km), whilst the median distance to the 50% SIC contour is 27 km (IQR = 10 to 136 km, range = 0.1 to 535 km) (Figure 12c, 12d). Within the assumed mean foraging range, the median area of sea ice between 15 – 50% SIC in February is 60,900 km^2 (IQR = 46,700 to 67,600 km^2, range = 4,840 to 174,000 km^2), and within the maximum foraging range, the median area of 15 – 50 % SIC is 201,000 km^2 (IQR = 146,000 to 265,000 km^2 , range = 110,000 to 398,000 km^2).

3.3 Discussion

3.3.1 Geographic distribution

Geographically, more snow petrel breeding sites are known within East Antarctica (69 breeding sites, between 76°E and 112°E), and the north-west Antarctic Peninsula (61 breeding sites, between 61°S and 69°S) than in other regions (Figure 6). From known population counts, East Antarctica also holds the highest numbers of breeding pairs (at least 21,160 pairs), followed by the South Orkney Islands (at least 20,129 pairs) due to the estimation of 20,000 breeding pairs on Laurie Island (Clarke, 1906; Croxall et al., 1995). As a loosely colonial cavity-nesting species, defining the extent of a snow petrel breeding site and colony is difficult, and many population sizes may be underestimated. However, the population estimate for Laurie Island probably represents multiple colonies (Coria et al., 2011).

The distribution of breeding sites in relation to distance to the coastline suggests that the furthest inland breeding site at Greenall Glacier (440 km inland) is an outlier compared to the rest of the distribution (323 breeding sites ≤ 10 km of the coastline). However, the distance from breeding sites to the MIZ, their main foraging habitat, is more biologically relevant. At “Skiltvakta” in the Shackleton Range (Transantarctic Mountains), breeding is unconfirmed, but snow petrels that are suspected to be breeding here are 1680 km from the November ice edge, and 740 km from the November 50% SIC contour. Therefore this breeding site, relative to accessible foraging habitat, is more remote. In total, 64 breeding sites in the Transantarctic Mountains and Dronning Maud Land are > 1000 km from the November ice edge.

3.3.2 Regional absences

Updating the circumpolar breeding distribution of snow petrels highlights that there are extensive regions of exposed bedrock where breeding has not been recorded. These gaps could be due to lack of search effort or true absences. Most notably, no sites have been recorded on the east coast of the Antarctic Peninsula south of 69°5'S, adjacent to the western edge of the Weddell Sea (Figure 6). This contrasts with the rest of the Antarctic Peninsula, a region of relatively high seabird abundance (Schrimpf et al., 2020), with at least 89 snow petrel breeding sites and minimum 1264 breeding pairs. Similarly, there are only 8 known breeding sites in North and South Victoria Land, one of continental Antarctica's biggest ice-free regions. With a large proportion of exposed low-elevation coastal bedrock (Kim et al., 2015), the number of breeding snow petrels here is thus unlikely to be limited by the availability of bedrock. Furthermore, the disparity between the estimated number of breeding pairs from land-based observations in Victoria Land and adjacent islands (~5300; Appendix A) and the estimate of 1.97 million snow petrels in the Ross Sea region based on densities recorded at sea (Ainley et al., 1984), seems likely to indicate that there are numerous unknown breeding sites in this area.

These results demonstrate a geographical bias in where breeding sites are known that is clearly related to the proximity to Antarctic research stations, with a systematic decline in the number of breeding sites in areas of bedrock with distance from the nearest research station (Figure 8). Both dedicated surveys and opportunistic observations are presumably more likely in the vicinity of research stations, due to logistical constraints. Though research stations are also predominantly located at coastal sites with exposed rock, snow petrels are confirmed to breed up to 440 km inland. Thus, the lack of breeding sites further from stations (and further inland) where bedrock remains available (Figure 8), suggests it is highly likely that these more distant areas are under-sampled, and that many more remote sites remain undiscovered. This would explain obvious gaps in the circumpolar breeding distribution in North and South Victoria Land, where exposed bedrock is readily available and at sea density distributions suggest there are millions of snow petrels, but only 8 breeding sites are known.

From several surveys, snow petrel absence sites have been inferred with a varying degree of certainty. In East Antarctica, 5 small unnamed islands within the Davis Islands, 10 sites within the Larsemann Hills, and 6 sites within the Haswell Archipelago have been surveyed and no snow petrel breeding detected (Melick et al., 1996; Pande et al., 2020; Golubev, 2022). Similarly, there is an absence of snow petrel breeding at Jutulrora and Straumsvola in Dronning Maud Land (Ryan & Watkins, 1988), and a confirmed absence of snow petrel

breeding at Vesleskarvet (Steele & Hiller, 1997). In Adélie Land, surveys indicate a total of 9 absence sites along the coast and a further 3 on inland mountains (Barbraud et al., 1999). A partial survey of Southern Masson in the Framnes Mountains (inland Prince Charles Mountains) also found no snow petrel nests (Olivier & Wotherspoon, 2008). These sites with no evidence of breeding are close to localities where snow petrels do breed (e.g., 12 known breeding sites in the Larsemann Hills, and minimum 470 breeding pairs). Hence the distribution of confirmed absence sites is insufficient to explain any large regional gaps in Figure 6. The proximity of presence and absence sites suggests that regional sea-ice conditions are likely to be the same, so that distance to suitable foraging habitat is unlikely to be a limiting factor that would explain why breeding does not take place (Ainley et al., 1984). Instead, it is possible that these local absences reflect nesting-habitat availability or preferences, as discussed in the following section.

3.3.3 Potential environmental limits on breeding distribution

Nest-site selection is a critical decision for any bird (Stauffer & Best, 1982). As central-place foragers breeding terrestrially and foraging at sea, snow petrels face a distance-dependent cost of accessing food, and seabird populations in general are regulated by bottom-up processes and food availability (Wakefield et al., 2014; Sauser et al., 2021b). Breeding sites may therefore be chosen based both on the quality and proximity of foraging habitat (Bolton et al., 2019), as well as the suitability of local nest sites (Li & Martin, 1991; Lõhmus & Remm, 2005). Ainley et al. (1984) hypothesised that the breeding distribution of snow petrels is affected by the existence of accessible pack ice during the breeding season. These results support this hypothesis, given the distribution of distance from breeding sites to 15% SIC and 50% SIC in November (medians of 430 km and 136 km, respectively). As such, the persistence of high SIC in the western Weddell Sea, which is highly variable in extent but survives summer melt (Figure 11b; Turner et al., 2020), could explain the lack of breeding sites on the eastern Antarctic Peninsula.

At a local scale, as rock cavity-nesters, snow petrels are constrained to pre-existing cavities provided by the substrate (Ramos et al., 1997). They are therefore subject to intraspecific, as well as interspecific competition for these resources with other seabirds that have a similar habitat preference (Lõhmus & Remm, 2005; Wiebe, 2011; Radford & Fawcett, 2014). The availability of suitable cavities for snow petrels is inherently linked to rock type, weathering, and jointing. The results demonstrate that snow petrels breed most frequently in cavities in high-grade metamorphic and intrusive igneous rocks (Figure 10). Estimated breeding population sizes are highest on high-grade metamorphic rocks, despite the higher

availability of igneous intrusive and sedimentary rocks (Figure 10), suggesting that metamorphic rocks are more likely to incorporate suitable cavities. Additionally, specific selection of lithologies by snow petrels at a local scale is implied in multiple localities. For example, at Edisto Inlet in Cape Hallett, no suitable nesting cavities were observed on the eastern cliffs composed of volcanic rocks, whereas the western cliffs, composed of fine grained metamorphic rock, were extensively occupied by snow petrel nests over an area 6 miles in length (Maher, 1962). Frequent strong winds and precipitation at this locality during the austral summer of 1960/1961 resulted in nesting cavities being packed/buried with snow (Maher, 1962). Therefore, it is unlikely that nests on the western cliffs were selected due to favourable aspect, but that there were no suitable cavities in the eastern volcanic cliffs. By contrast, in the northern Prince Charles Mountains, there are relatively few snow petrels nesting in the high grade metamorphic rock (Precambrian basement gneisses), despite it being the dominant exposed bedrock in the region. Instead, the majority of known nests are in the Amery group sandstones, where suitable nesting cavities form through salt wedging (Heatwole et al., 1991). Furthermore, Verkulich & Hiller (1994) suggest that snow petrels in the Bunger Hills select mainly metamorphic and igneous rocks for nesting, since they are least susceptible to weathering, but they also highlight the importance of aspect for protection against strong winds and snow accumulation. Therefore, it is hypothesised that lithology, and specifically the availability of high-grade metamorphic and intrusive igneous rocks, is an important local-scale control on snow petrel nesting-habitat selection, given its association with both cavity availability and durability.

In the predominantly high-grade metamorphic mountains of Dronning Maud Land (Cox et al., 2023a), the availability of cavities is unlikely to be limiting the distribution of snow petrels. Here, observations report most breeding sites face north, which may provide shelter from katabatic winds and therefore a more favourable microclimate (Bowra et al., 1966; Mehlum et al., 1988; Ryan & Watkins, 1989; Johansson & Thor, 2004). Nests with a favourable aspect have higher breeding success (Olivier et al., 2005). Therefore, where the availability of cavities is not limited, the interplay between nest aspect and local climate may determine nest site selection (Olivier & Wotherspoon, 2006).

Based on these results, breeding location and cavity selection by snow petrels is likely to be driven by a hierarchy of regional and local environmental conditions, most importantly limited by suitable breeding substrate availability (bare rock) within a sustainable distance of suitable foraging habitat (MIZ) (Ainley et al., 1984). At locations within the foraging range of suitable foraging habitat, snow petrels may then select specific cavities based on availability

(related to lithology), and local conditions such as cavity size (for predation protection) and aspect (Olivier & Wotherspoon, 2006). Therefore, models of habitat selection that incorporate both distance to the MIZ and the availability of exposed high-grade metamorphic rock could be used to estimate the breeding distribution of snow petrels throughout their range.

3.3.4 Past and future breeding distribution

Radiocarbon dates for deposits of snow petrel stomach-oil, which often accumulate in thick layers outside their nests, demonstrate the discontinuous but persistent occupation of breeding sites throughout Dronning Maud Land, coastal East Antarctica, the inland Prince Charles Mountains and the Shackleton Mountains since before the last glacial maximum [LGM] and throughout the Holocene (Hiller et al., 1988; Thor & Low, 2011; Berg et al., 2019; McClymont et al., 2022). Conditions at these breeding sites and in foraging areas must have remained favourable during this period to facilitate nesting. However, the reconstructed LGM summer sea-ice edge was located beyond the modern foraging, so it has been proposed that coastal polynyas within the sea ice, or at ice-shelf fronts, must have provided suitable foraging habitat (Thatje et al., 2008; McClymont et al., 2022). Although these ice-free areas may have supported large population sizes during the LGM (Carrea et al., 2019), it is hypothesised that these populations were reproductively isolated, resulting in the evolution of two morphologically distinct subspecies of snow petrel (Jouventin & Viot, 1985; Henri & Schön, 2017; Carrea et al., 2019). During the review of breeding records, presence of the lesser (*P.n. nivea*) vs. greater snow petrel (*P.n. confuse/major*) was rarely distinguished, so their relative breeding distributions remain poorly quantified. A summary of the distribution of most known forms is given in Hobbs (2019), though that compilation omits known breeding of lesser snow petrels on Cockburn Island (Cowan, 1981).

Snow petrels respond to environmental factors operating both at breeding sites and in foraging areas, and, as high-trophic-level predators, their breeding and foraging success are potentially valuable indicators of ecosystem health (Croxall et al., 1988; Sydeman et al., 2012; González-Zevallos et al., 2013). Climate-driven changes in either breeding or foraging habitats could drive changes in the breeding distribution of this species. Most commonly, the effects of climate on seabirds are indirect and bottom-up, driven by spatial and temporal changes in prey distribution resulting from climate-driven changes in the pelagic environment (González-Zevallos et al., 2013). Seabird distributions in the future could be affected by decreases in prey availability in some regions, and increasing thermal suitability in others (Gonzalez et al., 2023). Snow petrel population size is hypothesised to be

negatively affected by a reduction in sea-ice extent (Jenouvrier et al., 2005). Winter sea ice is necessary to maintain Antarctic krill *Euphausia superba* abundance, and so its extent and duration affects food supply for snow petrels during the following breeding season (Loeb et al., 1997). Greater than average winter SIE thus improves the survival and breeding performance of snow petrels (Barbraud et al., 2000; Barbraud & Weimerskirch, 2001; Jenouvrier et al., 2005). Summer SIE also affects their breeding success, which is depressed if November SIE is lower, whilst fledgling body condition is higher when the November SIE is greater than average (Barbraud & Weimerskirch, 2001). Despite the surprising stability overall of Antarctic SIE over the past decades, recent years have experienced major declines and record minima in both winter and summer SIE, and the trend of more extreme lows is predicted to continue (Fogt et al., 2022; Raphael & Handcock, 2022). Dependence of snow petrels on the proximity of the MIZ suggests that with the projected southwards retreat of SIE, they will lose substantial areas of foraging habitat. The small snow petrel population size at their northern limit on South Georgia (~ 3000 breeding pairs) is suggested to result from limited sea ice nearby during the breeding season (Ainley et al., 1984). Regional variability in future sea-ice trends (Purich & Doddridge, 2023) may result in abandonment of breeding sites in some regions as foraging habitat becomes unsuitable, resulting in a southwards contraction of the breeding distribution.

By contrast, new exposed coastal breeding habitats may emerge as the climate warms. A high proportion (71%) of known breeding sites are located ≤ 10 km from the coast. As such, increased availability of ice-free rock may increase the options for snow petrels to expand in these areas, acknowledging that competition for this habitat with other seabirds may also increase.

Direct climate effects such as extreme weather can also have a significant impact on seabird distribution and breeding success at a local scale. Whilst nesting in crevices shelters snow petrels from much extreme weather, the timing and duration of local snow accumulation has a known influence on snow petrel breeding success (Croxall et al., 2002), affecting breeding probability (Chastel et al., 1993), hatching success (Olivier et al., 2005), and fledging probability (Sauser et al., 2021b) at breeding sites in Adélie Land and East Antarctica. Specifically, increased or prolonged snowfall can affect nest accessibility, and a simultaneous increase in local temperatures increases the risk of nest flooding (Chastel et al., 1993). Extreme storm activity (severe winds and high precipitation) in Dronning Maud Land during the 2021/2022 austral summer caused near complete breeding failure and mass mortality of snow petrels and conspecifics across multiple breeding sites extending

across more than 700 km (Descamps et al., 2023). Mass mortality events can have major lasting effects on seabirds which are long-lived and slow to reproduce (Mitchell et al., 2020), with the distribution of some (e.g., black-legged kittiwakes *Rissa tridactyla*) known to change as a result of poor breeding performance in particular areas (Boulinier et al., 2008). However, long-term demographic studies of snow petrels are spatially limited (Figure 6), with datasets only from the Pointe Géologie Archipelago (Adélie Land) and Reeve Hill at Casey Station (East Antarctica). Most long-term studies conclude intraspecific differences between sexes and neighbouring breeding sites in how snow petrels respond to local weather effects and larger scale climatic patterns (Sauser et al., 2021a). Therefore, longer term impacts of extreme breeding season weather, such as the recent storm activity in Dronning Maud Land, on the snow petrel breeding distribution remains uncertain. Investigating distributional shifts of breeding populations is a major target in seabird ecology (Grémillet & Boulinier, 2009), and by quantifying average climatic conditions at breeding sites, this provides important baseline data against which future distributional shifts can be assessed. This also highlights the need for more widespread long-term monitoring of snow petrel colonies, including at least population trends and breeding success, and ideally, long-term demographic studies. In addition, tracking studies and the development of species distribution models of habitat suitability in foraging areas would help in predicting the future distribution of snow petrels in relation to climate-driven change.

CHAPTER 4: Can snow petrels be detected from space?

The focus of this chapter is to investigate the final aim and research objective: testing whether known snow petrel breeding sites can be sensed remotely in satellite imagery with different spatial and spectral resolutions. Remote sensing is developing as an effective method for spatio-temporal monitoring of the Antarctic ecosystem, and to date has been successfully used to identify and quantify populations of adélie, emperor and chinstrap penguins, plus Antarctic petrels (Schwaller et al., 1989; Fretwell & Trathan, 2009; Fretwell et al., 2015; Schwaller et al., 2018; Román et al., 2022). However, the technique has not yet been tested on cavity-nesting species. Therefore, this chapter presents a first attempt at utilising satellite imagery to detect snow petrel nesting sites.

4.1 Methods

4.1.1 Selecting areas of interest

Two study sites were selected as areas of interest for investigating the spectral signature of snow petrel breeding sites: Svarthamaren (Dronning Maud Land), and Mount Henderson (Framnes Mountains, inland Prince Charles Mountains). These sites both have large known populations of snow petrels, thus maximising the likelihood of identifying any possible spectral signature. It is estimated that several 1000 pairs of snow petrels breed on Svarthamaren (Ewan Wakefield, pers. com.), and many snow petrel stomach-oil deposits (Antarctic mumiyo) occur there (Mehlum et al., 1988; ANTSIE, Durham University, unpub. data). A regional survey of snow petrels at Mount Henderson recorded 2750 active snow petrel nests, with a nest density of 11.9 nests per ha (Olivier & Wotherspoon, 2008). As the spectral signature of guano is the basis of detecting other Antarctic seabird colonies (Fretwell et al., 2015; Schwaller et al., 2018), high elevation and inland breeding sites with higher numbers of breeding pairs where any guano and deposits will be preserved throughout the breeding season were favoured for this analysis. Furthermore, no other seabirds (such as Antarctic petrels) nest sympatrically with snow petrels within the Mount Henderson range, reducing the chance of detecting non-snow petrel guano (errors of commission) (Schwaller et al., 2018). At Svarthamaren, around 50,000 Antarctic petrels nest sympatrically with the snow petrels, thus allowing comparison of the results between these sites.

4.1.2 Selecting satellite imagery

Initial exploration and analysis of each site was conducted in freely available Landsat 8 OLI, Landsat 9, and Sentinel 2 imagery (Table 2), accessed from USGS Earth Explorer and Copernicus (United States Geological Survey, https://earthexplorer.usgs.gov; Copernicus Climate Data Store, https://cds.climate.copernicus.eu). Both Landsat 8 OLI and Landsat 9 imagery were sourced from Landsat collection 2 level 2, providing accurate calibrated surface reflectance data.

Table 2: Spectral band wavelength ranges (nm) of Landsat and Sentinel imagery. Sentinel 2 has 3 red edge bands.

Spectral region	Landsat 8 OLI	Landsat 9	Sentinel 2
Coastal blue	435 – 451	433 – 453	-
Blue	452 – 512	450 – 515	458 – 523
Green	533 – 590	525 – 600	543 – 578
Red	636 – 673	630 – 680	650 – 680
Red edge	-	-	698-713; 733-748; 773-793
NIR	851 – 879	885 – 865	785 – 899
NIR narrow	-	-	855 – 875
SWIR 1	1566 – 1651	1560 – 1660	1565 – 1655
SWIR 2	2107 – 2294	2100 – 2300	2100 – 2280

Multiple criteria were imposed for the selection of suitable satellite imagery. Firstly, images were only considered from austral summer months November – February, aligning with the core breeding period and therefore capturing the time of definite nest occupation. Secondly, an additional criteria of cloud cover < 20 % was set to maximise the visual quality of the imagery used. For image clarity and minimal shadow, lower sun elevation angles were preferred (e.g., < 27 °, Fretwell et al., 2011). However, this was not a specific criteria; due to a lack of available imagery it could not be distinguished when shadow became a problem.

A single scene from each satellite that fit the criteria was then downloaded for each test site, resulting in the use of 6 freely available satellite images (Table 3).

Table 3: Image details of Landsat 8 OLI, Landsat 9, and Sentinel 2 products used for analysis.

Site name	Satellite	Image path and row	Image date	Cloud cover (%)	Sun elevation angle (°)	Scene ID	Spatial resolution
Svarthamaren	Landsat 8 OLI	168 111	26/12/2022	0.00	33.01	LC81681112022360LGN00	30 m
	Landsat 9	168 111	04/02/2023	0.00	25.30	LC91681112023035LGN01	30 m
	Sentinel 2		16/01/2023	0.82			20 m
Mount Henderson	Landsat 8 OLI	135 108	21/ 02/2023	0.01	23.53	LC81351082023052LGN00	30 m
	Landsat 9	135 108	13/02/2023	0.27	26.13	LC91351082023044LGN01	30 m
	Sentinel 2		14/02/2022	1.95			20 m

After exploring freely satellite imagery, a very high resolution 8-band multispectral Worldview 3 image of each study site was selected to investigate whether higher spatial and spectral resolution imagery increased the detection of snow petrel breeding sites (Table 4; Table 5). The images were similarly selected based on timing, low cloud cover, and low sun elevation angle. 8-band short wave infrared [SWIR] Worldview 3 imagery was available and downloaded for Mount Henderson, but was not available for Svarthamaren.

Table 4: Spectral band wavelength ranges (nm) of Worldview 3 imagery.

Spectral region	Worldview 3	Spectral region	Worldview 3
Coastal blue	400 – 450	SWIR 1	1195 – 1225
Blue	450 – 510	SWIR 2	1550 – 1590
Green	510 – 580	SWIR 3	1640 – 1680
Yellow	585 – 625	SWIR 4	1710 – 1750
Red	630 – 690	SWIR 5	2145 – 2185
Red edge	705 – 745	SWIR 6	2185 – 2225
NIR 1	770 – 895	SWIR 7	2235 – 2285
NIR 2	860 – 1040	SWIR 8	2295 – 2365

Table 5: Image details of Worldview 3 products used for analysis.

Site name	Satellite	Bands available	Image date	Cloud cover (%)	Spatial resolution
Svarthamaren	Worldview 3	8-band multispectral	31/12/2018	0.00	1.3 m
Mount Henderson	Worldview 3	8-band multispectral	27/11/2022	0.00	1.3 m
		8-band SWIR	27/11/2022	0.00	1.3 m

4.1.3 Pre-processing

For the medium resolution Landsat 8/9 and Sentinel 2 imagery, pre-processing was conducted using the Semi-Automatic Classification Plugin (QGIS). Firstly, the multiband rasters were split into individual bands, which were then clipped to the study area. All bands from each image were then atmospherically corrected to convert raw digital numbers [DN] (pixel values) to top-of-atmosphere reflectance. This step (radiometric calibration) corrects for varying illumination and is essential for allowing multiple images from different sensors and areas to be compared (Kuester, 2016). Because of the low atmospheric temperatures and minimum aerosol levels in Antarctica, top-of-atmosphere reflectance values do not need to be converted to bottom-of-atmosphere reflectance, so the results of the conversion were used for subsequent image enhancement (Bindschadler et al., 2008).

Pre-processing followed similar steps for the very high resolution Worldview 3 imagery. For both of the study sites, there were several individual multiband rasters. These multiband rasters were merged to create a single scene, and then split into individual bands. Next, radiometric calibration of the individual bands was calculated using equation 1,

$$L = GAIN * DN * \left(\frac{abscalfactor}{effectivebandwidth}\right) + OFFSET \qquad (1)$$

where *L* is the top-of-atmosphere reflectance ($W\mu m^{-1}\ m^{-2}\ sr^{-1}$), *Gain* and *Offset* are band specific absolute radiometric calibration adjustment factors for Worldview 3 given by DigitalGlobe, *abscalfactor* and *effectivebandwith* are numbers provided for each band in the metadata file, and *DN* is the pixel value of the imagery (Kuester, 2016).

Following pre-processing, digital image processing is typically conducted through image enhancement, and then classification (Phiri & Morgenroth, 2017). For this analysis, multiple approaches for image processing were undertaken to visually investigate the spectral characteristics of each site.

4.1.4 Image enhancement

Image enhancement began by constructing true-colour red-green-blue [RGB] composites of each Landsat, Sentinel and Worldview image. Lab based tests of adélie penguin guano demonstrate distinctly high reflectance in the short-wave infrared [SWIR] when compared to other bands, a spectral signature which has been successfully used to identify known and unknown Antarctic seabird colonies (Fretwell et al., 2015). Specifically, maximum reflectance occurs at wavelengths between 1100 – 1300 nm with a secondary peak at 1650 nm, and absorption is greatest below 500 nm and above 2400 nm (Figure 5). Though the spectral signature of snow petrel guano is currently unknown, the predominant dietary components of adélie penguins and snow petrels are the same: fish and krill. Therefore, it is likely that snow petrel guano reflects and absorbs solar irradiance at similar wavelengths, and the profile of adélie penguin guano (Figure 5) was used as a guide for this analysis.

False-colour composites [FCCs] assign bands outside of the visible spectrum (such as SWIR) to either the red, green, or blue bands, and the use of FCCs is a common technique for land mapping to enhance differences in land cover, lithology, minerology etc (e.g., Mars, 2018). Based on Figure 5, FCCs including SWIR bands were more likely to enhance and discriminate any spectral signature of snow petrel guano at the study sites than true-colour composites alone. Different FCCs were used for the different satellite images, but all included bands with high guano reflectance (SWIR) and low guano reflectance (blue/coastal). In the Landsat 8/9 images, a FCC of bands 2-7-6 (blue, SWIR2, SWIR1) was constructed. Similarly, in the Sentinel images, a FCC of 12-11-1 (SWIR2, SWIR1, coastal blue) was used. The wavelengths of SWIR bands in Worldview 3 more closely cover the peaks in reflectance of guano than do the SWIR bands of Landsat 8/9 and Sentinel 2, and with the SWIR bands available for Mount Henderson, a FCC of 2-9-12 (blue, SWIR1, SWIR4) was constructed.

Band ratioing is another effective way to enhance spectral differences between bands, as it increases the difference in reflectance (brightness) between target and neighbouring phenomena (Jahanbani et al., 2022). Band ratioing also normalises the effect of factors such as: surface slope, aspect, and changing illumination (Fretwell et al., 2015).

To investigate ways to discriminate any snow petrel guano signature at the test sites, a customised normalised difference spectral index ratio for guano was tested in the Landsat 8/9 imagery. Based on the normalised difference indexes for vegetation, water, and snow [NDVI, NDWI, NDSI, respectively], customised spectral index ratios have been

demonstrated to improve the interpretation and extraction of land cover information in Antarctica by discriminating the target class from the rest of the image (Jawak & Luis, 2013). The NDVI exploits the difference between the near infrared and red bands, in which vegetation reflectance is highest and lowest respectively. To emulate this, Landsat bands 6 (SWIR1) and band 1 (coastal blue) in which guano reflectance is highest and lowest, respectively, were determined to be the most useful for this ratio. The spectral index ratio was then calculated using equation 2,

$$spectral\ index\ ratio\ for\ guano = \frac{(SWIR\ 1 - Coastal\ Blue)}{(SWIR\ 1 + Coastal\ Blue)} \qquad (2)$$

This was also tested in the Worldview 3 imagery, using the respective SWIR 1 and coastal blue bands.

Utilising the higher spectral resolution of Worldview 3, a second band ratio was tested to try and discriminate guano in the study areas. This followed the band ratio technique in Jahanbani et al. (2022), using the two bands with most reflection and the band with the most absorption in equation 3,

$$band\ ratio\ for\ guano = \frac{SWIR\ 1 + SWIR\ 4}{Coastal\ Blue} \qquad (3)$$

4.1.5 Unsupervised classification

Classification is a key stage in image processing and can either be supervised or unsupervised. In this analysis, where areas of snow petrel guano were unknown, and the objective was to test whether or not snow petrel guano can be detected in satellite imagery, unsupervised classification was conducted to segment the study areas into regions with similar spectral attributes without the input of training data. Unsupervised classification was conducted through the *k*-means clustering algorithm, a widely used, iterative classification that generates a user-determined number of classes by dividing the data into the specified number of classes (*k*), finding the mean of each class, and assigning each pixel to the closest mean to create the output classes (Lloyd, 1982).

K-means clustering was conducted on the Worldview 3 satellite imagery for Svarthamaren and Mount Henderson as the highest spatial resolution images available. For Svarthamaren, where SWIR bands were not available (highest guano reflectance), the true-colour RGB was used as the input band set in the Semi-Automatic Classification Plugin. Instead, for Mount Henderson, the 2-9-12 FCC which enhances the bands with highest reflectance of guano was used as the input band set. Initially, for both sites, the default number of iterations was set to 10, the seed signatures that start the iteration were set to be random, and minimum

distance set as the algorithm for calculating spectral distance. Three versions of the classification were run for each site, with 10, 20, and 50 classes respectively. Based on field knowledge of snow petrels at Svarthamaren (Mehlum et al., 1988) and coordinate locations of mumiyo deposits (ANTSIE, Durham University, unpub. data), a second round of *k*-means classifications with 10, 20, and 50 classes were run on the NE corner of the nunatak.

To remove noise and enhance the classification output, sieving was carried out as a post-processing step on the output of each *k*-means classification (Bakr & Afifi, 2019).

4.2 Results

4.2.1 Medium resolution imagery

At Svarthamaren, little difference can be seen between the results of FCCs and band ratioing in Landsat 8 OLI imagery and Landsat 9 imagery (Figure 13a – f). In the false-colour composites, the NE side of the nunatak (blue) is distinguished from the rest of the exposed bedrock (light blue) and snow/ice (red) (Figure 13c, 13d), and this region corresponds to pixels values close to 0 (white) in the spectral index ratio results (Figure 13e, 13f).

Despite slightly higher spatial resolution in the Sentinel 2 imagery (20 m, compared to 30 m for Landsat; Table 2), the true-colour composite shows much less detail than in Landsat 8 and 9 (Figure 13g). However, the false-colour composite similarly distinguishes areas on the NE side of the nunatak (green) from the rest of the bedrock (yellow) and snow/ice (dark blue).

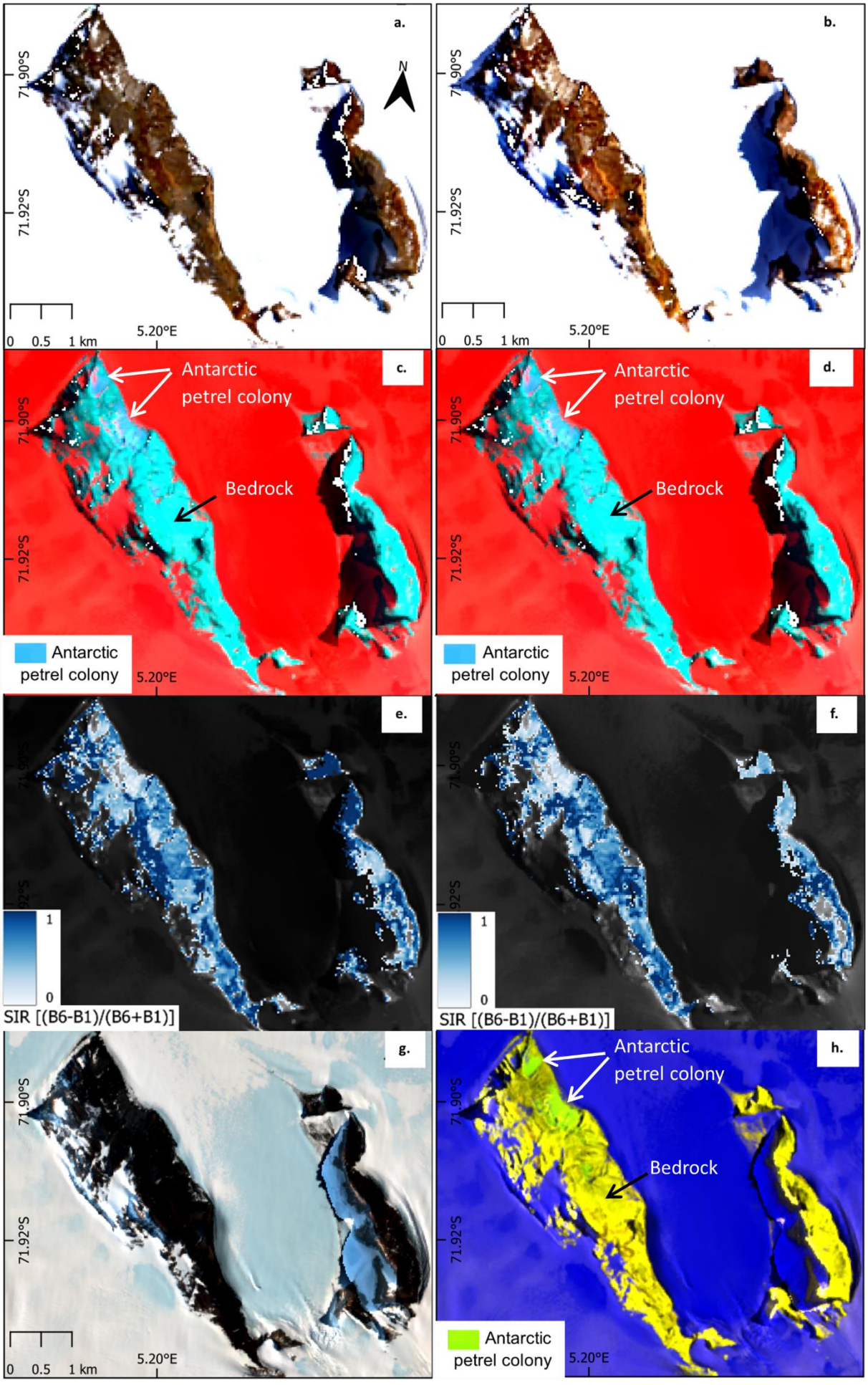
a.
b.
c.
d.
e.
f.
g.
h.
71.90°S
71.92°S
5.20°E
0 0.5 1 km
N
Antarctic
petrel colony
Bedrock
1
0
SIR [(B6-B1)/(B6+B1)]

Figure 13. Inspection of Svarthamaren, Dronning Maud Land. **(a)** RGB in Landsat 8 OLI, **(b)** RGB in Landsat 9. **(c)** False-colour composite (band 2 = red, band 7 = green, band 6 = blue) in Landsat 8 OLI, **(d)** false-colour composite (band 2 = red, band 7 = green, band 6 = blue) in Landsat 9. **(e)** spectral index ratio emulating NDVI using band 6 (maximum guano reflectance) to band 1 (minimum guano reflectance) in Landsat 8 OLI, **(f)** spectral index ratio emulating NDVI in Landsat 9. **(g)** RGB in Sentinel 2B, **(h)** false-colour composite (band 12 = red, band 11 = green, band 2 = blue) in Sentinel 2B.

At Mount Henderson, Landsat 9 imagery similarly does not provide any more detail than Landsat 8 (Figure 14a-f). In the false-colour composites, shadow obscures the western sides of the exposed rock, and no areas of the nunatak are distinguished by the same blue colour as the NE side of Svarthamaren (Figure 14c, 14d). In the spectral index ratios, the pixels with the highest values (white) and therefore most reflective in SWIR are located differently between Landsat 8 and Landsat 9, with little overlap between the two results. In the false-colour composite from Sentinel 2, no detail on the bedrock apart from shadow is visible (Figure 14h).

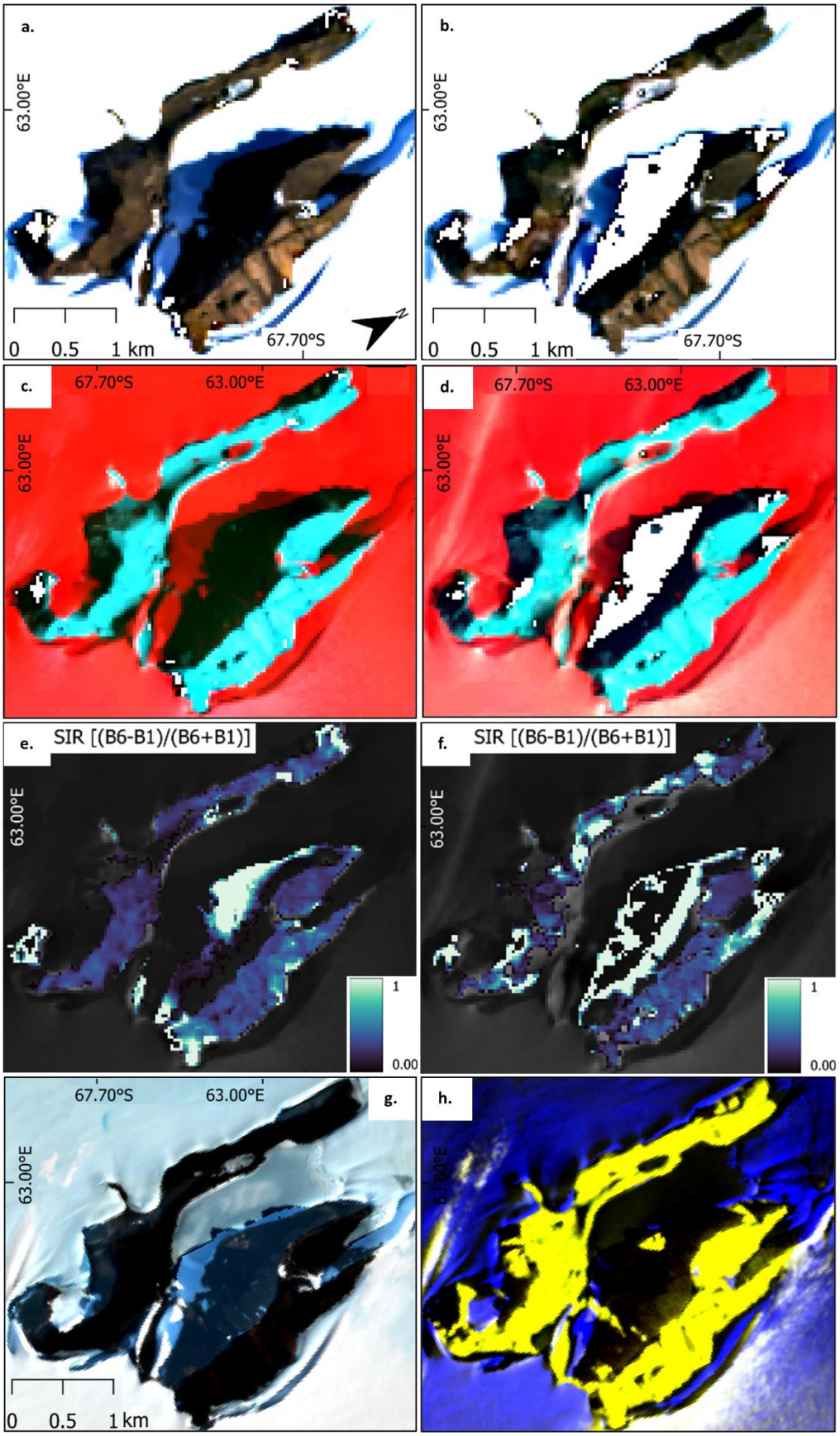

Figure 14. Inspection of Mount Henderson, coastal Prince Charles Mountains. **(a)** RGB in Landsat 8 OLI, **(b)** RGB in Landsat 9. **(c)** False-colour composite (band 2 = red, band 7 = green, band 6 = blue) in Landsat 8 OLI, **(d)** false-colour composite (band 2 = red, band 7 = green, band 6 = blue) in Landsat 9. **(e)** spectral index ratio emulating NDVI using band 6 (maximum guano reflectance) to band 1 (minimum guano reflectance) in Landsat 8 OLI, **(f)** spectral index ratio emulating NDVI in Landsat 9. **(g)** RGB in Sentinel 2B, **(h)** false-colour composite (band 12 = red, band 11 = green, band 2 = blue) in Sentinel 2B.

4.2.2 Very high resolution imagery

At Svarthamaren, without SWIR bands, visual contrasts on the nunatak are clearer in the band 7-3-2 false-colour composite than in the true-colour composite (Figure 15a, 15b). The higher spatial resolution (1.3 m) provides much clearer surface details, demonstrating the varying topography at each location of stomach oil deposit samples.

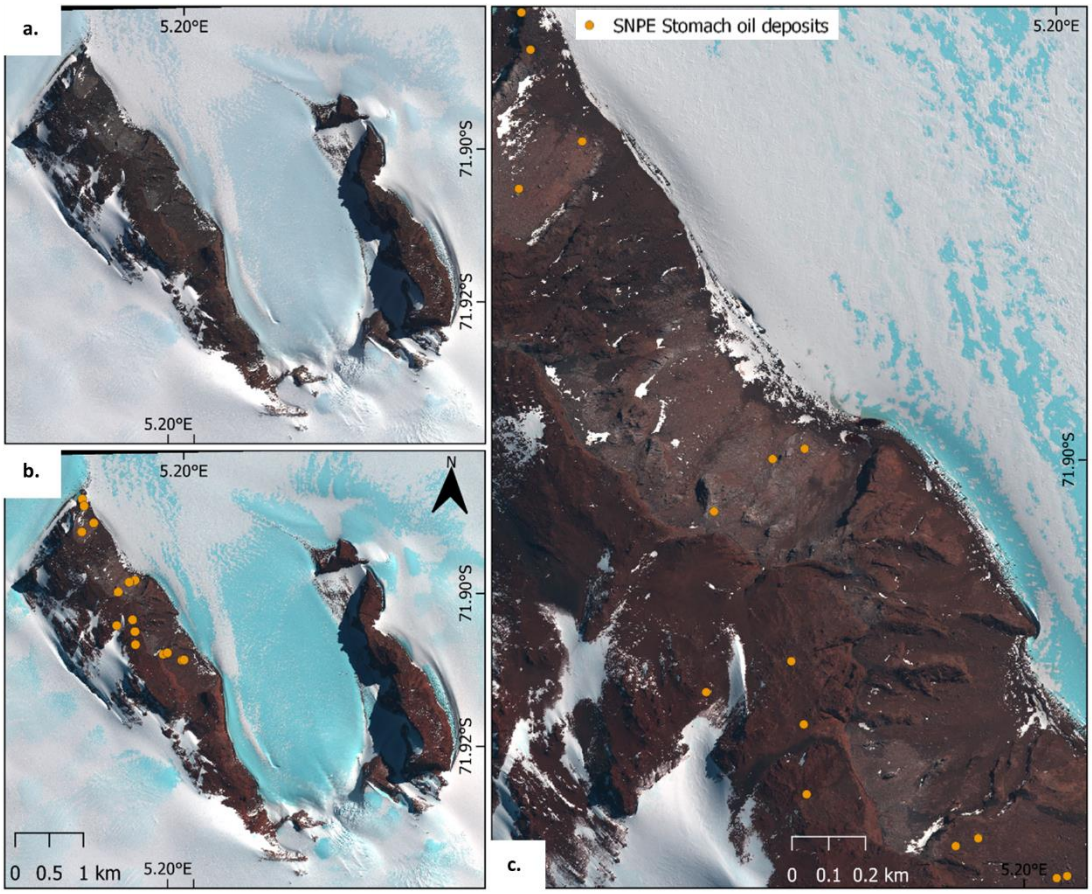

Figure 15. (a) RGB composite of Svarthamaren in Worldview 3 imagery, **(b)** false-colour composite (NIR 1 = red, blue = blue, green = green), and **(c)** close up of the NE side of Svarthamaren in false-colour composite. Snow petrel (SNPE) stomach oil deposits sourced from ANTSIE, Durham University unpub. data.

The Worldview 3 imagery for Mount Henderson provides better spatial and spectral resolution than both Landsat and Sentinel (Figure 16). Visually, the false-colour composite (2-9-12) is more informative than the true-colour image in distinguishing areas more reflective in SWIR where, for example, adélie penguin guano is known to be most reflective (Fretwell et al., 2015). The NE slope of the nunatak marked by the arrow, appears differently to the rest of the exposed bedrock (dark blue), ice/snow (red, orange, and white), and shadow (black) (Figure 16b). This area corresponds to high reflectance in band 1 of the SWIR (Figure 16c), but in the true-colour image looks similar to snow (Figure 16a).

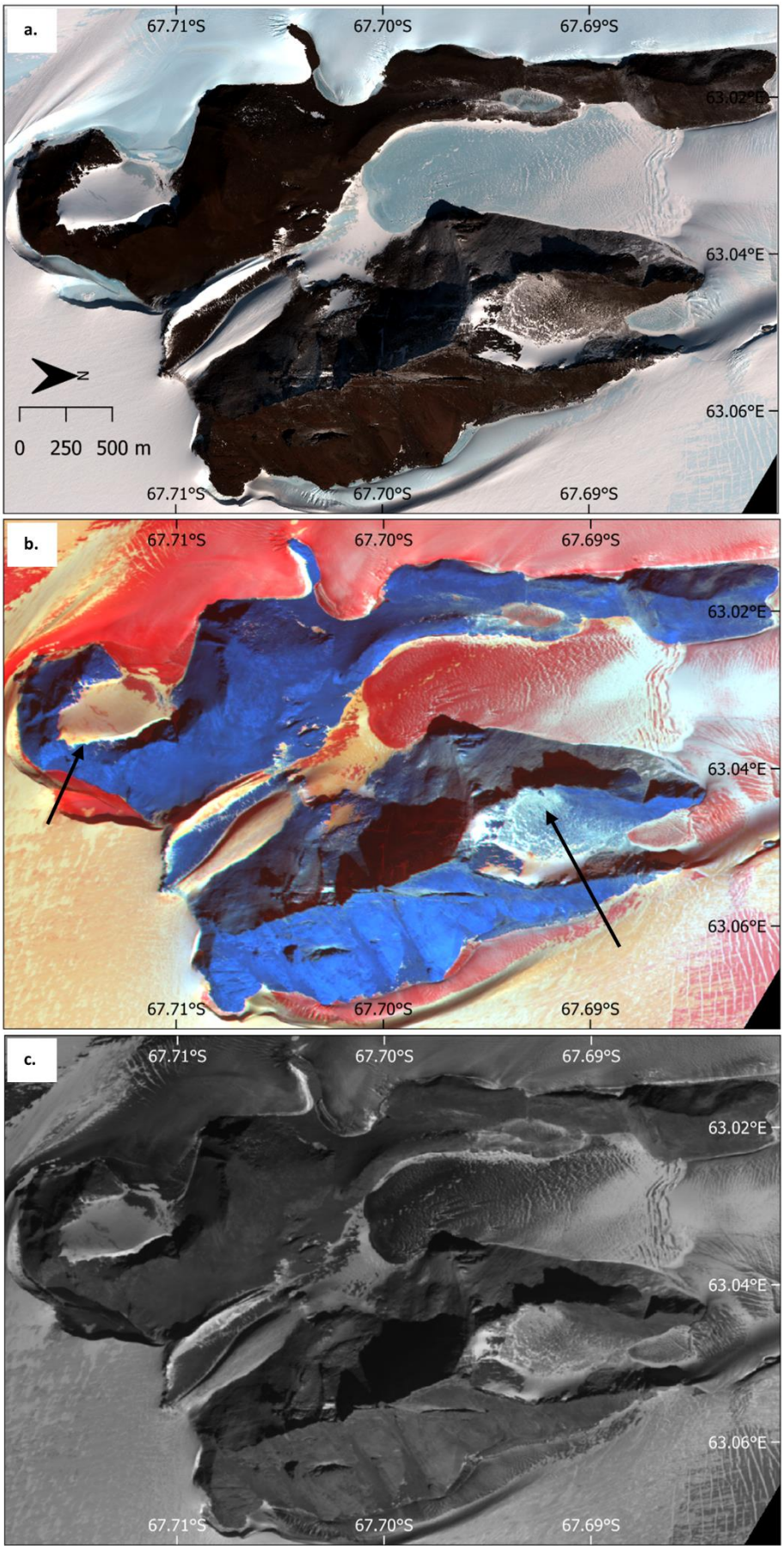

Figure 16. (a) RGB composite of Mount Henderson in Worldview 3 imagery, **(b)** false-colour composite (blue = red, SWIR 1 = green, SWIR 4 = blue), and **(c)** SWIR band 1 (wavelengths 1195 to 1225 nm).

The results of both the spectral index ratio and band ratios (Figure 17a, 17b) show the pixels with the highest values on Mount Henderson located both individually and in clusters. The main clusters are located on the NE facing slope of the nunatak (67°69'6"S 63°05'E), as well as at the base of multiple slopes at the boundary between ice/snow and bedrock (e.g., 67°71'S 63°04'E) (Figure 17c).

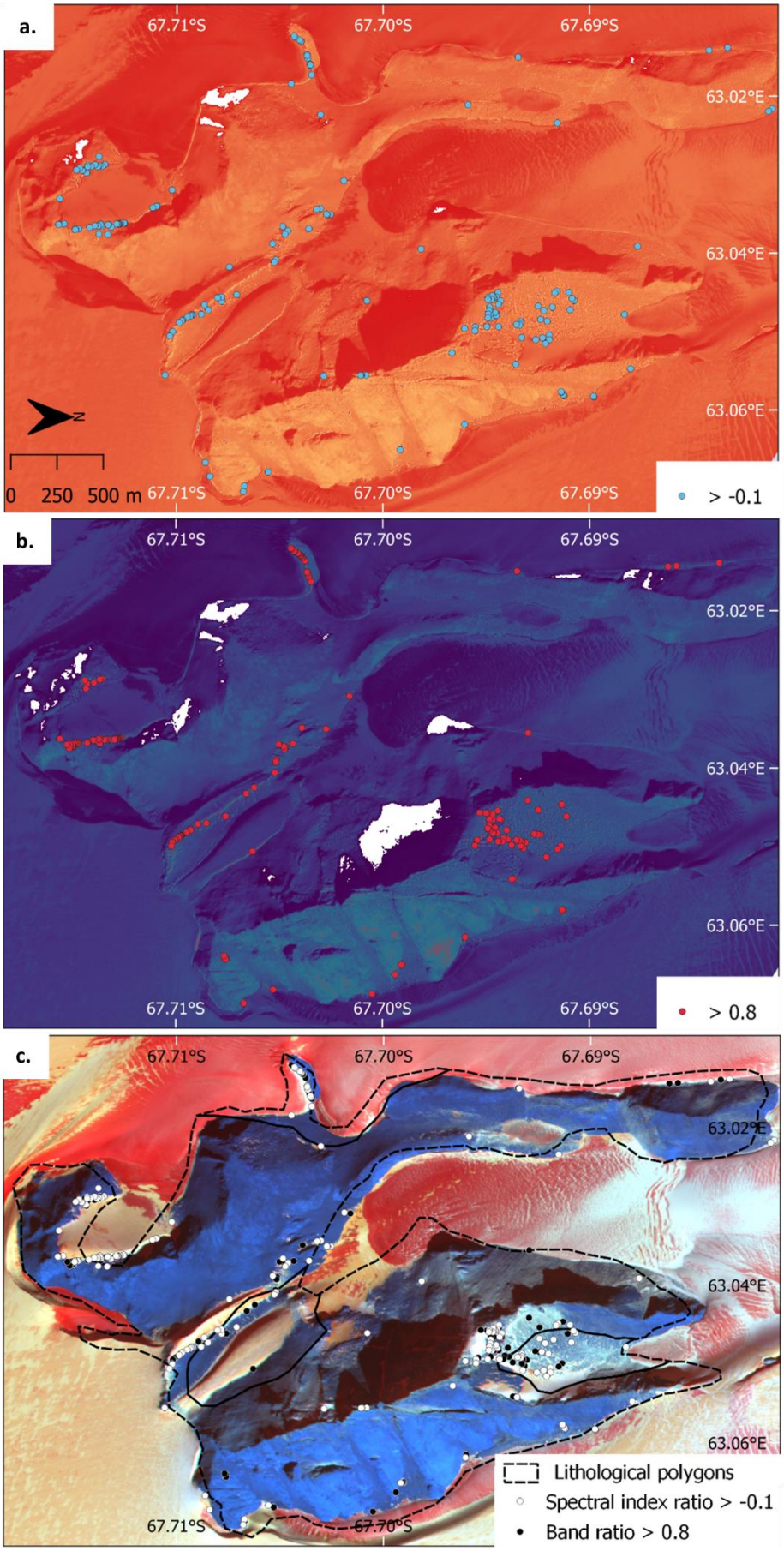

Figure 17. (a) Product of equation 1 (spectral index ratio for guano). Highest pixel values shown by blue points for clarity. **(b)** Product of equation 2 (band ratio for guano). Highest pixel values shown by red points for clarity. **(c)** Highest values pixels from (a) and (b) overlain on the 2-9-12 FCC. The outlines of lithological polygons from the SCAR GeoMAP (Cox et al., 2023a) are also displayed in black to show that the high pixel values do not appear to relate to a change in lithology. Solid black line outlines unconsolidated sediment. Dashed black line outlines igneous intrusive bedrock.

4.2.3 Unsupervised classification

Unsupervised *k*-means classification of Svarthamaren does not massively improve when the number of classes specified (*k*) in the algorithm is increased. When *k* = 10, 7 classes represent ice/snow in the image, and when *k* = 50, 45 classes represent ice/snow (Figure 18a, 18b). Neither classification clearly classifies the structural lithology known from the SCAR GeoMAP (Cox et al., 2023a) (Figure 18c). In figure 18b, stomach oil deposits are located on classes 1 and 3, and in figure 18a, they locate on all 5 classes. At this scale, unsupervised classification does not identify a single class which could relate to stomach oil deposit (and therefore known potential nesting sites) locations.

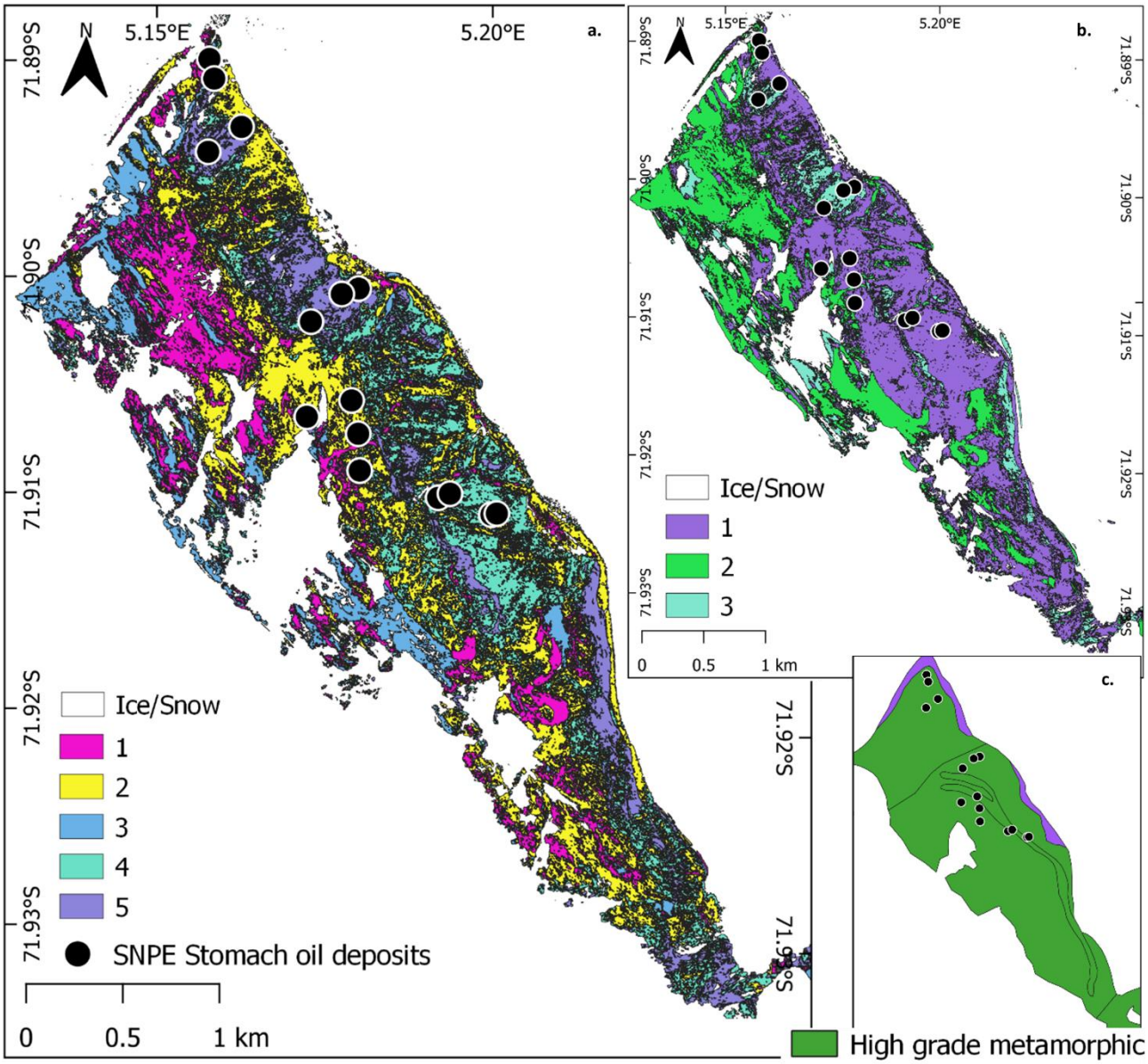

Figure 18. (a) *K*-means classification of Svarthamaren with 50 classes. 45 classes were merged into Ice/Snow. **(b)** *K*-means classification of Svarthamaren with 10 classes. 7 classes were merged into Ice/Snow. **(c)** Lithological polygons of Svarthamaren from SCAR GeoMAP (Cox et al., 2023a).

As observational records report snow petrels to be nesting in the NE corner of Svarthamaren (Mehlum et al., 1988), unsupervised classification was also tested here at a smaller scale (Figure 19). This test of known nesting (and stomach oil deposit) sites similarly does not indicate a clear landcover pattern where stomach oil deposits are located. In each version of the classification, no single class is associated with the location of stomach oil deposits. For example, when the algorithm was run with 20 classes (Figure 19b), the deposits were located on classes 1, 2, 3 and 4, all of which also appear elsewhere in the classification and thus cannot relate specifically to a deposit signal.

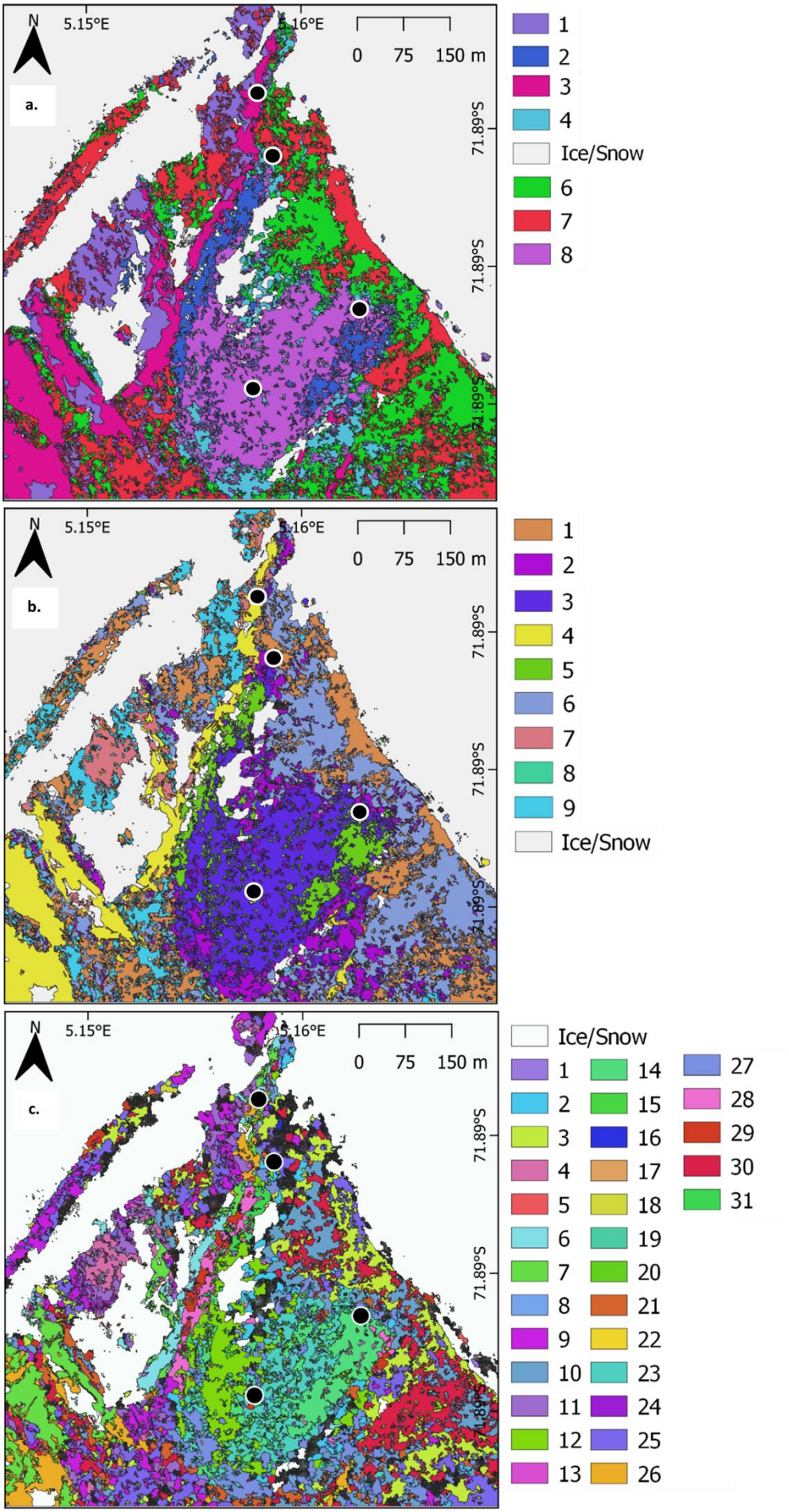

Figure 19. (a) *K*-means classification of the NE corner of Svarthamaren with 10 classes. 3 classes were merged into Ice/Snow. **(b)** *K*-means classification with 20 classes. 11 classes were merged into Ice/Snow. **(c)** *K*-means classification with 50 classes. 19 classes were merged into Ice/Snow.

At Mount Henderson, when *k*-means was run with 50 classes, only 24 represented exposed bedrock, but classified a lot of detail (Figure 20a). Without ground truth data, these classes cannot be merged into specific known landcover classes. However, overlaying the pixels with highest values from the outputs of spectral index ratio and band ratioing, demonstrates that these pixels are not represented by a single class (Figure 20b).

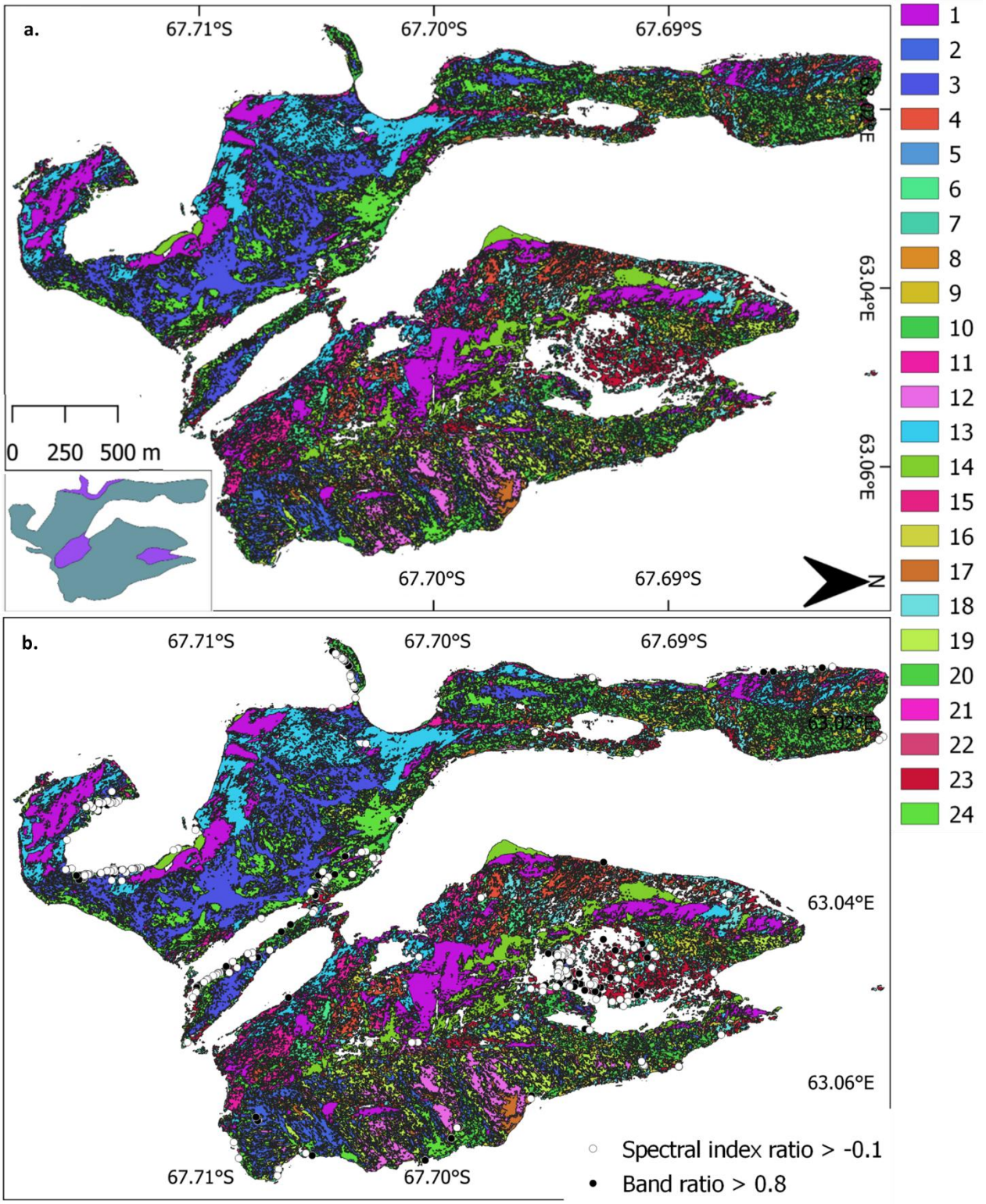

Figure 20. (a) *K*-means classification of Mount Henderson with 50 classes. 26 classes were merged into Ice/Snow. Inset shows lithological polygons for Mount Henderson from Cox et al. (2023), with intrusive igneous in blue, and unconsolidated sediment in purple. **(b)** Same classification, overlain by highest value pixels from the outputs of spectral index ratio and band ratioing in Figure 17.

4.3 Discussion

4.3.1 Can known breeding sites be detected from space?

Remote sensing analysis of the spectral signature from known snow petrel nesting sites is limited without the availability of ground truthing data. Ground truthed data are essential to verify and reduce uncertainty in identifying the location of Antarctic seabird colonies and typically, for the remote sensing of seabirds, knowledge of the spectral signature, specific coordinates, and size of local populations are used as ground truth data (Fretwell et al., 2012; Schwaller et al., 2013; Fretwell et al., 2015). Though approximate population sizes for snow petrels at Svarthamaren and Mount Henderson are known (Mehlum et al., 1988; Olivier & Wotherspoon, 2008), snow petrels are loosely colonial, nesting in cavities at densities partly controlled by nunatak structure (Ryan & Watkins, 1989; Hodum, 1999; Olivier & Wotherspoon, 2006). Therefore, whilst high-density surface nesting colonial seabirds can be clearly identified in satellite imagery by large areas of guano (Schwaller et al., 1989; Fretwell & Trathan, 2009; Fretwell et al., 2012; Schwaller et al., 2018), snow petrel deposits are likely to be less clustered or extensive. As such, knowledge of active nest coordinates and the spectral profile of snow petrel guano and stomach-oil deposits is critical to ground truth remote sensing of these sites.

The results from this analysis demonstrate that the spatial and spectral resolution of Landsat 8 OLI, Landsat 9, and Sentinel 2 imagery is too coarse to detect any possible signs of snow petrel nesting (Figures 13, 14). Whilst 30 m / 20 m pixels are sufficient to detect all but the smallest colonies of surface nesting birds (Schwaller et al., 2013; Fretwell et al., 2015), image enhancement of Landsat and Sentinel imagery at Svarthamaren and Mount Henderson does not specifically identify any areas where snow petrels could be nesting. At Svarthamaren, the false-colour composites in both Landsat and Sentinel distinguish NE facing parts of the nunatak from the rest of the exposed bedrock (Figure 13). This is likely to be the large Antarctic petrel colony (~50,000 breeding pairs; Descamps et al., 2023) that has been identified by both field observations (Mehlum et al., 1988; Descamps et al., 2023) and remote sensing (Schwaller et al., 2018). Snow petrels are reported to nest most densely in the NE corner of the nunatak, where Antarctic petrels are fewer (Mehlum et al., 1988; Ewan Wakefield, pers. com.), but any spectral signature of these snow petrels cannot be distinguished from the spectral signature of the Antarctic petrels at this spatial and spectral resolution. Furthermore, the absence of this same signature on Mount Henderson (where Antarctic petrels do not nest; Figure 14), suggests that if snow petrel guano has similar

reflective properties to Antarctic petrel guano (resulting from similar diet), it cannot be identified in the spatial and spectral resolution of medium resolution satellite imagery.

As well as showing much greater surface detail of both sites than either the Landsat or Sentinel imagery (Figures 15, 16), image enhancement using the SWIR bands of Worldview imagery may indicate areas of Mount Henderson on which snow petrels are nesting. The false-colour composite in Figure 16b distinguishes a north facing slope with uneven terrain from the rest of the exposed bedrock on Mount Henderson. Similarly, many of the highest value pixels from the results of the spectral index ratio and band ratio (designed to highlight pixels with the similar reflectance to adélie penguin guano; Fretwell et al., 2015) overlap with this area (Figure 17). Therefore, assuming the signature of snow petrel guano is similar to that of adélie penguin guano (Figure 5), snow petrels may be nesting on this northern slope of Mount Henderson. At Svarthamaren, where Worldview SWIR bands were not available, it is difficult to determine where snow petrels could be nesting from the Worldview imagery available. Therefore, high spectral resolution in the SWIR is likely to be necessary for any possible detection of snow petrel nests.

No ground truth data are available for Mount Henderson. Survey data recorded 2750 active nests with a nest density of 11.9 nests per ha, but do not provide any specific coordinates or descriptions of their location or aspect (Olivier & Wotherspoon, 2008). To hypothesise that snow petrels are nesting on the north facing slope of Mount Henderson (described above) without ground truth data, it is important to rule out any other ground cover or surface materials that may result in high reflectance in SWIR. This area is clearly distinguished from snow and ice (red/orange in Figure 17c). Similarly, it is not a distinct lithological polygon (Figure 17c), thus the high value pixels probably do not reflect a variation in minerology. However, these pixels are typically close to lithological boundaries, where cavities might be more likely to occur. At this distance inland (approximately 13km; Appendix A), vegetation is likely to be sparse to non-existent, with possibly only a few lichens present. The high value pixels are thus unlikely to be vegetation, which furthermore is typically most reflective in the near-infrared region (Fretwell et al., 2011). Although spectral profiles of Antarctic soil moisture are different to that of adélie penguin guano, soil moisture reflectance is generally high in SWIR (Levy et al., 2014). Whilst this could be an alternative explanation for pixels with high reflectance from the spectral image and band ratio results (Figure 17b), it should also be considered that the formation of ornithogenic soils, derived from concentrations of guano, carcasses, feathers and eggshells, and enriched in specific nutrients, has been associated with snow petrel nests at inland nunataks (Cocks et al., 1999). Therefore, if this

high-SWIR reflectance area is instead identifying soil moisture, it does not mean this is not part of the spectral signature of snow petrel nesting sites. Based on these results, it is justifiable to hypothesise that snow petrels are nesting on the north facing slope of Mount Henderson that is highlighted by multiple image enhancement techniques, but evidently, ground truth data are needed to be able to confirm this.

The results of unsupervised classification are also difficult to interpret without ground truth data, which would allow classes to be merged into known ground covers other than ice/snow versus bedrock. With plenty of freedom, and when targeted to an area of known stomach-oil deposits and snow petrel nesting on Svarthamaren (Figure 19), the deposits all appear on different classes. Similarly, on Mount Henderson, the highest value pixels from the spectral image ratio and band ratio results are associated with multiple classes (Figure 20). Therefore, despite being a commonly used technique for landcover classification, with the input information available and lack of ground truth data, unsupervised classification does not work to identify any possible nest sites in areas of known snow petrel nesting.

CHAPTER 5

5.1 Discussion

The purpose of the following discussion is to discuss the findings from all previous chapters, and how knowledge of the breeding distribution and breeding habitat use of snow petrels has, and can still be, improved.

5.1.1 Knowledge of breeding sites and populations

Through quantifying the global breeding distribution of snow petrels from field observations and surveys, it is clear that understanding of the breeding distribution could be improved with more consistent, standardised data collection at breeding sites themselves. Firstly, knowledge of approximately 70% of known breeding sites rely on data collected before the year 2000, which have not been revisited to provide more updated information about either the breeding site or the breeding population (Appendix A). Similarly, only 28% of breeding sites have been recorded from surveys (e.g., Convey et al., 1999; Barbraud et al., 2000; Olivier & Wotherspoon, 2008; Pande et al., 2020), about 75% of which have been conducted since 2000 (Appendix A). Therefore, whilst targeted surveys of snow petrel populations provide better quantitative descriptions of local breeding habitat and local populations, the majority of breeding site information is over 20 years old, and does not contain the same level of detail as more recent survey records do. Furthermore, only 222 breeding sites have population estimates, 67% of which were recorded before 2000. Therefore, there is huge uncertainty about total and regional population sizes. For wildlife conservation and management, accurate breeding population estimates are critical. For the snow petrel in particular, which is regarded as an ecological indicator for the Southern Ocean, it is vital to acquire and monitor total and regional population sizes to understand the species' response to climate change (Grémillet & Boulinier, 2009; González-Zevallos et al., 2013; Petry et al., 2016; Pande & Sivakumar, 2022; Gonzalez et al., 2023). Whilst we now have a better picture of where snow petrels breed (Figure 6), the discrepancy in descriptive and quantitative data recorded between different breeding sites illustrates that more accurate information, particularly regarding breeding population estimates, is very important for improving the understanding of the global breeding distribution.

A similar issue arises from the spatial resolution at which data are recorded. As a loosely-colonial cavity-nesting species, defining the spatial extent of a snow petrel colony is difficult. Using breeding sites instead of colonies (defined in Chapter 3) to describe the global

breeding distribution avoids the need to define the extent of a colony, but some issues still remain. Although all breeding sites in Appendix A have an associated coordinate location, for localities such as Mount Henderson, only one general coordinate is known for an estimated 2750 nests with a density of 11.9 nests per ha (Olivier & Wotherspoon, 2008). Similarly, for the neighbouring Northern Masson, one coordinate represents 2705 nests with a density of 8.6 nests per ha (Olivier & Wotherspoon, 2008), and for Laurie Island, one coordinate represents 20,000 breeding pairs (Clarke, 1906 in Croxall et al., 1995). At breeding sites such as these, it is not known where within the range encompassed/represented by the locality's coordinates snow petrel nests are. Better descriptions of the location of nests, including aspect (only recorded for 11% of breeding sites in Appendix A) (Pande & Sivakumar, 2022), and the specific coordinates of some active nests would help improve knowledge of breeding sites. At the same time, this type of data would serve as important ground truth data, to enable the capability of remote sensing to detect snow petrel nesting sites to be tested more accurately (e.g., Schwaller et al., 2013). With the current mismatch of information known about current breeding sites, it is difficult to locate known breeding sites in satellite imagery.

5.1.2 Gaps in the breeding distribution

Spatial analysis of the circumpolar breeding distribution in Chapter 3 demonstrates that there are large gaps in the breeding distribution, which could be due either to under-sampling of remote and inaccessible regions, or true absences. The results of characterising environmental conditions local to breeding sites and within their foraging range has advanced the understanding of suitable breeding habitats, and identifies that the breeding distribution is likely limited by distance to the Marginal Ice Zone during the breeding season (Ainley et al., 1984), and within sustainable distances of this, lithologies that form suitable cavities (such as high-grade metamorphic and intrusive igneous rock). Therefore, whilst the absence of known breeding sites in regions such as the eastern Antarctic Peninsula may result from unsuitable foraging habitat, these results also demonstrate that much of the breeding population likely remains undiscovered. Without being able to identify known breeding sites robustly using remote sensing, it is not possible to use this technique to discover unknown breeding sites. Therefore, habitat selection modelling will be a vital step in predicting the location of breeding sites throughout the snow petrels' range (e.g., Olivier & Wotherspoon, 2006). In turn, this would allow surveys/searches for breeding sites, which face challenging logistical constraints due to remoteness, to be targeted to certain areas.

5.1.3 Long-term monitoring

Finally, increasing the number of breeding sites at which long-term (multidecadal) demographic studies of snow petrels are conducted would improve the understanding of the global breeding population and its distribution. Current long-term demographic studies have been instrumental in analysing the response of snow petrels to both local and regional climatic variations (Chastel et al., 1993; Barbraud et al., 2000; Barbraud & Weimerskirch, 2001; Jenouvrier et al., 2005; Olivier et al., 2005; Sauser et al., 2021a; 2021b), and enable estimations of how the breeding populations will respond to climate-driven changes. Until recently, this understanding has been based upon snow petrel populations at only two locations (Figure 6), with different responses to climate variations observed between different sexes and the two locations. Long-term (decadal) monitoring of snow petrel demographics has now commenced at other localities such as Svarthamaren, where near complete breeding failure of snow petrels and other seabirds occurred in 2021/2022 due to exceptionally violent storms (Descamps et al., 2023). More widespread long-term monitoring of snow petrel populations such as this will improve understanding of the global breeding distribution, and how the total and regional populations might be impacted by climate change. Fundamentally, this work will need to be done through direct observation, as with the current spectral and spatial resolution of satellite imagery available, remote sensing is unable to robustly identify either breeding sites on the whole, or individual nests.

CHAPTER 6: Conclusions

The aim of this thesis was to develop an updated database of the known breeding distribution of snow petrels and to identify whether further breeding sites could be located using remote sensing techniques. By updating the known circumpolar breeding distribution and characterising environmental conditions at breeding sites and within their foraging range, this work has advanced the understanding of the world's most southerly breeding vertebrate in a number of specific ways.

The primary output of chapter 3 is a new database of snow petrel breeding locations (Appendix A), which includes 456 confirmed and suspected breeding sites and increases the number of known sites by 158 compared to the only previous Antarctic-wide inventory (Croxall et al., 1995). This database will be published in an open access repository and will be linked to the future publication of a paper (Appendix B) describing the database compilation and quantification of the breeding distribution and habitat. The database provides a baseline understanding of the circumpolar snow petrel breeding distribution to which more breeding sites can be added in the future. For both conservation and management, such knowledge of a species' breeding distribution is critical.

Quantifying the breeding distribution indicates that known breeding sites are predominantly situated very close to the coastline, but breeding occurs as far inland as 440 km. Most sites are also proximal to Antarctic research stations, systematically declining in frequency with distance from stations, despite the availability of exposed bedrock. This likely suggests a geographical bias relating to accessibility for scientific study, and indicates that more remote breeding sites may currently remain undiscovered.

Characterisation of local environmental conditions at breeding sites demonstrates that snow petrels use cavities in intrusive igneous and high-grade metamorphic lithologies in greater proportions than their availability, whilst less commonly nest in cavities of sedimentary rock, despite its higher availability. Moreover, the majority of the known breeding population (> 45,000 pairs; Appendix A) are located on high-grade metamorphic rock. Though nest-site selection is complex, this, in combination with field observations of specific selection of lithologies, may suggest that high-grade metamorphic rock forms more suitable nesting cavities for the snow petrel.

The accessibility of low concentration sea ice is proposed to be an important control on the breeding distribution of snow petrels (Ainley et al., 1984). Given the distribution of breeding

sites from the sea ice edge in November (median distance = 430 km), the analysis supports this hypothesis. The results also demonstrate that the upper limit on distance to the Marginal Ice Zone is apparent at breeding sites in the Shackleton Mountains which are furthest from this key foraging habitat (> 1000 km). It is likely that this limiting factor also explains the absence of snow petrel breeding sites on the eastern Antarctic Peninsula, because in the western Weddell Sea near complete sea ice cover persists throughout the year. The results of this analysis have the potential to provide the basis for habitat selection modelling that could be used to estimate the breeding distribution of snow petrels throughout their range.

The demonstrable gaps in the known breeding distribution illustrate that the discovery of new breeding sites is an important next step in understanding the breeding distribution of snow petrels. As a relatively cheap and successful method of identifying known and unknown colonies of other Antarctic seabird species this work tested whether satellite imagery could also be used to identify known snow petrel breeding sites. However, the results of various tests show that the use of medium resolution imagery is clearly unsuitable for identifying this loosely colonial cavity-nesting species. Though the use of very high spatial and spectral resolution imagery may indicate that snow petrel breeding sites are a possible cause of high reflection in SWIR on the north facing slope of Mount Henderson, this hypothesis can only be tested if various forms of ground truth data are provided, and it is likely that better spatial and spectral resolution imagery than currently available is needed if snow petrel breeding sites are to be detected in the future.

To better understand the breeding distribution of snow petrels, it is clear that more detailed data from field observations would yield more understanding of breeding sites and the spatial extent of snow petrel colonies, whilst simultaneously providing ground truth data to more accurately assess the capability of remote sensing to identify known snow petrel breeding sites. Furthermore, the absence of population data from over half of the known breeding sites indicates that working towards a more accurate census of the snow petrel breeding population is an important target for further research. Similarly, characterising the average local climatic conditions at breeding sites provides important baseline data against which future distributional shifts in the breeding distribution of snow petrels can be assessed, and highlights the importance of increasing the spatial extent across which long-term monitoring of snow petrels is conducted.

References

Ainley, D. G., & Jacobs, S. S. (1981). Sea-bird affinities for ocean and ice boundaries in the Antarctic. *Deep-Sea Research*, *28A*(10), 1173–1185.

Ainley, D. G., Jacobs, S. S., Ribic, C. A., & Gaffney, I. (1998). Seabird distribution and oceanic features of the Amundsen and southern Bellingshausen seas. *Antarctic Science*, *10*(2), 111–123. https://doi.org/10.1017/s0954102098000169

Ainley, D. G., O'Connor, E. F., & Boekelheide, R. J. (1984). The Marine Ecology of Birds in the Ross Sea, Antarctica. *Ornithological Monographs*, *32*, iii–97. https://www.jstor.org/stable/40166773?seq=1&cid=pdf-

Bakr, N., & Afifi, A. A. (2019). Quantifying land use/land cover change and its potential impact on rice production in the Northern Nile Delta, Egypt. *Remote Sensing Applications: Society and Environment*, *13*, 348–360. https://doi.org/10.1016/J.RSASE.2018.12.002

Barbraud, C., Delord, K. C., Micol, T., & Jouventin, P. (1999). First census of breeding seabirds between Cap Bienvenue (Terre Adélie) and Moyes Islands (King George V Land), Antarctica: new records for Antarctic seabird populations. *Polar Biology*, *21*, 146–150.

Barbraud, C., Vasseur, J., & Delord, K. (2018). Using distance sampling and occupancy rate to estimate abundance of breeding pairs of Wilson's Storm Petrel (Oceanites oceanicus) in Antarctica. *Polar Biology*, *41*(2), 313–322. https://doi.org/10.1007/s00300-017-2192-2

Barbraud, C., & Weimerskirch, H. (2001). Contrasting effects of the extent of sea-ice on the breeding performance of an antarctic top predator, the snow petrel pagodroma nivea. *Journal of Avian Biology*, *32*(4), 297–302. https://doi.org/10.1111/j.0908-8857.2001.320402.x

Barbraud, C., Weimerskirch, H., Guinet, C., & Jouventin, P. (2000). Effect of sea-ice extent on adult survival of an Antarctic top predator: The snow petrel Pagodroma nivea. *Oecologia*, *125*(4), 483–488. https://doi.org/10.1007/s004420000481

Berg, S., Melles, M., Hermichen, W. D., McClymont, E. L., Bentley, M. J., Hodgson, D. A., & Kuhn, G. (2019). Evaluation of Mumiyo Deposits From East Antarctica as Archives for the Late Quaternary Environmental and Climatic History. *Geochemistry, Geophysics, Geosystems*, *20*(1), 260–276. https://doi.org/10.1029/2018GC008054

Bindschadler, R., Vornberger, P., Fleming, A., Fox, A., Mullins, J., Binnie, D., Paulsen, S. J., Granneman, B., & Gorodetzky, D. (2008). The Landsat Image Mosaic of Antarctica. *Remote Sensing of Environment*, *112*(12), 4214–4226. https://doi.org/10.1016/j.rse.2008.07.006

Bolton, M., Conolly, G., Carroll, M., Wakefield, E. D., & Caldow, R. (2019). A review of the occurrence of inter-colony segregation of seabird foraging areas and the implications for marine environmental impact assessment. *Ibis*, *161*(2), 241–259. https://doi.org/10.1111/ibi.12677

Boulinier, T., McCoy, K. D., Yoccoz, N. G., Gasparini, J., & Tveraa, T. (2008). Public information affects breeding dispersal in a colonial bird: Kittiwakes cue on neighbours. *Biology Letters*, *4*(5), 538–540. https://doi.org/10.1098/rsbl.2008.0291

Bowra, G. T., Holdgate, M. W., & Tilbrook, P. J. (1966). Biological investigations in Tottanfjella and central Heimefrontfjella. *British Antarctic Survey Bulletin*, *9*, 63–70.

Brook, D., & Beck, J. R. (1972). Antarctic petrels, snow petrels and south polar skuas breeding in the Theron Mountains. *British Antarctic Survey Bulletin*, *27*, 131–137.

Burton-Johnson, A., Black, M., Fretwell, P. T., & Kaluza-Gilbert, J. (2016) An automated methodology for differentiating rock from snow, clouds and sea in Antarctica from Landsat 8 imagery: a new rock outcrop map and area estimation for the entire Antarctic continent. *The Cryosphere, 10*, 1665-1677, https://doi.org/10.5194/tc-10-1665-2016.

Carneiro, A. P. B., Pearmain, E. J., Oppel, S., Clay, T. A., Phillips, R. A., Bonnet-Lebrun, A. S., Wanless, R. M., Abraham, E., Richard, Y., Rice, J., Handley, J., Davies, T. E., Dilley, B. J., Ryan, P. G., Small, C., Arata, J., Arnould, J. P. Y., Bell, E., Bugoni, L., … Dias, M. P. (2020). A framework for mapping the distribution of seabirds by integrating tracking, demography and phenology. *Journal of Applied Ecology*, *57*(3), 514–525. https://doi.org/10.1111/1365-2664.13568

Carrea, C., Burridge, C. P., Wienecke, B., Emmerson, L. M., White, D., & Miller, K. J. (2019). High vagility facilitates population persistence and expansion prior to the Last Glacial Maximum in an antarctic top predator: The Snow petrel (Pagodroma nivea). *Journal of Biogeography*, *46*(2), 442–453. https://doi.org/10.1111/jbi.13513

Chastel, O., Weimerskirch, H., & Jouventin, P. (1993). High annual variability in reproductive success and survival of an Antarctic seabird, the snow petrel Pagodroma nivea: A 27-year study. *Oecologia*, *94*, 278–285.

Clarke, W. E. (1906). Ornithological Results of the Scottish National Antarctic Expedition.—II. On the Birds of the South Orkney Islands. *Ibis*, *48*(1), 145–187.

Clarke, A., Croxall, J. P., Poncet, S., Martin, A. R., & Burton, R. (2012). Important Bird Areas: South Georgia. *British Birds*, *105*, 118–144.

Cline, D. R., Siniff, D. B., & Erickson, A. W. (1969). *Summer Birds of the Pack Ice in the Weddell Sea, Antarctica* (Vol. 86, Issue 4). https://about.jstor.org/terms

Cocks, M. P., Harris, J. M., Steele, W. K., & Balfour, D. A. (1999). The influence of ornithogenic products on the nutrient status of soils surrounding nests on nunataks in Dronning Maud Land, Antarctica. *Polar Research*, *18*(1), 19–26. https://doi.org/10.1111/j.1751-8369.1999.tb00274.x

Convey, P., Chown, S. L., Clarke, A., Barnes, D. K. A., Bokhorst, S., Cummings, V., Ducklow, H. W., Frati, F., Green, T. G. A., Gordon, S., Griffiths, H. J., Howard-Williams, C., Huiskes, A. H. L., Laybourn-Parry, J., Lyons, W. B., McMinn, A., Morley, S. A., Peck, L. S., Quesada, A., … Wall, D. H. (2014). The spatial structure of Antarctic biodiversity. *Ecological Monographs*, *84*(2), 203–244. https://doi.org/10.1890/12-2216.1

Convey, P., Morton, A., & Poncet, J. (1999). Survey of marine birds and mammals of the South Sandwich Islands. *Polar Record*, *35*(193), 107–124. https://doi.org/10.1017/S0032247400026450

Cooper. J., & Woehler, E. J. (1994). Consumption of Antarctic krill (Euphausia superba) by seabirds during summer in the Prydz Bay region, Antarctica. In *Southern Ocean ecology: the BIOMASS perspective* (pp. 247–260). Cambridge University Press.

Coria, N. R., Montalti, D., Rombola, E. F., Santos, M. M., Garcia Beteno, M. I., & Juares, M. A. (2011). Birds at Laurie Island, South Orkney Islands, Antarctica: breeding species and their distribution. *Marine Ornithology*, *39*, 207–213.

Cowan, A. N. (1981). Size variation in Snow Petrel (Pagodroma nivea). *Notornis*, *28*, 169–188.

Cox, S. C., Smith Lyttle, B., Elkind, S., Smith Siddoway, C., Morin, P., Capponi, G., Abu-Alam, T., Ballinger, M., Bamber, L., Kitchener, B., Lelli, L., Mawson, J., Millikin, A., Dal Seno, N., Whitburn, L., White, T., Burton-Johnson, A., Crispini, L., Elliot, D., … Wilson, G. (2023b). A continent-wide detailed geological map dataset of Antarctica. *Scientific Data*, *10*(1). https://doi.org/10.1038/s41597-023-02152-9

Cox, S. C., Smith Lyttle, B., Elkind, S., Smith Siddoway, C. S., Morin, P., Capponi, G., Abu-Alam, T., Ballinger, M., Bamber, L., Kitchener, B., Lelli, L., Mawson, J. F., Millikin, A., Dal Seno, N., Whitburn, L., White, T., Burton-Johnson, A., Crispini, L., Elliot, D., … Wilson, G. S. (2023a). The GeoMAP (v.2022-08) continent-wide detailed geological dataset of Antarctica. In *PANGAEA*. https://doi.org/https://doi.org/10.1594/PANGAEA.951482

Croxall, J. P., McCann, T. S., Prince, P. A., & Rothery, P. (1988). Reproductive performance of seabirds and seals at South Georgia and Signy Island, South Orkney Islands, 1976 - 1987: implications for Southern Ocean monitoring studies. In D. Sahrhage (Ed.), *Antarctic Ocean and resource variability* (pp. 261–285). Springer.

Croxall, J. P., & Prince, P. A. (1980). Food, feeding ecology and ecological segregation of seabirds at South Georgia. *Biological Journal of the Linnean Society*, *14*, 103–131.

Croxall, J. P., Steele, W. K., McInnes, S. J., & Prince, P. A. (1995). Breeding Distribution of the snow petrel Pagodroma nivea. *Marine Ornithology*, *23*(2), 69–99.

Croxall, J. P., Trathan, P. N., & Murphy, E. J. (2002). Environmental change and Antarctic seabird populations. (Review). *Science*, *297*(5586).

Delord, K., Pinet, P., Pinaud, D., Barbraud, C., De Grissac, S., Lewden, A., Cherel, Y., & Weimerskirch, H. (2016). Species-specific foraging strategies and segregation mechanisms of sympatric Antarctic fulmarine petrels throughout the annual cycle. *Ibis*, *158*(3), 569–586. https://doi.org/10.1111/ibi.12365

Descamps, S., Hudson, S., Sulich, J., Wakefield, E., Grémillet, D., Carravieri, A., Orskaug, S., & Steen, H. (2023). Extreme snowstorms lead to large-scale seabird breeding failures in Antarctica. *Current Biology*, *33*(5), R176–R177. https://doi.org/10.1016/j.cub.2022.12.055

Dias, M. P., Martin, R., Pearmain, E. J., Burfield, I. J., Small, C., Phillips, R. A., Yates, O., Lascelles, B., Borboruglu, P. Garcia., & Croxall, J. P. (2019). Threats to seabirds: A global assessment. *Biological Conservation*, *237*, 525–537.

Durant, J. M., Hjermann, D. Ø., Frederiksen, M., Charrassin, J. B., Le Maho, Y., Sabarros, P. S., Crawford, R. J. M., & Stenseth, N. C. (2009). Pros and cons of using seabirds as ecological indicators. *Climate Research*, *39*(2), 115–129. https://doi.org/10.3354/cr00798

Einoder, L. D., Emmerson, L. M., Southwell, D. M., & Southwell, C. J. (2014). Cavity characteristics and ice accumulation affect nest selection and breeding in Snow Petrels Pagodroma Nivea. *Marine Ornithology*, *42*, 175–182.

Fogt, R. L., Sleinkofer, A. M., Raphael, M. N., & Handcock, M. S. (2022). A regime shift in seasonal total Antarctic sea ice extent in the twentieth century. *Nature Climate Change*, *12*(1), 54–62. https://doi.org/10.1038/s41558-021-01254-9

Fretwell, P. T., Convey, P., Fleming, A. H., Peat, H. J., & Hughes, K. A. (2011). Detecting and mapping vegetation distribution on the Antarctic Peninsula from remote sensing data. *Polar Biology*, *34*(2), 273–281. https://doi.org/10.1007/s00300-010-0880-2

Fretwell, P. T., LaRue, M. A., Morin, P., Kooyman, G. L., Wienecke, B., Ratcliffe, N., Fox, A. J., Fleming, A. H., Porter, C., & Trathan, P. N. (2012). An Emperor Penguin Population Estimate: The First Global, Synoptic Survey of a Species from Space. *PLoS ONE*, *7*(4). https://doi.org/10.1371/journal.pone.0033751

Fretwell, P. T., Phillips, R. A., Brooke, M. de L., Fleming, A. H., & McArthur, A. (2015). Using the unique spectral signature of guano to identify unknown seabird colonies. *Remote Sensing of Environment*, *156*, 448–456. https://doi.org/10.1016/j.rse.2014.10.011

Fretwell, P. T., & Trathan, P. N. (2009). Penguins from space: faecal stains reveal the location of emperor penguin colonies. *Global Ecology and Biogeography*, *18*(5), 543–552. https://doi.org/10.1111/j.1466-8238.2009.00467.x

Gerrish, L., Fretwell, P., & Cooper, P. (2022). High resolution vector polylines of the Antarctic coastline (7.5) [Data set]. In *UK Polar Data Centre, Natural Environment Research Council, UK Research & Innovation*.

Gibson, J. A. E. (2000). *The Environment of the Bunger Hills*.

Goldsworthy, P. M., & Thomson, P. G. (2000). An extreme inland breeding locality of snow petrels (Pagodroma nivea) in the southern Prince Charles Mountains, Antarctica. *Polar Biology*, *23*, 717–720.

Golubev, S. (2022). Analysis of the attempts to breed seabirds in uninhabited territories of the Haswell archipelago and Adams Island (East Antarctica). *Czech Polar Reports*, *12*(1), 44–59. https://doi.org/10.5817/cpr2022-1-4

Gonzalez, J. C., Orgeira, J. L., Jimenez, Y. G., Nieto, C., Romero, C., Alegre, A., & Quiñones, J. (2023). Habitat suitability under future climate scenarios in black-browed albatross

(Thalassarche melanophris) in Southern South America and Antarctica. *Polar Biology*, *46*, 545–557. https://doi.org/10.1007/s00300-023-03143-7

González-Zevallos, D., Santos, M. M., Rombolá, E. F., Juáres, M. A., & Coria, N. R. (2013). Abundance and breeding distribution of seabirds in the northern part of the Danco Coast, Antarctic Peninsula. *Polar Research*, *32*. https://doi.org/10.3402/polar.v32i0.11133

Greenfield, L. G., & Smellie, J. M. (1992). Known, New and Probable Snow Petrel Breeding Locations in the Ross Dependency and Marie Byrd Land. *Notornis*, *39*, 119–124. https://www.researchgate.net/publication/265318589

Grémillet, D., & Boulinier, T. (2009). Spatial ecology and conservation of seabirds facing global climate change: a review. *Marine Ecology Progress Series*, *391*, 121–137. https://doi.org/10.3354/meps08212

Heatwole, H., Betts, M., Webb, J., & Crosthwaite, P. (1991). Birds of the Northern Prince Charles Mountains Antarctica. *Corella*, *15*(4), 120–122.

Henri, R., & Schön, I. (2017). Phylogeography and taxonomy of the Snow Petrel (Pagodroma nivea sl). In *Book of Abstracts* (p. 82).

Hiller, A., Hermichen, W. D., & Wand, U. (1995). Radiocarbon-dated subfossil stomach oil deposits from petrel nesting sites: novel paleoenvironmental records from continental Antarctica. *Radiocarbon*, *37*(2), 171–180. https://doi.org/10.1017/S0033822200030617

Hiller, A., Wand, U., Kampf, H., & Stackebrandt, W. (1988). Occupation of the Antarctic Continent by Petrels During the Past 35 000 Years: Inferences from a 14C Study of Stomach Oil Deposits. *Polar Biology*, *9*, 69–77.

Hobbs, J. (2019). *List of Fulmarine Type Petrels with References*.

Hodum, P. J. (1999). *Foraging Ecology and Reproductive Energetics of Antarctic Fulmarine Petrels*.

Jahanbani, M., Vahidnia, M. H., & Aspanani, M. (2022). Geographical agent-based modeling and satellite image processing with application to facilitate the exploration of minerals in Behshahr, Iran. *Arabian Journal of Geosciences*, *15*(9). https://doi.org/10.1007/s12517-022-10165-8

Jawak, S. D., & Luis, A. J. (2013). A spectral index ratio-based Antarctic land-cover mapping using hyperspatial 8-band WorldView-2 imagery. *Polar Science*, *7*(1), 18–38. https://doi.org/10.1016/j.polar.2012.12.002

Jenouvrier, S., Barbraud, C., & Weimerskirch, H. (2005). Long-term contrasted responses to climate of two Antarctic seabird species. *Ecology*, *86*(11), 2889–2903. https://doi.org/10.1890/05-0514

Johansson, P., & Thor, G. (2004). Observations on the birds of the Vestfjella and Heimefrontfjella, Dronning Maud Land, Antarctica, 1991/92 and 2001/02. *Marine Ornithology*, *32*, 43–46.

Jouventin, P., & Bried, J. (2001). The effect of mate choice on speciation in snow petrels. *Animal Behaviour*, *62*(1), 123–132. https://doi.org/10.1006/anbe.2001.1713

Jouventin, P., & Viot, C.-R. (1985). Morphological and genetic variability of Snow Petrels Pagodroma nivea. *Ibis*, *127*(4), 430–441.

Kim, M., Cho, A., Lim, H. S., Hong, S. G., Kim, J. H., Lee, J., Choi, T., Ahn, T. S., & Kim, O. S. (2015). Highly Heterogeneous Soil Bacterial Communities around Terra Nova Bay of Northern Victoria Land, Antarctica. *PLoS ONE*, *10*(3). https://doi.org/10.1371/journal.pone.0119966

Kuester, M. (2016). *Radiometric Use of WorldView-3 Imagery, Technical Note*.

LaRue, M. A., Lynch, H. J., Lyver, P. O. B., Barton, K., Ainley, D. G., Pollard, A., Fraser, W. R., & Ballard, G. (2014). A method for estimating colony sizes of Adélie penguins using remote sensing imagery. *Polar Biology*, *37*(4), 507–517. https://doi.org/10.1007/s00300-014-1451-8

Lawther, E., & Macallister, N. (1973). *British Antarctic Survey Biology Report*.

Levy, J., Nolin, A., Fountain, A., & Head, J. (2014). Hyperspectral measurements of wet, dry and saline soils from the McMurdo Dry Valleys: Soil moisture properties from remote sensing. *Antarctic Science*, *26*(5), 565–572. https://doi.org/10.1017/S0954102013000977

Li, P., & Martin, T. E. (1991). Nest-site selection and nesting success of cavity-nesting birds in high elevation forest drainages. *The Auk*, *108*, 405–418. https://academic.oup.com/auk/article/108/2/405/5172742

Lloyd, S. P. (1982). Least Squares Quantization in PCM. In *IEEE TRANSACTIONS ON INFORMATION THEORY* (Vol. 28, Issue 2).

Loeb, V., Siegel, V., Holm-Hansen, O., Hewitt, R., Fraser, W., Trivelpiece, W., & Trivelpiece, S. (1997). Effects of sea-ice extent and krill or salp dominance on the Antarctic food web. *Nature*, *387*, 897–900.

Lõhmus, A., & Remm, J. (2005). Nest quality limits the number of hole-nesting passerines in their natural cavity-rich habitat. *Acta Oecologica*, *27*(2), 125–128. https://doi.org/10.1016/j.actao.2004.11.001

Lynch, H. J., & LaRue, M. A. (2014). First global census of the Adélie Penguin. *Auk*, *131*(4), 457–466. https://doi.org/10.1642/AUK-14-31.1

Maher, W. J. (1962). Breeding Biology of the Snow Petrel near Cape Hallett, Antarctica. *The Condor*, *64*(6), 488–499. https://www.jstor.org/stable/1365472?seq=1&cid=pdf-

Mars, J. C. (2018). Mineral and lithologic mapping capability of worldview 3 data at Mountain Pass, California, using true- and false-color composite images, band ratios, and logical operator algorithms. *Economic Geology*, *113*(7), 1587–1601. https://doi.org/10.5382/econgeo.2018.4604

McClymont, E. L., Bentley, M. J., Hodgson, D. A., Spencer-Jones, C. L., Wardley, T., West, M. D., Croudace, I. W., Berg, S., Gröcke, D. R., Kuhn, G., Jamieson, S. S. R., Sime, L., & Phillips, R. A. (2022). Summer sea-ice variability on the Antarctic margin during the last glacial period reconstructed from snow petrel (Pagodroma nivea) stomach-oil deposits. *Climate of the Past*, *18*(2), 381–403. https://doi.org/10.5194/cp-18-381-2022

Mehlum, F., Gjessing, Y., Haftorn, S., & Bech, C. (1988). Census of breeding Antarctic petrels Thalassoica antarctica and physical features of the breeding colony at Svarthamaren, Dronning Maud Land, with notes on breeding snow petrels Pagodroma nivea and south polar skuas Catharacta maccormicki. *Polar Research*, *6*(1), 1–9. https://doi.org/10.3402/polar.v6i1.6841

Melchior Van Wessem, J., Jan Van De Berg, W., Noël, B. P. Y., Van Meijgaard, E., Amory, C., Birnbaum, G., Jakobs, C. L., Krüger, K., Lenaerts, J. T. M., Lhermitte, S., Ligtenberg, S. R. M., Medley, B., Reijmer, C. H., Van Tricht, K., Trusel, L. D., Van Ulft, L. H., Wouters, B., Wuite, J., & Van Den Broeke, M. R. (2018). Modelling the climate and surface mass balance of polar ice sheets using RACMO2 - Part 2: Antarctica (1979-2016). *Cryosphere*, *12*(4), 1479–1498. https://doi.org/10.5194/tc-12-1479-2018

Melick, D., Jackson, A., & Petz, W. (1996). An initial biological survey of the Davis Islands, Vincennes Bay, East Antarctica. *Polar Record*, *32*(180), 67–69. https://doi.org/10.1017/S0032247400027674

Mitchell, I., Daunt, F., Frederiksen, M., & Wade, K. (2020). Impacts of climate change on seabirds, relevant to the coastal and marine environment around the UK. *MCCIP Science Review*, 382–399. https://doi.org/10.14465/2020.arc17.sbi

Muñoz Sabater, J. (2019). *ERA5-Land monthly averaged data from 1950 to present. Copernicus Climate Change Service (C3S) Climate Data Store (CDS)*.

Olivier, F., Lee, A. V., & Woehler, E. J. (2004). Distribution and abundance of snow petrels Pagodroma nivea in the Windmill Islands, East Antarctica. *Polar Biology*, *27*(5), 257–265. https://doi.org/10.1007/s00300-004-0595-3

Olivier, F., Van Franeker, J. A., Creuwels, J. C. S., & Woehler, E. J. (2005). Variations of snow petrel breeding success in relation to sea-ice extent: detecting local response to large-scale processes? *Polar Biology*, *28*(9), 687–699. https://doi.org/10.1007/s00300-005-0734-5

Olivier, F., & Wotherspoon, S. J. (2006). Modelling habitat selection using presence-only data: Case study of a colonial hollow nesting bird, the snow petrel. *Ecological Modelling*, *195*(3–4), 187–204. https://doi.org/10.1016/j.ecolmodel.2005.10.036

Olivier, F., & Wotherspoon, S. J. (2008). Nest selection by snow petrels Pagodroma nivea in East Antarctica. Validating predictive habitat selection models at the continental scale. *Ecological Modelling*, *210*(4), 414–430. https://doi.org/10.1016/j.ecolmodel.2007.08.006

Pande, A., Mondol, S., Sathyakumar, S., Mathur, V. B., Ray, Y., & Sivakumar, K. (2020). Past records and current distribution of seabirds at Larsemann Hills and Schirmacher Oasis, east Antarctica. *Polar Record*. https://doi.org/10.1017/S0032247420000364

Pande, A., & Sivakumar, K. (2022). Climate Change and Seabirds: Insights from Ecological Monitoring of Snow Petrels in the Indian Antarctic Program. *Assessing the Antarctic Environment from a Climate Change Perspective: An Integrated Approach*, 207–234. https://doi.org/10.1007/978-3-030-87078-2_5

Petry, M. V., Valls, F. C. L., Petersen, E. de S., Krüger, L., Piuco, R. da C., & dos Santos, C. R. (2016). Breeding sites and population of seabirds on Admiralty Bay, King George

Island, Antarctica. *Polar Biology*, *39*(7), 1343–1349. https://doi.org/10.1007/s00300-015-1846-1

Phillips, R. A., Lewis, S., González-Solís, J., & Daunt, F. (2017). Causes and consequences of individual variability and specialization in foraging and migration strategies of seabirds. In *Marine Ecology Progress Series* (Vol. 578, pp. 117–150). Inter-Research. https://doi.org/10.3354/meps12217

Phiri, D., & Morgenroth, J. (2017). Developments in Landsat land cover classification methods: A review. In *Remote Sensing* (Vol. 9, Issue 9). MDPI AG. https://doi.org/10.3390/rs9090967

Purich, A., & Doddridge, E. W. (2023). Record low Antarctic sea ice coverage indicates a new sea ice state. *Communications Earth and Environment*, *4*(1). https://doi.org/10.1038/s43247-023-00961-9

Radford, A. N., & Fawcett, T. W. (2014). Conflict between Groups Promotes Later Defense of a Critical Resource in a Cooperatively Breeding Bird. *Current Biology*, *24*(24), 2935–2939. https://doi.org/10.1016/j.cub.2014.10.036

Ramos, J. A., Monteiro, L. R., And, S., & Moniz, Z. (1997). Characteristics and competition for nest cavities in burrowing Procellariiformes. *The Condor*, *99*, 634–641. https://academic.oup.com/condor/article/99/3/634/5124478

Rankin, L. M., Gibson, J. A. E., Franzrnann', P. D., & Burton, H. R. (1999). The Chemical Stratification and Microbial Communities of Ace Lake, Antarctica: A Review of the Characteristics of a Marine-Derived Meromictic Lake. *Polarforschung*, *66*(2), 33–52.

Raphael, M. N., & Handcock, M. S. (2022). A new record minimum for Antarctic sea ice. *Nature Reviews Earth and Environment*, *3*(4), 215–216. https://doi.org/10.1038/s43017-022-00281-0

Ridoux, V., & Offredo, C. (1989). The Diets of Five Summer Breeding Seabirds in Adélie Land, Antarctica. *Polar Biology*, *9*, 137–145.

Rodríguez, A., Arcos, J. M., Bretagnolle, V., Dias, M. P., Holmes, N. D., Louzao, M., Provencher, J., Raine, A. F., Ramírez, F., Rodríguez, B., Ronconi, R. A., Taylor, R. S., Bonnaud, E., Borrelle, S. B., Cortés, V., Descamps, S., Friesen, V. L., Genovart, M., Hedd, A., … Chiaradia, A. (2019). Future directions in conservation research on petrels

and shearwaters. *Frontiers in Marine Science*, *6*(94). https://doi.org/10.3389/fmars.2019.00094

Román, A., Navarro, G., Caballero, I., & Tovar-Sánchez, A. (2022). High-spatial resolution UAV multispectral data complementing satellite imagery to characterize a chinstrap penguin colony ecosystem on deception island (Antarctica). *GIScience and Remote Sensing*, *59*(1), 1159–1176. https://doi.org/10.1080/15481603.2022.2101702

Ryan, P. G., & Watkins, B. P. (1989). Snow Petrel Breeding Biology at an Inland Site in Continental Antarctica. In *Waterbirds* (Vol. 12, Issue 2). https://www.jstor.org/stable/1521338

Ryan, P., & Watkins, B. (1988). Birds of the inland mountains of western Dronning Maud Land, Antarctica. *Cormorant*, *16*, 34–40.

Santora, J. A., LaRue, M. A., & Ainley, D. G. (2020). Geographic structuring of Antarctic penguin populations. *Global Ecology and Biogeography*, *29*(10), 1716–1728. https://doi.org/10.1111/geb.13144

Sauser, C., Delord, K., & Barbraud, C. (2021a). Demographic sensitivity to environmental forcings: a multi-trait, multi-colony approach. *Oikos*, *130*(6), 943–957. https://doi.org/10.1111/oik.07441

Sauser, C., Delord, K., & Barbraud, C. (2021b). Sea ice and local weather affect reproductive phenology of a polar seabird with breeding consequences. *Ornithological Applications*, *123*(4). https://doi.org/10.1093/ornithapp/duab032

Schrimpf, M. B., Che-Castaldo, C., & Lynch, H. J. (2020). Regional breeding bird assessment of the Antarctic Peninsula. *Polar Biology*, *43*(2), 111–122. https://doi.org/10.1007/s00300-019-02613-1

Schwaller, M. R., Lynch, H. J., Tarroux, A., & Prehn, B. (2018). A continent-wide search for Antarctic petrel breeding sites with satellite remote sensing. *Remote Sensing of Environment*, *210*, 444–451. https://doi.org/10.1016/j.rse.2018.02.071

Schwaller, M. R., Olson Jr, C. E., Ma, Z., & Zhu, Z. (1989). A Remote Sensing Analysis of Adélie Penguin Rookeries. *Remote Sensing of the Environment*, *28*, 199–206.

Schwaller, M. R., Southwell, C. J., & Emmerson, L. M. (2013). Continental-scale mapping of Adélie penguin colonies from Landsat imagery. *Remote Sensing of Environment*, *139*, 353–364. https://doi.org/10.1016/j.rse.2013.08.009

Schwaller, M. R., Benninghoff, W. S., & Olson Jr, C. E. (1984). Prospects for satellite remote sensing of Adelie penguin rookeries. *International Journal of Remote Sensing*, *5*(5), 849–853.

Smith, W. O., & Comiso, J. C. (2008). Influence of sea ice on primary production in the Southern Ocean: A satellite perspective. *Journal of Geophysical Research: Oceans*, *113*(5). https://doi.org/10.1029/2007JC004251

Smith, W. O., & Nelson, D. M. (1985). Phytoplankton Bloom Produced by a Receding Ice Edge in the Ross Sea: Spatial Coherence with the Density Field. *Science*, *227*, 163–166. https://www.science.org

Southwell, C., Smith, D., Bender, A., & Emmerson, L. (2021). A spatial reference and identification system for coastal ice-free land in East Antarctica. *Polar Record*, *57*. https://doi.org/10.1017/s0032247421000280

Southwell, D. M., Einoder, L. D., Emmerson, L. M., & Southwell, C. J. (2011). Using the double-observer method to estimate detection probability of two cavity-nesting seabirds in Antarctica: The snow petrel (Pagodroma nivea) and the Wilson's storm petrel (Oceanites oceanicus). *Polar Biology*, *34*(10), 1467–1474. https://doi.org/10.1007/s00300-011-1004-3

Starck, W. (1980). The avifauna of Haswell Island (East Antarctica) in summer of 1978/1979. *Polish Polar Research*, 183–196.

Stauffer, D. F., & Best, L. B. (1982). Nest-Site Selection by Cavity-Nesting Birds of Riparian Habitats in Iowa. *The Wilson Bulletin*, *94*(3), 329–337.

Steele, W. K., & Hiller, A. (1997). Radiocarbon dates of snow petrel (Pagodroma nivea) nest sites in central Dronning Maud Land, Antarctica. *Polar Record*, *33*(184), 29–38.

Sydeman, W. J., Thompson, S. A., & Kitaysky, A. (2012). Seabirds and climate change: roadmap for the future. *Marine Ecology Progress Series*, *454*, 107–117. https://doi.org/10.3354/meps09806

Terauds, A., & Lee, J. R. (2016). Antarctic biogeography revisited: updating the Antarctic Conservation Biogeographic Regions. *Diversity and Distributions*, *22*(8), 836–840. https://doi.org/10.1111/ddi.12453

Thatje, S., Hillenbrand, C. D., Mackensen, A., & Larter, R. (2008). Life hung by a thread: Endurance of Antarctic fauna in glacial periods. *Ecology*, *89*(3), 682–692. https://doi.org/10.1890/07-0498.1

Thor, G., & Low, M. (2011). The persistence of the snow petrel (Pagodroma nivea) in Dronning Maud Land (Antarctica) for over 37,000 years. *Polar Biology*, *34*(4), 609–613. https://doi.org/10.1007/s00300-010-0912-y

Turner, J., Guarino, M. V., Arnatt, J., Jena, B., Marshall, G. J., Phillips, T., Bajish, C. C., Clem, K., Wang, Z., Andersson, T., Murphy, E. J., & Cavanagh, R. (2020). Recent Decrease of Summer Sea Ice in the Weddell Sea, Antarctica. *Geophysical Research Letters*, *47*(11). https://doi.org/10.1029/2020GL087127

Verkulich, S. R., & Hiller, A. (1994). Holocene deglaciation of the Bunger Hills revealed by 14C measurements on stomach oil deposits in snow petrel colonies. *Antarctic Science*, *6*(3), 395–399. http://journals.cambridge.org

Wakefield, E. D., Phillips, R. A., & Matthiopoulos, J. (2014). Habitat-mediated population limitation in a colonial central-place forager: the sky is not the limit for the black-browed albatross. *Proceedings of the Royal Society B: Biological Sciences*, *281*(1778). https://doi.org/10.1098/rspb.2013.2883

Walton, D. (1984). “The Terrestrial Environment.” In R. Laws (Ed.), *Antarctic Ecology* (Vol. 1, pp. 1–60). Academic Press.

Wand, U., & Hermichen, W.-D. (2005). Late Quaternary Ice Level Changes in Central Dronning Maud Land, East Antarctica, as Inferred from 14C ages of Mumiyo Deposits in Snow Petrel Colonies. *Geol Jahrbuch*, *B97*, 237–254.

Wang, Y., Zhang, X., Ning, W., Lazzara, M. A., Ding, M., Reijmer, C. H., Smeets, P. C. J. P., Grigioni, P., Heil, P., Thomas, E. R., Mikolajczyk, D., Welhouse, L. J., Keller, L. M., Zhai, Z., Sun, Y., & Hou, S. (2023). The AntAWS dataset: a compilation of Antarctic automatic weather station observations. *Earth System Science Data*, *15*(1), 411–429. https://doi.org/10.5194/essd-15-411-2023

Wiebe, K. L. (2011). Nest sites as limiting resources for cavity-nesting birds in mature forest ecosystems: A review of the evidence. *Journal of Field Ornithology*, *82*(3), 239–248. https://doi.org/10.1111/j.1557-9263.2011.00327.x

Winther, J.-G. (1994). Spectral bi-directional reflectance of snow and glacier ice measured in Dronning Maud Land, Antarctica. *Annals of Glaciology*, *20*, 1–5. https://doi.org/10.3189/1994aog20-1-1-5

Zink, R. M. (1981). Observations of seabirds during a cruise from Ross Island to Anvers Island, Antarctica. *Wilson Bulletin*, *93*(1), 1–20.

Appendix

Appendix A: Snow petrel database. A csv version of this database will be located, open access, in the UKPDC.

id	Locality	ACBR / BBR	Spatial SubGroup	SiteID(s)	LatDec	LonDec	References	Start Date Year	Start Date Month	Duration	EndDateYear	EndDateMonth
1	Cape Circoncision, Bouvet Island	Antarctic Bouvet			-54.40000	3.30000	Ozawa (1967); Solyanik (1964) in Croxall et al (1995)	1961		Years	1967	
2	Utpostane Nunatak vicinity, Vestfjella	Dronning Maud Land			-73.89417	-15.69278	Somme (1977) in Croxall et al. (1995); Berg et al (2018)	1977	January			
3	Audunfjellet Nunatak, Vestfjella	Dronning Maud Land			-73.92611	-15.63000	Somme (1977) in Croxall et al (1995); Mehlum et al (1988)	1977	January			
4	Skuafjellet, Vestfjella	Dronning Maud Land			-73.90000	-15.61667	Somme (1977) in Croxall et al (1995); Mehlum et al (1988)	1977	January			
5	Basen Nunatak, Vestfjella	Dronning Maud Land			-73.03333	-13.41667	Larsson (1990); Johansson and Thor (2004)	2001		Season	2002	
6	Fossilryggen Nunatak, Vestfjella	Dronning Maud Land			-73.38333	-13.05000	Johansson and Thor (2004)	2001	December	Season		
7	Plogen Nunatak, Vestfjella	Dronning Maud Land			-73.30000	-13.83333	Somme (1977) in Croxall et al. (1995); Johansson and Thor (2004)	1968			1969	
8	"Z.81" / Cottontoppen, Heimefrontfjella	Dronning Maud Land			-75.05000	-12.68333	Bowra et al (1966); Johansson and Thor (2004)	1963	November	Season	1964	
9	Tottan Hills	Dronning Maud Land			-75.00000	-12.00000	Thurston (1961); Chattopadhyay (1995)	1961	November			
10	"Z.92 / Peak K" / north end of Johnsonhogna, Tottanfjella	Dronning Maud Land			-74.80000	-12.16670	Ardus (1964); Bowra et al (1966); Johansson and Thor (2004)	1963	November	Season	1964	January
11	Steinnabben, Scharffenbergbotnen Valley,	Dronning Maud Land			-74.55333	-11.50000	Bowra (1966); Johansson and Thor (2004)	1992	January		2002	January

	Heimefront fjella											
12	Boyesennuten, Scharffenbergbotnen Valley, Heimefront fjella	Dronning Maud Land			-74.56667	-11.24167	Bowra (1966); Johansson and Thor (2004)	1992	January		2002	January
13	Svea-Haldorsentoppen, Scharffenbergbotnen Valley, Heimefront fjella	Dronning Maud Land			-74.58333	-11.21667	Bowra (1966); Johansson and Thor (2004)	1992	January		2002	January
14	Haldorsentoppen-Torsvikstoppen, Scharffenbergbotnen Valley, Heimefront fjella	Dronning Maud Land			-74.58667	-11.20833	Bowra (1966); Johansson and Thor (2004)	1992	January		2002	January
15	"Z.66-68 / Peaks W, X, Y" / Torsvikstoppen-Wrightthamaren, Scharffenbergbotnen Valley, Heimefront fjella	Dronning Maud Land			-74.58889	-11.13333	Bowra (1966); Johansson and Thor (2004)	1992	January		2002	January
16	Wrightthamaren-Engenhovet, Scharffenbergbotnen Valley, Heimefront fjella	Dronning Maud Land			-74.60167	-11.02500	Bowra (1966); Johansson and Thor (2004)	1992	January		2002	January
17	"Z.73" / Unnamed Nunatak	Dronning Maud Land					Bowra et al (1966); Johansson and Thor (2004)					
18	Johnsbrotet ("Nunataks III, V and VI"), northern Ahlmannryggen	Dronning Maud Land			-71.33333	-4.16667	La Grange (1962) in Steele and Newton (1995); Krynauw et al (1983); Steele and Newton (1995); Steele and Hiller (1997)	1992	January	Years	1993	January
19	Boreas and Passat Nunataks, northern Ahlmannryggenn	Dronning Maud Land			-71.30000	-3.95000	Krynauw et al (1983); Steele and Newton (1995); Steele and Hiller (1997)	1960	November	Days		

20	Ice Axe Peak complex, Robertskollen, northern Ahlmannryggen	Dronning Maud Land			-71.48333	-3.21667	Krynauw et al (1983); Ryan and Watkins (1989); Steele and Hiller (1997)	1987	December	Month	1988	January
21	Tumble Ice, Robertskollen, northern Ahlmannryggen	Dronning Maud Land			-71.45694	-3.30000	Krynauw et al (1983); Ryan and Watkins (1989); Steele and Hiller (1997)	1987	December	Month	1988	January
22	Petrel's Rest, Robertskollen, northern Ahlmannryggen	Dronning Maud Land			-71.47500	-3.31667	Krynauw et al (1983); Ryan and Watkins (1989); Steele and Hiller (1997)	1987	December	Month	1988	January
23	Ekberget, H.U. Sverdrupfjella	Dronning Maud Land			-72.28333	-0.35000	Dalenius and Wilson (1958); Ryan and Watkins (1988)	1950			1952	
24	Brattskarvet, NE H.U. Sverdrupfjella	Dronning Maud Land			-72.11667	1.41667	Ryan and Watkins (1988); Mehlum et al (1985)	1986		Season	1987	
25	Stornupen	Dronning Maud Land			-72.18333	2.38333	Ohta (1999)	1999				
26	Klovingen	Dronning Maud Land			-72.03333	2.45000	Ohta (1999)	1999				
27	Nonshogda	Dronning Maud Land			-72.00000	2.50000	Ohta (1999)	1999				
28	Troll	Dronning Maud Land			-72.03333	2.51667	Ohta (1999)	1999				
29	Troll Vicinity	Dronning Maud Land			-72.03333	2.58333	Ohta (1999)	1999				
30	Jutulsessen, Gjelsvikfjella	Dronning Maud Land			-72.05000	2.66667	Ryan and Watkins (1988); Mehlum et al (1988); Steele and Hiller (1997); Ohta (1993) in Croxall et al (1995); Njastad (2000)	1986		Season	1987	
31	Un-named Nunatak	Dronning Maud Land			-72.03333	2.68333	Ohta (1999)	1999				
32	Jutulhogget	Dronning Maud Land			-72.03333	2.85000	Ohta (1999)	1999				
33	Orvinfjella region	Dronning Maud Land			-71.95000	2.83333	Lovenskiold (1960)	1958	November			

34	Un-named rocks	Dronning Maud Land			-71.94500	2.83417	Descamps, pers. Comms. (2023)	2022				
35	Rempligen	Dronning Maud Land			-72.08333	4.30000	Ohta (1999)	1999				
36	Orvinfjella region	Dronning Maud Land			-72.00000	4.33333	Lovenskiold (1960)	1958	Febr uary	Seas on		
37	Skigarden	Dronning Maud Land			-71.91667	4.58333	Ohta (1999)	1999				
38	Svarthamaren, Muhlig-Hofmannfjella	Dronning Maud Land			-71.88333	5.16667	Mehlum et al (1985); Mehlum et al (1988); Steele and Hiller (1997); Ohta (1999); Njastad (2000)	1985	Janu ary	Mon th	1985	Febr uary
39	Un-named rocks	Dronning Maud Land			-71.89583	5.26667	Descamps, pers. Comms. (2023)	2022				
40	Kvitholten	Dronning Maud Land			-71.80000	5.88333	Ohta (1999)	1999				
41	Orvinfjella region	Dronning Maud Land			-71.91667	9.00000	Lovenskiold (1960); Mathews (1986)	1959	Janu ary	Seas on		
42	Dallmann Mountains, Wohlthat Massif	Dronning Maud Land			-71.76667	10.18333	Berg et al (2019); Berg et al (2023)					
43	Insel Range	Dronning Maud Land			-72.00000	11.00000	Hiller et al (1995); Thor and Low (2011)					
44	Orvinfjella	Dronning Maud Land			-71.50000	11.75000	Lovenskiold (1960)	1959	Janu ary	Seas on		
45	Schirmacher Oasis	Dronning Maud Land			-70.78333	11.66667	Pande et al (2020)	2014	Marc h	Years	2016	
46	Russian Bay, Nivlisen ice shelf	Dronning Maud Land			-69.98333	11.95000	Bhatnagar (1999) in Pande et al (2020)	1996				
47	India Bay, Nivlisen ice shelf	Dronning Maud Land			-69.98333	11.95000	Sathyakumar (1998) in Pande et al (2020)	1995				
48	Dakshin Gangotri, Nivlisen ice shelf	Dronning Maud Land			-70.08056	12.00250	Venkataraman (1998) and Sathyakumar (1998) in Pande et al (2020)	1995				
49	Petermann Range, Wohlthat Massif	Dronning Maud Land			-71.36667	12.58333	Berg et al (2019); Berg et al (2023)					
50	Lake Untersee Valley, Untersee Oasis	Dronning Maud Land			-71.36667	13.46667	Hiller et al (1988); Hiller et al (1995)	1983	Dece mber	Days		

51	Tanngarden Nunatak, Sor-Rondane Mountains	Dronning Maud Land			-72.00000	23.00000	Ohyama and Hiruta (1995)	1989		Season	1990	January
52	Vengen Nunatak, Sor Rondane Mountains	Dronning Maud Land			-72.33333	23.50000	Ohyama and Hiruta (1995)	1989		Season	1990	January
53	Pinvinane, Sor-Rondane Mountains	Dronning Maud Land			-72.00000	25.00000	Loy (1962)	1959	December	Season		
54	Menipa, Sor-Rondane Mountains	Dronning Maud Land			-71.95402	25.07099	Loy (1962)	1961	December	Season		
55	Yukidori Valley, Langhovde	Enderby Land	LUT_SG_02	R_1100	-69.24167	39.76670	Haga (1961); Fujii et al (2010); (ASPA report No. 141, 2019)	2006		Season	2007	
56	Ongul Island, Syowa Base	Enderby Land	LUT_SG_01	IS_92	-69.01667	39.53333	Watson et al (1971); Mehlum et al (1988)					
57	Casey Bay	Enderby Land	LEN_SG_01 to 08		-67.50000	48.00000	Woehler and Johnstone (1991) in Croxall et al (1995)	1961				
58	Mount Biscoe	Enderby Land	BIS_SG_01	R_17	-66.21667	51.36667	Bassett et al (1990)	1985	October	Days		
59	Proclamation Rock	Enderby Land	AAG_SG_03	IS_70092	-65.86667	53.80000	Falla (1937); Cowan (1981)	1930	January			
60	Taylor Rookery	Prince Charles Mountains (coastal)	COL_SG_05	R_626	-67.45000	60.86667	Bonner and Smith (1985)					
61	Rookery Island, Rookery Islands	Prince Charles Mountains (coastal)	HBW_SG_08	IS_74721	-67.61667	62.50000	Bonner and Smith (1985); Woehler (1990); ASPA No. 102 (2015); Southwell and Emmerson AAD *unpubl. data*			Years	2018	December
62	Giganteus Island, Rookery Islands	Prince Charles Mountains (coastal)	HBW_SG_07	IS_74487	-67.61667	62.53333	Bonner and Smith (1985)					
63	Jocelyn Island group, Holme Bay Islands	Prince Charles Mountains (coastal)	HBE_SG_18		-67.58333	62.70000	Olivier and Wotherspoon (2008); Southwell et al (2011)	2004	December	Years	2009	December
64	Trevillian Island, Holme Bay Islands	Prince Charles Mountains (coastal)	HBE_SG_15	IS_74830	-67.63333	62.70000	Olivier and Wotherspoon (2008)	2004	December			

65	Arrow Island, Holme Bay Islands	Prince Charles Mountains (coastal)	HBE_SG_14	IS_74570	-67.58703	62.70930	Olivier and Wotherspoon (2008); Southwell and Emmerson AAD *unpubl. data*	2004	December	Years	2009	January
66	Ring rocks, Holme Bay Islands	Prince Charles Mountains (coastal)	HBE_SG_16	IS_74831	-67.65000	62.71667	Olivier and Wotherspoon (2008)	2004	December			
67	Un-named Island	Prince Charles Mountains (coastal)	HBE_SG_19	IS_74636	-67.59272	62.77317	Southwell and Emmerson AAD *unpubl. data*	2010		Days	2010	
68	Un-named Island	Prince Charles Mountains (coastal)	HBE_SG_19	IS_74635	-67.59175	62.77505	Southwell and Emmerson AAD *unpubl. data*	2010		Days	2010	
69	Kerry Island	Prince Charles Mountains (coastal)	HBE_SG_19	IS_74640	-67.59739	62.77619	Southwell and Emmerson AAD *unpubl. data*	2009		Days	2009	
70	Evans Island, Holme Bay Islands	Prince Charles Mountains (coastal)	HBE_SG_19	IS_74679	-67.61333	62.80000	Olivier and Wotherspoon (2008); Southwell et al (2011)	2004	December	Years	2011	January
71	Bechervaise Island, Holme Bay Islands	Prince Charles Mountains (coastal)	HBE_SG_19	IS_74585	-67.58333	62.81667	Olivier and Wotherspoon (2008); Southwell et al (2011); Einoder et al (2014)	2004	December	Years	2009	December
72	Flat Island, Holme Bay Islands	Prince Charles Mountains (coastal)	HBE_SG_19		-67.61333	62.81667	Olivier and Wotherspoon (2008); Southwell et al (2011)	2004	December	Years	2011	January
73	Un-named Island	Prince Charles Mountains (coastal)	HBE_SG_19	IS_74526	-67.57925	62.81984	Southwell and Emmerson AAD *unpubl. data*	2011		Days	2011	
74	Un-named Island	Prince Charles Mountains (coastal)	HBE_SG_19	IS_74547	-67.58023	62.82981	Southwell and Emmerson AAD *unpubl. data*	2010		Days	2010	
75	West Budd Island	Prince Charles Mountains (coastal)	HBE_SG_19	IS_74503	-67.57551	62.83143	Southwell and Emmerson AAD *unpubl. data*	2010		Days	2010	
76	Stinear Island, Holme Bay Islands	Prince Charles Mountains (coastal)	HBE_SG_19	IS_74543	-67.58333	62.83333	Olivier and Wotherspoon (2008); Southwell et al (2011)	2004	December	Years	2009	December

77	Un-named Island	Prince Charles Mountains (coastal)	HBE_SG_19	IS_74557	-67.58226	62.83999	Southwell and Emmerson AAD *unpubl. data*	2010		Days	2010	
78	East Budd Island, Holme Bay Islands	Prince Charles Mountains (coastal)	HBE_SG_19	IS_74517	-67.59667	62.85000	Olivier and Wotherspoon (2008); Southwell et al (2011)	2004	December	Years	2009	December
79	Dyer Island, Holme Bay Islands	Prince Charles Mountains (coastal)	HBE_SG_21	IS_74639	-67.61333	62.86667	Olivier and Wotherspoon (2008)	2004	December			
80	Lee Island	Prince Charles Mountains (coastal)	HBE_SG_21	IS_74582	-67.58917	62.87237	Southwell and Emmerson AAD *unpubl. data*	2010		Days	2010	
81	Mawson (incl. Entrance, Hump Island), Holme Bay Islands	Prince Charles Mountains (coastal)	HBE_SG_21	IS_74646 /IS_74660 /R_718	-67.61333	62.88333	Woehler and Johnstone (1991) in Croxall et al (1995); Olivier and Wotherspoon (2008); Southwell and Emmerson AAD *unpubl. data*	2004	December	Years	2009	January
82	Un-named Island	Prince Charles Mountains (coastal)	HBE_SG_21	IS_74563	-67.58330	62.88791	Southwell and Emmerson AAD *unpubl. data*	2010		Days	2010	
83	Un-named Island	Prince Charles Mountains (coastal)	HBE_SG_21	IS_74569	-67.58557	62.89311	Southwell and Emmerson AAD *unpubl. data*	2010		Days	2010	
84	Petersen Island	Prince Charles Mountains (coastal)	HBE_SG_21	IS_74507	-67.57768	62.89360	Southwell and Emmerson AAD *unpubl. data*	2010		Days	2010	
85	Un-named Island	Prince Charles Mountains (coastal)	HBE_SG_21	IS_74548	-67.58146	62.89746	Southwell and Emmerson AAD *unpubl. data*	2010		Days	2010	
86	Teyssier Island, Holme Bay Islands	Prince Charles Mountains (coastal)	HBE_SG_21	IS_74619	-67.61333	62.90000	Olivier and Wotherspoon (2008); Southwell and Emmerson AAD *unpubl. data*	2004	December	Years	2009	January
87	Welch Island,	Prince Charles Mountain	HBE_SG_18	IS_74432	-67.58000	62.93333	Olivier and Wotherspoon (2008);	2004	December	Years	2010	December

	Holme Bay Islands	s (coastal)					Southwell and Emmerson AAD *unpubl. data*					
88	Un-named Island	Prince Charles Mountains (coastal)	HBE_SG_23	IS_74549	-67.58118	62.94734	Southwell and Emmerson AAD *unpubl. data*	2010		Days	2010	
89	Un-named Island	Prince Charles Mountains (coastal)	HBE_SG_23	IS_74521	-67.57863	62.94752	Southwell and Emmerson AAD *unpubl. data*	2010		Days	2010	
90	Rouse Island, Holme Bay Islands	Prince Charles Mountains (coastal)	HBE_SG_23	lS_74514	-67.58000	62.95000	Olivier and Wotherspoon (2008)	2004	December			
91	Un-named Island	Prince Charles Mountains (coastal)	HBE_SG_23	IS_74406	-67.55332	62.96512	Southwell and Emmerson AAD *unpubl. data*	2010		Days	2010	
92	Un-named Island	Prince Charles Mountains (coastal)	HBE_SG_22	IS_74337	-67.53082	62.98304	Southwell and Emmerson AAD *unpubl. data*	2010		Days	2010	
93	Canopus Island, Holme Bay Islands	Prince Charles Mountains (coastal)	HBE_SG_22	lS_74345	-67.54667	62.98333	Olivier and Wotherspoon (2008)	2004	December			
94	Klung Island, Holme Bay Islands	Prince Charles Mountains (coastal)	HBE_SG_23	IS_74386	-67.55000	62.98333	Olivier and Wotherspoon (2008)	2004	December			
95	Un-named Island	Prince Charles Mountains (coastal)	HBE_SG_22	IS_74315	-67.52056	63.01043	Southwell and Emmerson AAD *unpubl. data*	2010		Days	2010	
96	Un-named Island	Prince Charles Mountains (coastal)	HBE_SG_22	lS_74319	-67.52259	63.01055	Southwell and Emmerson AAD *unpubl. data*	2010		Days	2010	
97	Un-named Island	Prince Charles Mountains (coastal)	HBE_SG_22	lS_74305	-67.51763	63.01263	Southwell and Emmerson AAD *unpubl. data*	2010		Days	2010	
98	Un-named Island	Prince Charles Mountains (coastal)	HBE_SG_22	IS_74310	-67.51991	63.01273	Southwell and Emmerson AAD *unpubl. data*	2010		Days	2010	
99	Un-named Island	Prince Charles Mountain	HBE_SG_22	lS_74318	-67.52311	63.01304	Southwell and Emmerson AAD	2010		Days	2010	

		s (coastal)					*unpubl. data*					
100	Smith rocks, Holme Bay Islands	Prince Charles Mountains (coastal)	HBE_SG_22		-67.51667	63.01667	Olivier and Wotherspoon (2008)	2004	December			
101	Un-named Island	Prince Charles Mountains (coastal)	HBE_SG_22	IS_74338	-67.53043	63.02711	Southwell and Emmerson AAD *unpubl. data*	2010		Days	2010	
102	Un-named Island	Prince Charles Mountains (coastal)	HBE_SG_22	IS_74341	-67.53228	63.03103	Southwell and Emmerson AAD *unpubl. data*	2010		Days	2010	
103	Kitney Island, Holme Bay Islands	Prince Charles Mountains (coastal)	HBE_SG_24	IS_74286	-67.51667	63.06667	Olivier and Wotherspoon (2008)	2004	December			
104	Robinson Group Islands	Prince Charles Mountains (coastal)	ROB_SG_01 to 11		-67.45000	63.45000	Southwell et al (2011)	2009	December	Season	2010	February
105	Scullin Monolith	Prince Charles Mountains (coastal)	MON_SG_01	R_810	-67.79361	66.71889	Falla (1937); Woehler and Johnstone (1991) in Croxall et al (1995); (ASPA No. 164, 2022)	1987				
106	Murray Monolith	Prince Charles Mountains (coastal)	MON_SG_01	R_812	-67.78417	66.88806	(ASPA No. 164, 2022)					
107	Mt Horden Range, Framnes Mountains	Prince Charles Mountains (inland)			-67.92972	62.48667	Olivier and Wotherspoon (2008)	2005	January	Month	2005	February
108	David Range, Framnes Mountains	Prince Charles Mountains (inland)			-67.83333	62.53333	Olivier and Wotherspoon (2008)	2005	January	Month	2005	February
109	Northern Masson, Framnes Mountains	Prince Charles Mountains (inland)			-67.78333	62.81667	Olivier and Wotherspoon (2008); Southwell et al (2011); Southwell and Emmerson AAD *unpubl. data*	2005	January	Years	2017	December
110	Central Masson, Framnes Mountains	Prince Charles Mountains (inland)			-67.82750	62.85833	Olivier and Wotherspoon (2008)	2005	January	Month	2005	February
111	Mt Henderson Range, Framnes Mountains	Prince Charles Mountains (inland)			-67.70000	63.06667	Olivier and Wotherspoon (2008); Southwell and Emmerson	2005	January	Years	2017	December

							AAD *unpubl. data*					
112	Sandilands Nunatak, northern Amery Peaks	Prince Charles Mountains (inland)			-70.54222	67.45000	Heatwole et al (1991)	1989		Season	1990	
113	Mt Seaton, northern Amery Peaks	Prince Charles Mountains (inland)			-70.61111	67.45917	Heatwole et al (1991)	1989		Season	1990	
114	Northwestern Manning Massif, northern Amery Peaks	Prince Charles Mountains (inland)			-70.71556	67.75333	Heatwole et al (1991)	1989		Season	1990	
115	Dragons Teeth Cliffs	Prince Charles Mountains (inland)			-70.86677	67.91667	Heatwole et al (1991)	1989		Season	1990	
116	Eastern side of Radok Lake	Prince Charles Mountains (inland)			-70.86677	68.00000	Heatwole et al (1991)	1989		Season	1990	
117	Bainmedart Cove	Prince Charles Mountains (inland)			-70.84833	68.05417	Heatwole et al (1991)	1989		Season	1990	
118	Pagodroma Gorge, Prince Charles Mountains	Prince Charles Mountains (inland)			-70.83333	68.10000	Heatwole et al (1991); Brown (1966) in Goldsworthy and Thomson (2000)	1989		Season	1990	
119	Flagstone Bench	Prince Charles Mountains (inland)			-70.84389	68.17778	Heatwole et al (1991)	1989		Season	1990	
120	Greenall Glacier, Mawson Escarpment, Prince Charles Mountains	Prince Charles Mountains (inland)			-73.24500	68.20100	Goldsworthy and Thomson (2000)	1998	February	Days		
121	Rimington Bluff, south Mawson Escarpment, Prince Charles Mountains	Prince Charles Mountains (inland)			-73.65000	68.42000	Goldsworthy and Thomson (2000)	1998	January	Days		
122	Grovnes Peninsula, Larsemann Hills	East Antarctica	LAR_SG_10	R_1183	-69.41667	76.19722	Zipan and Norman (1993); Pande et al (2020)	2014	March	Years	2016	
123	Stornes Peninsula, Larsemann Hills	East Antarctica	LAR_SG_10		-69.41667	76.10000	Zipan and Norman (1993); (ASPA No. 174, 2014)					
124	Brattnevet Peninsula, Larsemann Hills	East Antarctica	LAR_SG_09	R_1184	-69.40694	76.25083	Zipan and Norman (1993); Pande et al (2020)	2014	March	Years	2016	

125	Stinear Peninsula, Larsemann Hills	East Antarctica	LAR_SG_09	R_1177	-69.40280	76.30260	Zipan and Norman (1993); Pande et al (2020)	2014	March	Years	2016	
126	Cook Island, Larsemann Hills	East Antarctica	LAR_SG_01	IS_75138	-69.40250	76.01389	Zipan and Norman (1993); Pande et al (2020)	2014	March	Years	2016	
127	Fisher Island, Larsemann Hills	East Antarctica	LAR_SG_05	IS_75130	-69.39180	76.25740	Zipan and Norman (1993); Pande et al (2020)	2014	March	Years	2016	
128	Broknes Peninsula, Larsemann Hills	East Antarctica	LAR_SG_08	R_1159	-69.39169	76.34999	Zipan and Norman (1993); Pande et al (2020)	2014	March	Years	2016	
129	Breadloaf Island, Larsemann Hills	East Antarctica	LAR_SG_05	IS_75093	-69.37889	76.21639	Zipan and Norman (1993); Pande et al (2020)	2014	March	Years	2016	
130	Easther Island, Larsemann Hills	East Antarctica	LAR_SG_05	IS_75069	-69.37667	76.23417	Zipan and Norman (1993); Pande et al (2020)	2014	March	Years	2016	
131	McLeod Island, Larsemann Hills	East Antarctica	LAR_SG_04	IS_75192	-69.36722	76.14028	Zipan and Norman (1993); Pande et al (2020)	2014	March	Years	2016	
132	Manning Island, Larsemann Hills	East Antarctica	LAR_SG_06	IS_74927	-69.35500	76.33333	Zipan and Norman (1993); Pande et al (2020)	2014	March	Years	2016	
133	Betts Island, Larsemann Hills	East Antarctica	LAR_SG_03	IS_74917	-69.34944	76.21333	Zipan and Norman (1993); Pande et al (2020)	2014	March	Years	2016	
134	Svenner Islands	East Antarctica	SVE_SG_01 to 04		-69.03333	76.83333	Woehler and Johnstone (1991) in Croxall et al (1995)					
135	Hop Island, Rauer Islands, Prydz Bay	East Antarctica	RAU_SG_07	IS_72721	-68.83333	77.75000	Green and Johnstone (1986) in Croxall et al (1995); Hodum (1999); Weathers et al (2000); Hodum (2002); Southwell and Emmerson AAD *unpubl.data*	1994		Years	2015	December
136	Filla Island	East Antarctica	RAU_SG_03	IS_72650	-68.80803	77.84146	Southwell and Emmerson AAD *unpubl. data*	2015		Days	2015	

137	Kazak Island	East Antarctica	VES_SG_12	IS_72461	-68.66358	77.83723	Southwell and Emmerson AAD *unpubl. data*	2017		Days	2017	
138	Crooked (Krok) Fjord Islands, Vestfold Hills	East Antarctica	VES_SG_13	R_10001	-68.65500	78.05250	Brown (1966); Johnstone et al (1973)	1966				
139	Mule Island, Vestfold Hills	East Antarctica	VES_SG_11	IS_72390	-68.64639	77.82722	Brown (1966); Johnstone et al (1973)	1966				
140	Mule Peninsula (multiple sites)	East Antarctica	VES_SG_13	R_10001	-68.63333	77.96667	Brown (1966) Johnstone et al (1973); Kiernan et al (2002); Southwell and Emmerson AAD *unpubl. data*	1996		Years	2017	January
141	Marine Plain, Mule Peninsula, Vestfold Hills	East Antarctica	VES_SG_13	R_10001	-68.63056	78.13194	(ASPA No. 143, 2013)					
142	Gardner Island, Vestfold Hills	East Antarctica	VES_SG_10	IS_72276	-68.57833	77.86972	Brown (1966); Johnstone et al (1973)	1966				
143	Broad Peninsula (multiple sites)	East Antarctica	VES_SG_13	R_10001	-68.56667	78.25000	Brown (1966); Johnstone et al (1973); Kiernan et al (2002); Southwell and Emmerson AAD *unpubl. data*	1996		Years	2017	January
144	Anchorage Island, Vestfold Hills	East Antarctica	VES_SG_09	IS_73683	-68.56167	77.93167	Brown (1966); Johnstone et al (1973); Southwell and Emmerson AAD *unpubl. data*	1966		Years	2018	February
145	Trigwell Island, Vestfold Hills	East Antarctica	VES_SG_09	IS_73680	-68.55722	77.94694	Brown (1966); Johnstone et al (1973); Southwell and Emmerson AAD *unpubl. data*	1966		Years	2018	February
146	Bluff Island, Vestfold Hills	East Antarctica	VES_SG_09	IS_72270	-68.55389	77.90833	Brown (1966); Johnstone et al (1973)	1966				

147	Eastern Long Fjord	East Antarctica	VES_SG_13	R_1001	-68.55000	78.25000	Brown (1966); Johnstone et al (1973)	1966				
148	Turner Island, Vestfold Hills	East Antarctica	VES_SG_09	IS_72266	-68.54694	77.89139	Brown (1966); Johnstone et al (1973)	1966				
149	Magnetic Island, Vestfold Hills	East Antarctica	VES_SG_09	IS_72260	-68.54306	77.90889	Brown (1966); Johnstone et al (1973); Southwell and Emmerson AAD *unpubl. data*	1966		Years	2018	February
150	Lugg Island, Vestfold Hills	East Antarctica	VES_SG_09	IS_73650	-68.53778	77.95694	Brown (1966); Johnstone et al (1973); Southwell and Emmerson AAD *unpubl. data*	1966		Years	2018	February
151	Plough (Plog) Island, Vestfold Hills	East Antarctica	VES_SG_09	IS_73635	-68.53333	78.00000	Brown (1966); Johnstone et al (1973)	1966				
152	Soldat Island, Long Fjord, Vestfold Hills	East Antarctica	VES_SG_13	IS_73597	-68.52250	78.17861	Brown (1966); Johnstone et al (1973)	1966				
153	Zvuchnyy Island, Long Fjord, Vestfold Hills	East Antarctica	VES_SG_13	IS_73578	-68.50806	78.11583	Brown (1966); Johnstone et al (1973)	1966				
154	Partizan Island, Long Fjord, Vestfold Hills	East Antarctica	VES_SG_13	IS_73557	-68.50000	78.18333	Brown (1966); Johnstone et al (1973)	1966				
155	Topografov Island, Long Fjord, Vestfold Hills	East Antarctica	VES_SG_13	IS_73546	-68.49639	78.17861	Brown (1966); Johnstone et al (1973)	1966				
156	Long Peninsula (five sites), Vestfold Hills	East Antarctica	VES_SG_13	R_1001	-68.48333	78.11667	Brown (1966); Johnstone et al (1973); Kiernan et al (2002); Southwell and Emmerson AAD unpubl. data	1996		Years	2017	January
157	Southern side of Tryne Fjord	East Antarctica	VES_SG_13	R_1001	-68.45833	78.37333	Brown (1966); Johnstone et al (1973)	1966				
158	Ace Lake, Vestfold Hills	East Antarctica	VES_SG_13	R_1001	-68.40000	78.18333	Rankin et al (1999)					

159	Gaussberg	East Antarctica	WIL_SG_04	R_294	-66.80000	89.20000	Falla (1937); Woehler and Johnstone (1991) in Croxall et al (1995)	1956				
160	Haswell Island, Haswell Archipelago	East Antarctica	WIL_SG_03	IS_70637	-66.51667	93.00000	Pryor (1968); Starck (1980); Golubev (2022); ASPA No. 127 (2022)	1999		Years	2001	
161	"The Hippo" Nunatak, David Island	East Antarctica			-66.41667	98.00000	Falla (1937)	1912	December			
162	"Watson Bluff" Nunatak, David Island	East Antarctica			-66.41667	99.00000	Falla (1937)	1912	December			
163	Bunger Hills (multiple sites)	East Antarctica			-66.16667	101.00000	Verkulich and Hiller (1994); Gibson (2000); Leishman et al (2020)					
164	"Island B", Davis Islands	East Antarctica	KNO_SG_04	IS_70732	-66.68333	108.40000	Melick et al (1996)	1993	December	Season	1994	
165	Hudson Island (three sites), Davis Islands	East Antarctica	KNO_SG_04	IS_70712	-66.65000	108.41667	Law (1962); Melick et al (1996)	1993	December	Season	1994	
166	Nelly Island, Frazier Islands	East Antarctica	CAS_SG_01	IS_70519	-66.23333	110.18333	Cowan (1981); ASPA No. 160 (2013)					
167	Dewart Island, Frazier Islands	East Antarctica	CAS_SG_01	IS_70505	-66.21667	110.16667	Cowan (1981); ASPA No. 160 (2013)					
168	Peterson Island, South Windmill Islands	East Antarctica	CAS_SG_09	IS_73864	-66.46667	110.50000	Murray and Luders (1990); Olivier et al (2004)	2002		Season	2003	
169	Browning Peninsula, South Windmill Islands	East Antarctica	CAS_SG_09	R_73	-66.46667	110.55000	Olivier et al (2004)	2002		Season	2003	
170	Browning Islands, South Windmill Islands	East Antarctica	CAS_SG_09		-66.46667	110.61667	Olivier et al (2004)	2002		Season	2003	
171	Holl Island, South Windmill Islands	East Antarctica	CAS_SG_07	IS_73846	-66.41667	110.41667	Olivier et al (2004)	2002		Season	2003	
172	O'Connor Island, South Windmill Islands	East Antarctica	CAS_SG_07	IS_73850	-66.41667	110.46667	Cowan (1981); Olivier et al (2004)	2002		Season	2003	

173	Cloyd Island, South Windmill Islands	East Antarctica	CAS_SG_08	IS_73848	-66.41667	110.55000	Olivier et al (2004)	2002		Season	2003	
174	Ford Island, South Windmill Islands	East Antarctica	CAS_SG_08	IS_73841	-66.40000	110.51667	Olivier et al (2004)	2002		Season	2003	
175	Herring Island, South Windmill Islands	East Antarctica	CAS_SG_08	IS_73847	-66.40000	110.63333	Murray and Luders (1990); Olivier et al (2004)	2002		Season	2003	
176	Robinson Ridge, South Windmill Islands	East Antarctica	CAS_SG_08	R_53/R_54	-66.36667	110.60000	Olivier et al (2004)	2002		Season	2003	
177	Mitchell Peninsula, North Windmill Islands	East Antarctica	CAS_SG_06	R_34	-66.33333	110.53333	Olivier et al (2004)	2002		Season	2003	
178	Warrington Island, North Windmill Islands	East Antarctica	CAS_SG_06	IS_73832	-66.33333	110.46667	Olivier et al (2004)	2002		Season	2003	
179	Ardery Island, South Windmill Islands	East Antarctica	CAS_SG_07	IS_73838	-66.33333	110.41667	Cowan (1981); Barbraud and Baker (1998); Barbraud et al (1999); Olivier et al (2004)	2002		Season	2003	
180	Odbert Island, South Windmill Islands	East Antarctica	CAS_SG_08	IS_73839	-66.33333	110.55000	Cowan (1981); Olivier et al (2004)	2002		Season	2003	
181	Pidgeon Island, North Windmill Islands	East Antarctica	CAS_SG_06	IS_73831	-66.31667	110.45000	Olivier et al (2004)	2002		Season	2003	
182	Hollin/Midgley Islands, North Windmill Islands	East Antarctica	CAS_SG_06	IS_70552/IS_70569	-66.31667	110.40000	Olivier et al (2004)	2002		Season	2003	
183	Beall Island, North Windmill Islands	East Antarctica	CAS_SG_06	IS_73818	-66.30000	110.48333	Olivier et al (2004)	2002		Season	2003	
184	Bailey Peninsula, North Windmill Islands	East Antarctica	CAS_SG_05	R_27	-66.28333	110.51667	Murray and Luders (1990); Olivier et al (2004)	2002		Season	2003	
185	Shirley Island, North Windmill Islands	East Antarctica	CAS_SG_05	IS_73811	-66.28333	110.50000	Olivier et al (2004)	2002		Season	2003	
186	Reeve Hill, Casey Station	East Antarctica	CAS_SG_05	R_27	-66.28333	110.53333	Olivier et al (2005)	1984		Years	2003	
187	Budnick Hill, Budd Coast	East Antarctica	CAS_SG_05		-66.28333	110.53333	(ASPA No. 135, 2013)					

188	Whitney Point, Casey Station area	East Antarctica	CAS_SG_05	R_18	-66.25000	110.53333	Woehler pers. comm. in Croxall et al (1995)	1989			1990	
189	Clark Peninsula, North Windmill Islands	East Antarctica	CAS_SG_05	R_18	-66.25389	110.56333	SCAR Bulletin (2002); Olivier et al (2004)	2002		Season	2003	
190	Balaena Islands	East Antarctica	BAL_SG_01	IS_70165/IS_70166	-66.01667	111.10000	Woehler and Johnstone (1991) in Croxall et al (1995)	1956				
191	Ifo Island, Point Geologie Archipelago	Adelie Land	DUM_SG_01	IS_70698	-66.62917	139.73889	Micol and Jouventin (2001)	1998		Season	1999	
192	Fram Island, Point Geologie Archipelago	Adelie Land	DUM_SG_01	IS_70700/IS_70703/IS_70704	-66.63333	139.83333	Micol and Jouventin (2001)	1998		Season	1999	
193	Le Mauguen Island, Point Geologie Archipelago	Adelie Land	DUM_SG_03	IS_70730	-66.67000	140.01000	Micol and Jouventin (2001); ASPA No. 120 (2022)	2019		Season	2020	
194	Dumont d'Urville, Ile des Petrels, Point Geologie Archipelago	Adelie Land	DUM_SG_03	IS_70717	-66.66667	140.00110	Chastel et al (1993); Barbraud et al (2000); Micol and Jouventin (2001)	1981		Years	1997	
195	Bon Docteur Nunatak, Point Geologie Archipelago	Adelie Land	DUM_SG_03	IS_70735	-66.66667	140.01667	Micol and Jouventin (2001); ASPA No. 120 (2022)	2019		Season	2020	
196	Rostand Island, Point Geologie Archipelago	Adelie Land	DUM_SG_03	IS_70727	-66.66861	140.01889	Micol and Jouventin (2001); ASPA No. 120 (2022)	2019		Season	2020	
197	Lamarck Island, Point Geologie Archipelago	Adelie Land	DUM_SG_03	IS_70725	-66.66611	140.02694	Micol and Jouventin (2001); ASPA No. 120 (2022)	2019		Season	2020	
198	Bernard Island, Point Geologie Archipelago	Adelie Land	DUM_SG_03	IS_70719	-66.66222	140.02944	Micol and Jouventin (2001); ASPA No. 120 (2022)	2019		Season	2020	
199	Pasteur Island, Point Geologie Archipelago	Adelie Land	DUM_SG_02	IS_70696	-66.62380	140.09160	Micol and Jouventin (2001)	1998		Season	1999	
200	Cap Bienvenue	Adelie Land	DUM_SG_04	R_247	-66.71667	140.51667	Barbraud et al (1999)	1997	December	Month	1998	January
201	Cap Jules	Adelie Land	DUM_SG_05	R_259	-66.73333	140.91667	Barbraud et al (1999)	1997	December	Month	1998	January

202	Cape Hunter	Adelie Land	GEO_SG_00	R_406	-66.96667	142.66667	Barbraud et al (1999)	1997	December	Month	1998	January
203	Cape Denison	Adelie Land	GEO_SG_02	R_99999	-67.00000	142.66667	Falla (1937); Isenmann et al (1970); Cowan (1981); ASPA No. 162 (2014)					
204	Cape Gray	Adelie Land	GEO_SG_08	IS_70824	-66.83333	143.55000	Falla (1937)					
205	Cape Pigeon Rocks	Adelie Land	GEO_SG_11	R_419	-66.98333	143.78333	Falla (1937); Barbraud et al (1999)	1997	December	Month	1998	January
206	"Island D"	Adelie Land	GEO_SG_11	IS_70983	-66.95000	143.90000	Barbraud et al (1999)	1997	December	Month	1998	January
207	Stillwell Island	Adelie Land	GEO_SG_10	IS_70934	-66.91667	143.91667	Barbraud et al (1999)	1997	December	Month	1998	January
208	"Island C"	Adelie Land	GEO_SG_11	IS_70988	-66.95000	143.91667	Barbraud et al (1999)	1997	December	Month	1998	January
209	Moyes Islands	Adelie Land	GEO_SG_12	IS_71038	-67.00000	143.93333	Barbraud et al (1999)	1997	December	Month	1998	January
210	"Island B"	Adelie Land	GEO_SG_11	IS_70957	-66.93333	143.95000	Barbraud et al (1999)	1997	December	Month	1998	January
211	"Island A"	Adelie Land	GEO_SG_11	IS_70996	-66.96667	143.95000	Barbraud et al (1999)	1997	December	Month	1998	January
212	Horn Bluff and Penguin Point	Adelie Land			-68.31667	149.61667	Falla (1937)					
213	Balleny Islands (inc. Sabrina Island)	Antarctic East			-66.91667	163.33333	Hatherton et al (1964); Kinsky (1965) and Robertson et al (1980) in Greenfield and Smellie (1992)	1964				
214	Scott Island	Antarctic East			-67.40000	179.91667	Greenfield and Smellie (1992); Wilson and Harper (1996)	1967		Years	1982	
215	Morozumi Range	North Victoria Land			-71.60222	161.83333	Watson et al (1991); Greenfield and Smellie (1992); Pinkerton et al (2015)					
216	Cape Adare	North Victoria Land			-71.30000	170.15000	Reid (1962); Greenfield and Smellie (1992)	1961	December			
217	Duke of York Island	North Victoria Land			-71.61667	170.06667	Watson et al (1971); Greenfield and Smellie (1992)					

218	Edisto Inlet, Cape Hallett Area	North Victoria Land			-72.33333	170.08333	Harrington (1960) in Greenfield and Smellie (1992); Maher (1962); Ricker (1964); Greenfield and Smellie (1992)	1960		Season	1961	
219	Felsite Island, Cape Hallett area	North Victoria Land			-72.43330	169.81667	Harrington (1960) in Greenfield and Smellie (1992); Maher (1962); Ricker (1964)	1960	December	Season		
220	Crater Cirque	North Victoria Land			-72.63333	169.36667	Harrington (1960) in Greenfield and Smellie (1992); Ricker (1964); Green et al (2015)	1958	December			
221	Cape Washington	North Victoria Land			-74.65000	165.41667	Greenfield and Smellie (1992)	1984	December			
222	Beaufort Island (multiple sites), McMurdo Sound, Ross Sea	South Victoria Land			-76.95000	166.95000	(ASPA No. 105, 2006; 2022)					
223	Mount Helen Washington, Rockefeller Mountains	Marie Byrd Land			-78.08333	-155.25000	Siple and Lindsey (1937)	1934	December	Season		
224	Washington Ridge Nunatak, Rockefeller Mountains	Marie Byrd Land			-78.10000	-154.80222	Broady et al (1989)	1997	November	Season	1998	January
225	Mount Paterson Nunatak (two sites), Rockefeller Mountains	Marie Byrd Land			-78.03333	-154.60222	Broady et al (1989)	1997	November	Season	1998	January
226	Saunders Mountain	Marie Byrd Land			-76.88333	-145.70000	Harper et al (1984) in Greenfield and Smellie (1992)					
227	Marujupu Peak, Fosdick Mountains	Marie Byrd Land			-76.51667	-145.61667	Perkins (1945); Greenfield and Smellie (1992)	1940	November	Season		
228	Mount McCoy	Marie Byrd Land			-75.86667	-141.16667	Greenfield and Smellie (1992)	1990		Season	1991	
229	Mount Prince, Perry Range	Marie Byrd Land			-75.96667	-134.18333	Strandtman (1978) in Greenfield	1990	December	Season		

							and Smellie (1992); Greenfield and Smellie (1992)					
230	Kennel Peak, Demas Range	Marie Byrd Land			-75.01667	-133.56667	Greenfield and Smellie (1992)	1990				
231	Western Martin Peninsula	Marie Byrd Land			-74.18333	-115.08333	Pankurst pers. comms. in Croxall et al (1995)	1991			1992	
232	Hedin Nunatak, Mt Murphy	Marie Byrd Land			-75.31667	-111.28333	Greenfield and Smellie (1992)	1990		Season	1991	
233	"Petrel Nunatak", Mt Murphy	Marie Byrd Land			-75.38333	-111.23333	Greenfield and Smellie (1992)	1990		Season	1991	
234	"Notebook Cliffs", Mt Murphy	Marie Byrd Land			-75.38333	-111.10000	Greenfield and Smellie (1992)	1990		Season	1991	
235	Sechrist Peak, Mt Murphy	Marie Byrd Land			-75.38333	-111.03333	Greenfield and Smellie (1992)	1990		Season	1991	
236	Kay Peak, Mt Murphy	Marie Byrd Land			-75.23333	-110.95000	Greenfield and Smellie (1992)	1990		Season	1991	
237	"Aubyn Ridge", Mt Murphy	Marie Byrd Land			-75.23333	-110.81667	Greenfield and Smellie (1992)	1990		Season	1991	
238	Mt Nickens	Ellsworth Land			-73.93333	-100.33333	Allen pers. comms. in Croxall et al (1995)	1968			1869	
239	Mt Moses	Ellsworth Land			-74.55000	-99.18333	Allen pers. comms. in Croxall et al (1995)	1968			1969	
240	Mt Faraway, Theron Mountains	Transantarctic Mountains			-79.20000	-28.83333	Fuchs and Hillary (1960) in Croxall et al (1995)	1967	January			
241	NE end of Coalseam Cliffs, Theron Mountains	Transantarctic Mountains			-79.16667	-28.83333	Brook and Beck (1972)	1967	January	Season		
242	Maro Cliffs near station Z.451	Transantarctic Mountains			-79.06667	-28.50000	Brook and Beck (1972)	1967	November	Season		
243	SW end of Lenton Bluff, Theron Mountains	Transantarctic Mountains			-79.00000	-28.21667	Brook and Beck (1972)	1966	December	Season		
244	Station Z.504, W of Jefferies Glacier, Theron Mountains	Transantarctic Mountains			-79.03333	-28.08333	Brook and Beck (1972)	1967	November	Season		
245	NE end of Lenton Bluff, Theron Mountains	Transantarctic Mountains			-79.00000	-28.00000	Brook and Beck (1972)	1967	November	Season		
246	Station Z.506,	Transantarctic			-78.80000	-27.83333	Brook and Beck (1972)	1967	November	Season		

	Theron Mountains	Mountains										
247	Station Z.508, W of Goldsmith Glacier, Theron Mountains	Transantarctic Mountains			-78.95000	-27.50000	Brook and Beck (1972)	1966	November	Season	1966	December
248	Genghis Hills	Transantarctic Mountains			-80.73333	-28.03333	Skidmore (1968) in Croxall et al (1995)	1968			1969	
249	"Skiltvakta", Shackleton Range	Transantarctic Mountains			-80.50000	-19.01667	Noble (1968) in Croxall et al (1995)	1967			1968	
250	Mt Provender, Shackleton Range	Transantarctic Mountains			-80.38333	-29.91667	Wright and Wyeth (1971), Wyeth (1971) and Marsh and Holden (1978) in Croxall et al (1995)	1971	January			
251	Mt Skidmore, Shackleton Range	Transantarctic Mountains			-80.31667	-28.95000	Skidmore (1968) in Croxall et al (1995)	1968			1969	
252	Fitzgerald Bluffs	South Antarctic Peninsula			-74.05000	-77.33333	Thomson pers. comms. in Croxall et al (1995)	1984			1985	
253	Mt McCann, Snow Mountains	South Antarctic Peninsula			-73.56667	-77.61667	Thomson pers. comms. in Croxall et al (1995)	1984			1985	
254	Mt Thornton, Snow Mountains	South Antarctic Peninsula			-73.56667	-77.11667	Thomson pers. comms. in Croxall et al (1995)	1984			1985	
255	Mt Benkert, Snow Mountains	South Antarctic Peninsula			-73.63333	-76.66667	Thomson pers. comms. in Croxall et al (1995)	1984			1985	
256	Stephenson Nunatak, Alexander Island	Central south Antarctic Peninsula			-72.13333	-69.13333	Norman (1969)	1969	December			
257	Mussorgsky Peaks, Beethoven Peninsula, Alexander Island	Central south Antarctic Peninsula			-71.50000	-73.31667	C.M.Bell BAS records in Croxall et al (1995)	1970	December			
258	Planet Heights, Alexander Island	Central south Antarctic Peninsula			-71.21667	-68.78333	A. Crame and S. Grice BAS records in Croxall et al (1995)	1985			1986	
259	South side of "Saltire Glacier", Lully Foothills, Alexander Island	Central south Antarctic Peninsula			-70.86667	-69.61667	Lawther and Macallister (1973)	1973				

260	Ablation Point, Alexander Island	Central south Antarctic Peninsula			-70.80000	-68.35000	Fuchs and Adie (1949); Bentley (2004); (ASPA No. 147, 2017)	2004				
261	Lully Foothills	Central south Antarctic Peninsula			-70.76667	-69.53333	Barrett (1974)	1974	December			
262	Un-named nunatak, Lully Foothills, Alexander Island	Central south Antarctic Peninsula			-70.71667	-69.56667	Lawther and Macallister (1973)	1973				
263	Belemnite Point, Alexander Island	Central south Antarctic Peninsula			-70.65000	-68.53333	Lawther and Macallister (1973)	1973	October			
264	"Petrel Point", Mt Lepus	Central south Antarctic Peninsula			-70.63333	-67.30000	R.C. Pashley and P. J. Rowe BAS records in Croxall et al (1995)	1969			1970	
265	"Petrel Ridge", Alexander Island	Central south Antarctic Peninsula			-70.61667	-68.80000	Lawther and Macallister (1973)	1973				
266	South side of Lamina Peak, Alexander Island	Central south Antarctic Peninsula			-70.56667	-68.78333	Lawther and Macallister (1973)	1973				
267	Mt Courtauld	Central south Antarctic Peninsula			-70.33333	-67.50000	R.C. Pashley and P. J. Rowe BAS records in Croxall et al (1995)	1969			1970	
268	Marion Nunataks, Charcot Island	Central south Antarctic Peninsula			-69.75000	-75.25000	(ASPA No. 170, 2018)					
269	Brindle Cliffs	Central south Antarctic Peninsula			-69.38333	-68.55000	S. and J. Poncet *in litt.* in Croxall et al (1995)	1990	January			
270	Mica Island	Central south Antarctic Peninsula			-69.33333	-68.60000	S. and J. Poncet *in litt.* in Croxall et al (1995)	1990	January			
271	Cape Walcott	Central south Antarctic Peninsula			-69.08333	-63.31667	Lawther and Macallister (1973)	1973	November			
272	Athene Glacier	Central south Antarctic Peninsula			-68.93333	-64.20000	Barrett (1974)	1974	December			
273	Cronus Glacier	Central south Antarctic Peninsula			-68.83333	-63.91667	Barrett (1974)	1974	December			
274	Victory Nunatak	Central south Antarctic Peninsula			-68.75000	-64.36667	Barrett (1974)	1974	December			

275	Kay Nunatak	Central south Antarctic Peninsula			-68.68333	-64.66667	Barrett (1974)	1974	December			
276	Neny Fjord	Central south Antarctic Peninsula			-68.26667	-66.83333	Poncet and Poncet (1978)	1978	September			
277	Trail Inlet	Central south Antarctic Peninsula			-68.16667	-65.58333	Barrett (1974)	1975	January			
278	Terra Firma Islands	North-west Antarctic Peninsula			-68.70000	-67.53333	Poncet and Poncet (1978)	1978	September		1979	
279	Refuge Islands	North-west Antarctic Peninsula			-68.35000	-67.16667	Poncet and Poncet (1978)	1978	September		1979	
280	Roman Four Cliff Face	North-west Antarctic Peninsula			-68.20000	-66.95000	Norman (1968)	1968	November			
281	Neny Island	North-west Antarctic Peninsula			-68.20000	-67.03333	Friedmann (1945); Freeman (1946); Cowan (1981)	1946	November	Season		
282	Camp Point	North-west Antarctic Peninsula			-67.96667	-67.25000	Norman (1968)	1968	October			
283	Southern Peak of Lagotellerie	North-west Antarctic Peninsula			-67.88333	-67.40000	McGowan (1958)	1958				
284	Square Bay	North-west Antarctic Peninsula			-67.85000	-67.00000	Freeman (1946)	1946	November			
285	Broken Island	North-west Antarctic Peninsula			-67.81667	-66.95000	Scotland (1956)	1956	September		1957	
286	The Guebriants	North-west Antarctic Peninsula			-67.80000	-68.41667	Killingbeck (1962)	1962				
287	Holdfast Point	North-west Antarctic Peninsula			-66.80000	-66.60000	S. and J. Poncet *in litt.* in Croxall et al (1995)	1984	February			
288	Nicholl Head	North-west Antarctic Peninsula			-67.78333	-67.08333	Scotland (1956); Procter (1957)	1956	September			
289	Lainez Point, Pourquoi Pas Island	North-west Antarctic Peninsula			-67.68333	-67.81667	Procter (1957); S. and J. Poncet *in litt.* in Croxall et al (1995)	1986	February			
290	Perplex Ridge, Pourquoi Pas Island	North-west Antarctic Peninsula			-67.65000	-67.71667	S. and J. Poncet *in litt.* in Croxall et al (1995)	1986	February			

291	Conseil Hill, Pourquoi Pas Island	North-west Antarctic Peninsula			-67.60000	-67.46667	S. and J. Poncet *in litt.* in Croxall et al (1995)	1986	February			
292	Mt Liotard	North-west Antarctic Peninsula			-67.61667	-68.58333	Killingbeck (1962)	1962				
293	Rothera, Adelaide Island	North-west Antarctic Peninsula			-67.56667	-68.13333	Poncet and Poncet (1978); Milius (2000)	1995	November	Years	1998	March
294	Cape Saenz Paena	North-west Antarctic Peninsula			-67.55000	-67.65000	McGowan (1958)	1958				
295	Stork Nunatak, Rothera Point Area	North-west Antarctic Peninsula			-67.51667	-68.16667	Killingbeck (1962); Norman (1968)	1968	November			
296	Hansen Island	North-west Antarctic Peninsula			-67.10000	-67.61667	S. and J. Poncet *in litt.* in Croxall et al (1995)	1984	February			
297	"Schmidt Point", Crystal Sound	North-west Antarctic Peninsula			-66.91667	-67.03333	S. and J. Poncet *in litt.* in Croxall et al (1995)	1990	January			
298	Nunatak to NW of Mt Haskel	North-west Antarctic Peninsula			-66.75000	-64.26667	Fletcher (1977)	1978	January			
299	NE side of Mt Denuce	North-west Antarctic Peninsula			-66.71667	-64.20000	Fletcher (1977)	1978	January			
300	"Six Egg Ridge", Anderson Glacier	North-west Antarctic Peninsula			-66.36670	-64.10000	Tindal (1963)	1964	December			
301	South Casey	North-west Antarctic Peninsula			-66.36667	-63.75000	Tindal (1963)	1963	December			
302	Un-named Nunatak	North-west Antarctic Peninsula			-66.25000	-62.91667	Fletcher (1977)	1977	December			
303	West side of Eden Glacier	North-west Antarctic Peninsula			-66.20000	-63.25000	Tindal (1963)	1963	December			
304	Lizard Island	North-west Antarctic Peninsula			-65.68333	-64.45000	S. and J. Poncet *in litt.* in Croxall et al (1995)	1990	January			
305	Starbuck Glacier	North-west Antarctic Peninsula			-65.61667	-62.41667	Tindal (1963)	1963			1964	
306	Cape Perez	North-west Antarctic Peninsula			-65.40000	-64.10000	Saunders (1979)	1979				
307	Mt Demaria, Cape Tuxen	North-west Antarctic Peninsula			-65.28333	-64.13333	Smith (1960); Potts (1962);	1958				

							(Rodger, 1974)					
308	Argentine Islands	North-west Antarctic Peninsula			-65.25000	-64.28333	Watson et al (1971) in Croxall et al (1995)					
309	Lower cliffs of Mt Balch	North-west Antarctic Peninsula			-65.25000	-63.98333	Potts (1962); Thomas (1960); Lewis (1963)	1962				
310	Nunatak to SE of Skontorp Cove	North-west Antarctic Peninsula			-64.90000	-62.85000	Araya (1965)	1962	November			
311	Almirante Brown Station	North-west Antarctic Peninsula			-64.88333	-62.85000	Araya (1965)	1962				
312	Spigot Peak	North-west Antarctic Peninsula			-64.63333	-62.56667	S. and J. Poncet *in litt.* in Croxall et al (1995)	1989	December			
313	Mt Francais, Anvers Island	North-west Antarctic Peninsula			-64.63333	-63.43333	Wylie (1957); Parmalee et al (1977)	1957			1958	
314	Andrews Point to Ryswyck Bay, Anvers Island	North-west Antarctic Peninsula			-64.50000	-62.91667	S. and J. Poncet *in litt.* in Croxall et al (1995)	1987	January			
315	Lockyer Island	North-west Antarctic Peninsula			-64.45000	-57.61667	Andersson (1905)	1902				
316	Brabant Island	North-west Antarctic Peninsula			-64.25000	-62.33333	Furse (1986)	1984				
317	Cockburn Island	North-west Antarctic Peninsula			-64.21667	-56.81667	Ross (1847); Cowan (1981)	1843	January			
318	Point 536, James Ross Island	North-west Antarctic Peninsula			-64.20000	-57.75000	Cain (1985)	1985			1986	
319	Rohss Bay/Ineson Glacier, James Ross Island	North-west Antarctic Peninsula			-64.08333	-58.13333	Cain (1985)	1985			1986	
320	Lagrelius Point, James Ross Island	North-west Antarctic Peninsula			-63.91667	-58.30000	Taylor (1945)	1945			1946	
321	Moss Islands	North-west Antarctic Peninsula			-64.16556	-61.03500	Gonzalez-Zevallos et al (2013)	2011	January	Season		
322	Cierva Point, Danco Coast	North-west Antarctic Peninsula			-64.15000	-60.95000	Quintana et al (2000)	1991		Years	1996	
323	Davis Island	North-west Antarctic Peninsula			-64.10000	-62.06667	S. and J. Poncet *in litt.* in Croxall et al (1995)	1988	December			

324	"Marr Island"	North-west Antarctic Peninsula			-63.93333	-58.25000	Lamb (1945); Taylor (1945)	1945			1946	
325	Mahogany Bluff, Vega Island	North-west Antarctic Peninsula			-63.88333	-57.21667	Andersson (1905)	1902				
326	Cape Gordon Cliffs, Vega Island	North-west Antarctic Peninsula			-63.85000	-57.05000	Lamb (1945); Marshall (1945)	1945	December			
327	Carlson Island	North-west Antarctic Peninsula			-63.88333	-58.26667	Lamb (1945); Taylor (1945)	1945			1946	
328	Devil Island	North-west Antarctic Peninsula			-63.80000	-57.28333	Marshall (1945)	1945	November	Month	1945	December
329	Eagle Island	North-west Antarctic Peninsula			-63.66677	-57.48333	Lamb (1945); Taylor (1945)	1945			1946	
330	Cape Wollaston, Trinity Island	North-west Antarctic Peninsula			-63.66667	-60.78333	S. and J. Poncet *in litt.* in Croxall et al (1995)	1987	January			
331	Andersson Island	North-west Antarctic Peninsula			-63.58333	-56.58333	Andersson (1905)	1902				
332	Paulet Island	North-west Antarctic Peninsula			-63.58333	-55.78333	Fritzsche (2005)					
333	Duse Bay	North-west Antarctic Peninsula			-63.56667	-57.25000	Andersson (1905)	1902				
334	Marescot Point	North-west Antarctic Peninsula			-63.48333	-58.58333	S. and J. Poncet *in litt.* in Croxall et al (1995)	1990	February			
335	Joinville Island	North-west Antarctic Peninsula			-63.25000	-55.75000	Taylor (1956)	1956			1957	
336	"South East Point", Deception Island	North-west Antarctic Peninsula			-62.95000	-60.63333	Bird (1965)	1965	December			
337	Bridgeman Island	North-west Antarctic Peninsula			-62.06667	-56.73333	Furse (1978)	1970			1971	
338	Elephant Island	North-west Antarctic Peninsula			-61.13333	-55.11667	Furse (1978); Furse and Bruce (1979)	1970				
339	Mt Lombard	North-east Antarctic Peninsula			-64.51667	-59.66667	Lewis (1980)	1981	January			
340	Red Island	North-east Antarctic Peninsula			-63.73333	-57.86667	Lamb (1945); Taylor (1945)	1945			1946	

341	Inaccessible Islands	South Orkney Islands			-60.56667	-46.73333	S. and J. Poncet *in litt.* in Croxall et al (1995)	1986	December			
342	Sandefjord Bay, Coronation Island	South Orkney Islands			-60.61667	-46.03333	Ardley (1936)	1933	January			
343	Moe Island	South Orkney Islands			-60.73333	-45.68333	Hall (1957)	1957			1958	
344	Signy Island	South Orkney Islands			-60.71667	-45.63333	Scotland (1958)	1957	October	Season	1958	February
345	Borge Bay	South Orkney Islands			-60.71667	-45.61667	Ardley (1936)	1933	January			
346	Olivine Point, Coronation Island	South Orkney Islands			-60.66667	-45.48333	Smith (1965)	1965	January			
347	Palmer Bay, Coronation Island	South Orkney Islands			-60.61667	-45.33333	Hall (1957)	1957			1958	
348	Saunders Point, Coronation Island	South Orkney Islands			-60.70000	-45.31667	Smith (1965)	1964	December			
349	S side of Mt Noble, Coronation Island	South Orkney Islands			-60.65000	-45.26667	Hall (1957)	1957			1958	
350	Pulpit Mountain, Coronation Island	South Orkney Islands			-60.68333	-45.21667	Hall (1957)	1957			1958	
351	"The Tower", Coronation Island	South Orkney Islands			-60.63333	-45.20000	Hall (1957)	1957			1958	
352	East Cape, Coronation Island	South Orkney Islands			-60.63333	-45.18333	Hall (1957)	1957			1958	
353	SW Gibbon Bay, Coronation Island	South Orkney Islands			-60.65000	-45.18333	Hall (1957)	1957			1958	
354	The Divide Range, Coronation Island	South Orkney Islands			-60.73333	-45.16667	Hall (1957)	1957			1958	
355	"Red Flag Hill", Coronation Island	South Orkney Islands			-60.66667	-45.15000	Hall (1957)	1957			1958	
356	The Turret, Coronation Island	South Orkney Islands			-60.66667	-45.15000	Hall (1957)	1957			1958	
357	Matthews Islands, Coronation Island	South Orkney Islands			-60.75000	-45.15000	Smith (1965)	1965	January			
358	Whale Skerries, Powell Island	South Orkney Islands			-60.70000	-45.10000	Hall (1957)	1957			1958	
359	"Camp Peninsula", Powell Island	South Orkney Islands			-60.68333	-45.03333	Scotland (1958)	1957				

360	Ellefsen Harbour, Powell Island	South Orkney Islands			-60.73333	-45.03333	Ardley (1936)	1933	January			
361	Michelsen Island	South Orkney Islands			-60.73333	-45.03333	Scotland (1958) in Croxall et al (1995)	1957			1958	
362	Crags inland of "Cow Point", Powell Island	South Orkney Islands			-60.66667	-45.01667	Hall (1957)	1957			1958	
363	Northern cliffs, Powell Island	South Orkney Islands			-60.63333	-45.01667	S. and J. Poncet *in litt.* in Croxall et al (1995)	1983	December			
364	East coast, Powell Island	South Orkney Islands			-60.70000	-45.01667	S. and J. Poncet *in litt.* in Croxall et al (1995)	1983	December			
365	Fredriksen Island	South Orkney Islands			-60.73333	-45.00000	Ardley (1936) in Croxall et al (1995); Hall (1957)	1932			1933	
366	Saddle Island	South Orkney Islands			-60.61667	-44.83333	Clarke (1906) in Croxall et al (1995)	1903			1904	
367	Weddell Islands	South Orkney Islands			-60.63333	-44.83333	Ardley (1936) in Croxall et al (1995)	1932			1933	
368	Laurie Island (multiple sites)	South Orkney Islands			-60.73333	-44.61667	Clarke (1906) in Croxall et al (1995)	1903			1904	
369	Twitcher Rock, Thule Island, South Sandwich Islands	Antarctic West			-59.45639	-27.28333	Convey et al (1999)	1997	January			
370	Cook Island, South Sandwich Islands	Antarctic West			-59.44161	-27.19021	Poncet (1997); Convey et al (1999)	1997	January	Days	1997	January
371	Thule Island, South Sandwich Islands	Antarctic West			-59.43733	-27.35780	Poncet (1997); Convey et al (1999)	1997	January	Days	1997	January
372	Bellingshausen Island, South Sandwich Islands	Antarctic West			-59.41251	-27.08310	Poncet (1997); Convey et al (1999)	1997	January	Days	1997	January
373	Freezland Rocks, South Sandwich Islands	Antarctic West			-59.02889	-26.72583	Poncet (1997); Convey et al (1999)	1997	January	Hours		
374	Wilson Rocks, South Sandwich Islands	Antarctic West			-59.02167	-26.68694	Poncet (1997); Convey et al (1999)	1997	January	Hours		

375	Grindle Rocks, South Sandwich Islands	Antarctic West			-59.01667	-26.65000	Poncet (1997); Convey et al (1999)	1997	January	Hours		
376	Bristol Island, South Sandwich Islands	Antarctic West			-59.01429	-26.53431	Poncet (1997); Convey et al (1999)	1997	January	Days	1997	January
377	Montagu Island, South Sandwich Islands	Antarctic West			-58.45871	-26.37400	Poncet (1997); Convey et al (1999)	1997	January	Days	1997	January
378	Saunders Island, South Sandwich Islands	Antarctic West			-57.80508	-26.38436	Poncet (1997); Convey et al (1999)	1997	January	Days	1997	January
379	Vindication Island, South Sandwich Islands	Antarctic West			-57.12049	-26.83072	Poncet (1997); Convey et al (1999)	1997	January	Days		
380	Visokoi Island, South Sandwich Islands	Antarctic West			-56.70664	-27.19460	Poncet (1997); Convey et al (1999)	1997	January	Days	1997	January
381	Crater Bay, Leskov Island, South Sandwich Islands	Antarctic West			-56.66667	-28.10000	Convey et al (1999)	1997	January	Days		
382	Pacific Point, Zavodovski Island, South Sandwich Islands	Antarctic West			-56.31667	-27.60000	Convey et al (1999)	1997	January	Days	1997	January
383	Candlemas Island, South Sandwich Islands	Antarctic West			-56.08333	-26.65000	Poncet (1997); Convey et al (1999)	1997	January	Month	1997	February
384	South Georgia (total population)	Transition			-54.25000	-36.75694	Leader-Williams (1975); Prince and Payne (1979); Croxall and Prince (1980); Prince and Croxall (1983); Clarke et al (2012)	1977		Years	1982	
385	Willis Islands	Transition			-54.00000	-38.20000	Prince and Poncet *unpubl. data* in Croxall et al (1995)	1987			1988	
386	Bird Island, South Georgia	Transition			-54.00000	-38.05000	Hunter et al (1978); Croxall and Prince (1980)					

387	SW Cape Paryadin	Transition			-54.06667	-38.01667	Prince and Poncet *unpubl. data* in Croxall et al (1995)	1986			1987	
388	Hesse Peak	Transition			-54.03333	-38.00000	M. R. Payne BAS records in Croxall et al (1995)	1972			1973	
389	SE Cape Paryadin	Transition			-54.06667	-38.00000	G. Thomas, T.S.McCann BAS records in Croxall et al (1995)	1976			1977	
390	Snow Peak	Transition			-54.01667	-37.91667	G. Thomas, T.S.McCann , L. Kearsley BAS records in Croxall et al (1995)	1976			1977	
391	N of Romerof Head	Transition			-54.05000	-37.86667	P. Martin BAS records in Croxall et al (1995)	1981			1982	
392	Schlieper Bay	Transition			-54.05000	-37.83333	G. Thomas BAS records in Croxall et al (1995)	1976			1977	
393	Cape North	Transition			-53.96667	-37.73333	Prince and Poncet *unpubl. data* in Croxall et al (1995)	1987			1988	
394	Ice Fjord	Transition			-54.06667	-37.68333	Prince and Poncet *unpubl. data* in Croxall et al (1995)	1986			1987	
395	N of Samuel Island	Transition			-54.18333	-37.61667	J. Hall BAS records in Croxall et al (1995)	1976			1977	
396	Nilse Hullett	Transition			-54.16667	-37.58333	J. Hall BAS records in Croxall et al (1995)	1976			1977	
397	Wales Head	Transition			-54.00000	-37.56667	Prince and Poncet *unpubl. data* in Croxall et al (1995)	1986			1987	
398	NE of MacDonald Cove	Transition			-54.00000	-37.48333	Prince and Poncet *unpubl. data* in Croxall et al (1995)	1987			1988	
399	Cape Rosa	Transition			-54.18333	-37.41667	Prince and Poncet *unpubl. data* in Croxall et al (1995)	1986			1988	
400	S of Cape Rosa	Transition			-54.18333	-37.41667	Prince and Poncet *unpubl. data* in Croxall et al (1995)	1986			1988	

401	Shallop Cove	Transition			-54.21667	-37.33333	D. I. M. MacDonald BAS records in Croxall et al (1995)	1976			1977	
402	S of King Haakon Bay	Transition			-54.15000	-37.33333	Prince and Poncet *unpubl. data* in Croxall et al (1995)	1986			1987	
403	Prince Olav Harbour	Transition			-54.06667	-37.13333	Prince and Poncet *unpubl. data* in Croxall et al (1995)	1987			1988	
404	SE of Possession Bay	Transition			-54.11667	-37.13333	A. Down BAS records in Croxall et al (1995)	1964			1965	
405	Annenkov Island	Transition			-54.48333	-37.08333	Prince and Poncet *unpubl. data* in Croxall et al (1995)	1986			1988	
406	E of Possession Bay	Transition			-54.08333	-37.06667	Prince and Poncet *unpubl. data* in Croxall et al (1995)	1986			1987	
407	W of Crean Glacier	Transition			-54.16667	-37.01667	A. Down BAS records in Croxall et al (1995)	1964			1965	
408	Fanning Ridge	Transition			-54.33333	-37.01667	Prince and Poncet *unpubl. data* in Croxall et al (1995)	1986			1987	
409	Larvik	Transition			-54.36667	-36.90000	C. Johnson BAS records in Croxall et al (1995)	1975			1976	
410	Jacobsen Bight	Transition			-54.41667	-36.85000	D. I. M. MacDonald BAS records in Croxall et al (1995)	1976			1977	
411	W of Fortuna Bay	Transition			-54.11667	-36.80000	A. Down BAS records in Croxall et al (1995)	1964			1965	
412	above Konig Glacier	Transition			-54.18333	-36.80000	Prince and Poncet *unpubl. data* in Croxall et al (1995)	1987			1988	
413	Three Brothers area (three sites)	Transition			-54.26667	-36.80000	A. Down BAS records in Croxall et al (1995)	1964			1965	
414	Stromness, Husvik	Transition			-54.16667	-36.71667	Prince and Poncet *unpubl. data* in Croxall et al (1995)	1987			1988	

415	S of Hercules Bay	Transition			-54.11667	-36.66667	Prince and Poncet *unpubl. data* in Croxall et al (1995)	1986			1987	
416	Rocky Bay	Transition			-54.48333	-36.66667	J. Hall BAS records in Croxall et al (1995)	1976			1977	
417	Mt Sugartop	Transition			-54.36667	-36.63333	A. Down BAS records in Croxall et al (1995)	1964			1965	
418	Ducloz Head	Transition			-54.51667	-36.63333	Prince and Poncet *unpubl. data* in Croxall et al (1995)	1986			1987	
419	Grytviken	Transition			-54.28333	-36.51667	Prince and Poncet *unpubl. data* in Croxall et al (1995)	1986			1987	
420	Maiviken area	Transition			-54.23333	-36.50000	S. Hunter BAS records in Croxall et al (1995)	1980			1981	
421	above Hesteslette n	Transition			-54.30000	-36.50000	S. Hunter BAS records in Croxall et al (1995)	1979			1980	
422	Leon Head	Transition			-54.55000	-36.50000	A. Burkitt, B. Mair BAS records in Croxall et al (1995)	1976			1977	
423	W of Nordenskjol d Glacier	Transition			-54.33333	-36.40000	Prince and Poncet *unpubl. data* in Croxall et al (1995)	1986			1987	
424	Barff Point	Transition			-54.23333	-36.40000	N. Leader-Williams BAS records in Croxall et al (1995)	1973			1976	
425	N of Brogger Glacier	Transition			-54.53333	-36.38333	A. Burkitt, B. Mair BAS records in Croxall et al (1995)	1976			1977	
426	Nordenskjol d Peak	Transition			-54.48333	-36.35000	Prince and Poncet *unpubl. data* in Croxall et al (1995)	1986			1987	
427	S of Wheeler Glacier	Transition			-54.60000	-36.35000	J. Tallowin BAS records in Croxall et al (1995)	1972			1973	
428	Barff Peninsula	Transition			-54.25000	-36.33333	N. Leader-Williams BAS records in Croxall et al (1995)	1973			1976	
429	Barff Peninsula	Transition			-54.30000	-36.33333	N. Leader-Williams BAS records	1973			1976	

							in Croxall et al (1995)					
430	E Nordenskjold	Transition			-54.33333	-36.33333	N. Leader-Williams BAS records in Croxall et al (1995)	1973			1976	
431	Barff Peninsula	Transition			-54.30000	-36.30000	N. Leader-Williams BAS records in Croxall et al (1995)	1973			1976	
432	Sorling Valley	Transition			-54.36667	-36.30000	N. Leader-Williams BAS records in Croxall et al (1995)	1973			1976	
433	Mt Kling	Transition			-54.50000	-36.30000	N. Leader-Williams BAS records in Croxall et al (1995)	1973			1976	
434	E of Diaz Cove	Transition			-54.75000	-36.30000	Prince and Poncet *unpubl. data* in Croxall et al (1995)	1986			1987	
435	Ranvik	Transition			-54.80000	-36.25000	Prince and Poncet *unpubl. data* in Croxall et al (1995)	1986			1987	
436	Tijuca Point	Transition			-54.35000	-36.21667	Prince and Poncet *unpubl. data* in Croxall et al (1995)	1986			1987	
437	Hound Bay	Transition			-54.36667	-36.20000	N. Leader-Williams BAS records in Croxall et al (1995)	1973			1976	
438	Luisa Bay	Transition			-54.38333	-36.16667	N. Leader-Williams BAS records in Croxall et al (1995)	1973			1976	
439	St Andrews Bay	Transition			-54.43333	-36.16667	N. Leader-Williams BAS records in Croxall et al (1995)	1973			1976	
440	Paradise Beach	Transition			-54.83333	-36.16667	J. Tallowin BAS records in Croxall et al (1995)	1972			1987	
441	Drygalski Fjord	Transition			-54.81667	-36.16667	Prince and Poncet *unpubl. data* in Croxall et al (1995)	1986			1987	
442	Cape Disappointment	Transition			-54.88333	-36.11667	J. Tallowin BAS records in Croxall et al (1995)	1972			1987	
443	Green Island	Transition			-54.88333	-36.10000	Prince and Poncet *unpubl. data* in	1986			1973	

							Croxall et al (1995)					
444	Drygalski Fjord	Transition			-54.81667	-36.08333	Prince and Poncet *unpubl. data* in Croxall et al (1995)	1986			1987	
445	Little Moltke Harbour	Transition			-54.53333	-36.06667	Prince and Poncet *unpubl. data* in Croxall et al (1995)	1986			1987	
446	Mt Krokisius	Transition			-54.50000	-36.05000	N. Leader-Williams BAS records in Croxall et al (1995)	1973			1976	
447	Moltke Harbour	Transition			-54.51667	-36.05000	Prince and Poncet *unpubl. data* in Croxall et al (1995)	1986			1987	
448	Doubtful Bay, Smaaland Cove	Transition			-54.86667	-36.05000	Prince and Poncet *unpubl. data* in Croxall et al (1995)	1986			1987	
449	Calf Head	Transition			-54.46667	-36.03333	N. Leader-Williams BAS records in Croxall et al (1995)	1973			1976	
450	Larsen Harbour	Transition			-54.83333	-36.00000	Prince and Poncet *unpubl. data* in Croxall et al (1995)	1986			1987	
451	Trendall Crag	Transition			-54.80000	-35.98333	Prince and Poncet *unpubl. data* in Croxall et al (1995)	1986			1987	
452	S side of Larsen Harbour	Transition			-54.83333	-35.98333	A. Burkitt, B. Mair BAS records in Croxall et al (1995)	1975			1976	
453	Rumbolds Point (Island)	Transition			-54.86667	-35.98333	Prince and Poncet *unpubl. data* in Croxall et al (1995)	1986			1987	
453	Nattriss Head	Transition			-54.85000	-35.93333	Prince and Poncet *unpubl. data* in Croxall et al (1995)	1986			1987	
455	Cooper Bay	Transition			-54.78333	-35.80000	Prince and Poncet *unpubl. data* in Croxall et al (1995)	1986			1987	

456	Cape Vahsel	Transition			-54.75000	-35.78333	Prince and Poncet *unpubl. data* in Croxall et al (1995)	1986			1987		
457	Cooper Island	Transition			-54.81667	-35.78333	Prince and Poncet *unpubl. data* in Croxall et al (1995)	1986			1987		

id	Method	Survey Area1	Survey Area2	SNPE presence	ConfirmedBreeding	UnconfirmedBreeding	MinColonySize	MeanColonySize	MaxColonySize	Units	Accuracy	Min NestAltitude	MeanNestAltitude	Max NestAltitude	Aspect
1	Observation			1	1										
2	Survey			1		1							374		S
3	Observation			1	1		500		1000	Pairs	Estimate				
4	Observation			1	1		500		1000	Pairs	Estimate				
5	Survey			1	1		200		500	Pairs	Estimate		584		N
6	Observation			1		1			10	Birds	Count		731		
7	Observation			1		1							898		
8	Observation			1		1									
9	Observation			1	1		500			Birds	Estimate		2000		NE
10	Observation			1	1		1000			Birds	Estimate				NE
11	Observation			1	1		200		400	Pairs	Estimate				N
12	Observation			1	1		600		1000	Pairs	Estimate				N/S
13	Observation			1	1		50		200	Pairs	Estimate				N/S
14	Observation			1	1		200		400	Pairs	Estimate				N/S
15	Observation			1	1		1200		2000	Pairs	Estimate				N
16	Observation			1	1			50		Pairs	Estimate				
17	Observation			1		1									
18	Observation			1	1		109			Nests	Count		355		N
19	Observation			1	1		100		150	Birds	Estimate				N

20	Survey			1	1			511		Nests	Count	340		420	
21	Survey			1	1			125		Nests	Count		350		
22	Survey			1	1			127		Nests	Count				
23	Observation			1		1									
24	Observation			1	1										N
25	Observation			1	1										
26	Observation			1	1			1000		Birds	Estimate				
27	Observation			1	1			50		Birds	Estimate				
28	Observation			1	1			50		Birds	Estimate				
29	Observation			1	1			100		Birds	Estimate				
30	Observation			1	1			2100		Pairs	Estimate	1330		1380	
31	Observation			1	1			100		Birds	Estimate				
32	Observation			1	1			800		Birds	Estimate				
33	Observation			1	1		1			Nest	Count				
34	Observation			1		1									
35	Observation			1	1			300		Birds	Estimate				
36	Observation			1	1			20		Nests	Count				
37	Observation			1	1			100		Birds	Estimate				
38	Observation			1	1		500		1000	Pairs	Estimate		1600		NE
39	Observation			1		1									
40	Observation			1	1			100		Birds	Estimate				
41	Observation			1	1			50		Nests	Count	1500		2000	N
42	Observation			1		1						1730		1830	
43	Observation			1	1			100		Birds	Estimate			1700	
44	Observation			1		1	1			Nest	Count				

45	Survey	3400	34	1		1	12		15	Birds	Count				
46	Observation			1		1	1		16	Birds	Count				
47	Observation			1		1		16		Birds	Count				
48	Observation			1		1		15		Birds	Count				
49	Observation			1		1						1190		1490	
50	Observation			1	1			1000		Birds	Estimate			850	
51	Observation			1		1		Many		Nests	Estimate		1400		N
52	Observation			1		1							1500		
53	Observation			1	1		100			Birds	Estimate				W
54	Observation			1	1		100			Birds	Estimate				
55	Observation			1	1		1000			Birds	Estimate				
56	Observation			1	1										
57	Observation			1	1										
58	Observation			1		1		200		Birds	Estimate				
59	Observation			1	1										
60	Observation			1	1										
61	Observation			1	1										
62	Observation			1	1										
63	Survey	41.5	0.415	1	1			174		Nests	Count				
64	Survey	9.3	0.093	1	1			8		Nests	Count				
65	Survey	15.1	0.151	1	1			43		Nests	Count				
66	Survey	34.2	0.342	1	1			64		Nests	Count				
67	Survey			1											
68	Survey			1											
69	Survey			1											
70	Survey	52.8	0.528	1	1			78		Nests	Count				
71	Survey	47.1	0.471	1	1			113		Nests	Count				

72	Survey	25.1	0.251	1	1			16		Nests	Count				
73	Survey			1											
74	Survey			1											
75	Survey			1											
76	Survey	40	0.4	1	1			67		Nests	Count				
77	Survey			1											
78	Survey	18.4	0.184	1	1			40		Nests	Count				
79	Survey	17.8	0.178	1	1			27		Nests	Count				
80	Survey			1											
81	Survey	33.7	0.337	1	1			36		Nests	Count				
82	Survey			1											
83	Survey			1											
84	Survey			1											
85	Survey			1											
86	Survey	15.6	0.156	1	1			75		Nests	Count				
87	Survey	90.6	0.906	1	1			162		Nests	Count				
88	Survey			1											
89	Survey			1											
90	Survey	15.4	0.154	1	1			113		Nests	Count				
91	Survey			1											
92	Survey			1											
93	Survey	22.5	0.225	1	1			6		Nests	Count				
94	Survey	35.1	0.351	1	1			35		Nests	Count				
95	Survey			1											
96	Survey			1											
97	Survey			1											
98	Survey			1											
99	Survey			1											
100	Survey	13	0.13	1	1			41		Nests	Count				
101	Survey			1											
102	Survey			1											
103	Survey	2.3	0.023	1	1			8		Nests	Count				
104	Survey			1	1										

105	Observation			1	1			1200		Pairs	Estimate				
106	Observation			1	1										
107	Survey	108.3	1.083	1	1			140		Nests	Count				
108	Survey	259.7	2.597	1	1			455		Nests	Count				
109	Survey	316.2	3.162	1	1			2705		Nests	Count				
110	Survey	206.1	2.061	1	1			575		Nests	Count				
111	Survey	228.7	2.287	1	1			2750		Nests	Count				
112	Observation			1		1									N
113	Observation			1		1									N
114	Observation			1		1									N
115	Observation			1	1			1		Nest	Estimate				
116	Observation			1	1										N/S
117	Observation			1	1										N/SE
118	Observation			1	1										N/S
119	Observation			1	1		3			Nests	Estimate				
120	Survey			1	1			13		Birds	Count				W
121	Survey			1		1		8		Birds	Count				
122	Survey			1	1			92		Nests	Count				
123	Observation			1	1										
124	Survey			1	1			3		Nests	Count				
125	Survey			1		1									
126	Survey			1	1			9		Nests	Count				
127	Survey			1	1			36		Nests	Count				
128	Survey			1	1			255		Nests	Count				

129	Survey			1	1			4		Nests	Count				
130	Survey			1	1			55		Nests	Count				
131	Survey			1	1			6		Nests	Count				
132	Survey			1	1			4		Nests	Count				
133	Survey			1	1			6		Nests	Count				
134	Observation			1	1										
135	Survey			1	1		800		1000	Pairs	Estimate				
136	Survey			1		1									
137	Survey			1		1									
138	Observation			1	1										
139	Observation			1	1										
140	Observation			1	1									155	
141	Observation			1	1										
142	Observation			1	1										
143	Observation			1	1									155	
144	Observation			1	1										
145	Observation			1	1										
146	Observation			1	1										
147	Observation			1	1									155	
148	Observation			1	1										
149	Observation			1	1										
150	Observation			1	1										
151	Observation			1	1										
152	Observation			1	1										

153	Observation			1	1										
154	Observation			1	1										
155	Observation			1	1										
156	Observation			1	1							30		140	
157	Observation			1	1										
158	Observation			1		1	2		3	Pairs	Estimate				
159	Observation			1	1										
160	Survey			1	1		60		75	Nests	Estimate	0		93	SE/N/E/S
161	Observation			1	1			1000		Birds	Estimate				
162	Observation			1	1			1000		Birds	Estimate				
163	Observation			1	1				1000	Birds	Estimate	50		100	
164	Survey			1	1			30		Pairs	Estimate				
165	Survey			1	1			200		Pairs	Estimate				N/E/S
166	Observation			1	1										
167	Observation			1	1										
168	Survey	65	0.65	1	1			2815		Nests	Estimate				
169	Survey	112.9	1.129	1	1			4575		Nests	Estimate				
170	Survey	10.5	0.105	1	1			760		Nests	Estimate				
171	Survey	64.6	0.646	1	1			1084		Nests	Estimate				
172	Survey	10.2	0.102	1	1			327		Nests	Estimate				NE
173	Survey	4.9	0.049	1	1			622		Nests	Estimate				
174	Survey	18.8	0.188	1	1			1092		Nests	Estimate				
175	Survey	53.6	0.536	1	1			2137		Nests	Estimate				
176	Survey	12.8	0.128	1	1			26		Nests	Estimate				

177	Survey	46.4	0.464	1	1			1103		Nests	Estimate				
178	Survey	9.9	0.099	1	1			354		Nests	Estimate				
179	Survey	10.4	0.104	1	1			752		Nests	Estimate				N/E
180	Survey	35.7	0.357	1	1			854		Nests	Estimate				N/E
181	Survey	23.3	0.233	1	1			470		Nests	Estimate				
182	Survey	15.5	0.155	1	1			414		Nests	Estimate				
183	Survey	19.8	0.198	1	1			452		Nests	Estimate				
184	Survey	18	0.18	1	1			329		Nests	Estimate				
185	Survey	8.6	0.086	1	1			61		Nests	Estimate				
186	Survey			1	1				95	Nests	Estimate				
187	Observation			1	1										
188	Observation			1	1			5		Pairs	Estimate				
189	Survey	65.8	0.658	1	1			259		Nests	Estimate				
190	Observation			1	1										
191	Survey			1	1			4		Pairs	Count				
192	Survey			1	1			10		Pairs	Count				
193	Survey			1	1			15		Pairs	Count				
194	Survey			1	1		440	550	706	Pairs	Estimate				
195	Survey			1	1			2		Pairs	Count				
196	Survey			1	1			44		Pairs	Count				
197	Survey			1	1			27		Pairs	Count				
198	Survey			1	1			132		Pairs	Count				
199	Survey			1	1			16		Pairs	Count				
200	Survey			1	1			20		Pairs	Count				

201	Survey			1	1			93		Pairs	Count				
202	Survey			1	1			53		Pairs	Count				
203	Observation			1	1			30		Pairs	Estimate				
204	Observation			1	1										
205	Survey			1	1			97		Pairs	Count				
206	Survey			1	1			21		Pairs	Count				
207	Survey			1	1			10		Pairs	Count				
208	Survey			1	1			54		Pairs	Count				
209	Survey			1	1			2		Pairs	Count				
210	Survey			1	1			114		Pairs	Count				
211	Survey			1	1			336		Pairs	Count				
212	Observation			1	1										
213	Observation			1	1		5000			Nests	Estimate				
214	Observation			1	1										
215	Observation			1		1									
216	Observation			1		1									E
217	Observation			1		1									
218	Observation			1	1		110			Nests	Estimate				W
219	Observation			1	1										N/NW
220	Observation			1	1										
221	Observation			1	1		27			Nests	Count				E/S
222	Observation			1		1			6	Pairs	Estimate				
223	Observation			1	1										
224	Observation			1	1			12		Nests	Count				E/S

225	Observation			1	1		100			Birds	Estimate				
226	Observation			1	1										
227	Observation			1	1										
228	Observation			1	1		100			Nests	Estimate				E
229	Observation			1	1			5		Nests	Estimate				
230	Observation			1	1		60			Nests	Estimate				
231	Observation			1		1									
232	Observation			1	1				50	Nests	Estimate				
233	Observation			1	1				100	Nests	Estimate				
234	Observation			1	1		1000			Nests	Estimate				
235	Observation			1	1				100	Nests	Estimate				
236	Observation			1	1				50	Nests	Estimate				
237	Observation			1	1				50	Nests	Estimate				
238	Observation			1		1									
239	Observation			1		1									
240	Observation			1	1										
241	Observation			1	1		10		20	Pairs	Estimate				
242	Observation			1		1		50		Birds	Estimate				
243	Observation			1		1	10		20	Pairs	Estimate		450		
244	Observation			1		1	80		100	Pairs	Estimate				
245	Observation			1		1									
246	Observation			1		1		Large numbers		Birds	Estimate				
247	Observation			1	1		50			Pairs	Estimate	580		670	
248	Observation			1		1									

249	Observation			1		1									
250	Observation			1	1										
251	Observation			1		1									
252	Observation			1		1									
253	Observation			1		1									
254	Observation			1		1									
255	Observation			1	1										
256	Observation			1	1			500		Birds	Estimate				
257	Observation			1	1										
258	Observation			1		1									
259	Observation			1	1		3			Nests	Estimate				N
260	Observation			1		1									
261	Observation			1	1										
262	Observation			1	1			5		Nests	Estimate		1000		N
263	Observation			1		1		15		Birds	Estimate				
264	Observation			1	1		100			Birds	Estimate				
265	Observation			1		1		6		Pairs	Estimate		500		
266	Observation			1	1		75		100	Pairs	Estimate				E
267	Observation			1		1	100			Birds	Estimate				
268	Observation			1		1									
269	Observation			1		1	10			Birds	Estimate				
270	Observation			1		1									
271	Observation			1		1	100			Birds	Estimate				
272	Observation			1		1	4			Pairs	Estimate				

273	Observation			1	1			15		Pairs	Count				
274	Observation			1		1		100		Pairs	Estimate				
275	Observation			1		1	10			Pairs	Estimate				
276	Observation			1		1	4			Birds	Count				
277	Observation			1		1		14	14	Pairs	Count				
278	Observation			1		1	2			Birds	Count				
279	Observation			1		1	2			Birds	Count				
280	Observation			1	1			6		Nests	Estimate				
281	Observation			1	1			100		Birds	Estimate	150		300	
282	Observation			1		1		200		Birds	Estimate	152		183	
283	Observation			1		1									
284	Observation			1	1										N
285	Observation			1		1			10	Birds	Count				
286	Observation			1		1									
287	Observation			1		1									
288	Observation			1		1		50		Birds	Estimate				
289	Observation			1		1	100			Birds	Estimate				
290	Observation			1		1	100			Birds	Estimate				
291	Observation			1		1									
292	Observation			1		1									
293	Survey			1	1										
294	Observation			1		1									
295	Observation			1	1			6		Pairs	Count		305		
296	Observation			1		1									

297	Observation			1		1								
298	Observation			1		1		1		Bird	Count			
299	Observation			1		1								
300	Observation			1	1		80		100	Pairs	Estimate			
301	Observation			1	1			30		Pairs	Estimate			
302	Observation			1		1								
303	Observation			1		1	12			Pairs	Estimate			S
304	Observation			1		1								
305	Observation			1		1								
306	Observation			1	1									N
307	Observation			1		1	3		25	Birds	Estimate			
308	Observation			1	1									
309	Observation			1		1								
310	Observation			1		1								
311	Observation			1		1								
312	Observation			1		1	10			Pairs	Estimate			
313	Observation			1		1								
314	Observation			1		1								
315	Observation			1	1									
316	Observation			1		1								
317	Observation			1	1									
318	Observation			1	1									
319	Observation			1	1									
320	Observation			1		1								

321	Survey			1		1									
322	Survey			1	1			1		Pair	Count				
323	Observation			1		1	100			Pairs	Estimate				
324	Observation			1		1									
325	Observation			1	1										
326	Observation			1	1								30		
327	Observation			1		1									
328	Observation			1	1										
329	Observation			1		1									
330	Observation			1		1									
331	Observation			1		1									
332	Observation			1	1										N
333	Observation			1		1									
334	Observation			1		1									
335	Observation			1		1									
336	Observation			1		1		2		Birds	Count				
337	Observation			1		1		5		Birds	Estimate				
338	Observation			1	1			50		Pairs	Estimate				
339	Observation			1		1	20			Birds	Estimate				
340	Observation			1		1									
341	Observation					1									
342	Observation			1	1										
343	Observation			1	1		34			Birds	Count				
344	Observation			1	1		100			Birds	Estimate				

345	Observation			1	1										
346	Observation			1		1	2			Nests	Count				
347	Observation			1	1										
348	Observation			1		1									
349	Observation			1	1										
350	Observation			1	1										
351	Observation			1	1										
352	Observation			1	1										
353	Observation			1	1										
354	Observation			1	1										
355	Observation			1	1										
356	Observation			1	1										
357	Observation			1	1										
358	Observation			1	1										
359	Observation			1		1			100	Birds	Estimate				
360	Observation			1	1										
361	Observation			1	1										
362	Observation			1	1										
363	Observation			1		1									
364	Observation			1		1			10	Pairs	Estimate				
365	Observation			1	1										
366	Observation			1	1										
367	Observation			1	1										
368	Observation			1	1			20000		Pairs	Estimate				

369	Survey			1	1										
370	Survey			1	1			300		Pairs	Estimate	0		200	N/E/SE/S/W
371	Survey			1	1			1000		Pairs	Estimate				NE/E/SW/W/NW
372	Survey			1	1			400		Pairs	Estimate				E/SE/W
373	Observation			1	1			9		Pairs	Count				
374	Observation			1	1			10		Pairs	Estimate				
375	Observation			1	1			10		Pairs	Estimate				
376	Survey			1	1			300		Pairs	Estimate	0		400	NE/W
377	Survey			1	1			400		Pairs	Estimate				N/E/SW/W
378	Survey			1	1			10		Pairs	Estimate				N/SE/W
379	Survey			1	1			100		Pairs	Estimate				NE/SE
380	Survey			1	1			100		Pairs	Estimate				NE/S
381	Survey			1	1										N/NE/E/SE
382	Survey			1	1			100		Pairs	Estimate		20		
383	Survey			1	1			500		Pairs	Estimate				NE/SW
384	Survey			1	1			3000		Pairs	Estimate		300		
385	Observation			1	1										
386	Observation			1	1			2		Pairs	Estimate				
387	Observation			1		1	10			Pairs	Estimate				
388	Observation			1		1									
389	Observation			1	1										
390	Observation			1	1										
391	Observation			1		1									

392	Observation			1		1									
393	Observation			1		1									
394	Observation			1		1									
395	Observation			1	1										
396	Observation			1	1										
397	Observation			1		1									
398	Observation			1		1	10			Pairs	Estimate				
399	Observation			1		1									
400	Observation			1		1									
401	Observation			1		1									
402	Observation			1		1									
403	Observation			1		1									
404	Observation			1		1	2			Pairs	Estimate				
405	Observation			1	1										
406	Observation			1		1									
407	Observation			1		1	5			Pairs	Estimate				
408	Observation			1		1									
409	Observation			1		1									
410	Observation			1	1										
411	Observation			1		1	5			Pairs	Estimate				
412	Observation			1		1	5			Pairs	Estimate				
413	Observation			1		1		100		Pairs	Estimate				
414	Observation			1		1	10			Pairs	Estimate				
415	Observation			1		1									

416	Observation			1	1										
417	Observation			1		1									
418	Observation			1		1									
419	Observation			1		1									
420	Observation			1		1									
421	Observation			1		1									
422	Observation			1	1										
423	Observation			1		1									
424	Observation			1		1									
425	Observation			1		1									
426	Observation			1		1									
427	Observation			1		1	1			Pairs	Estimate				
428	Observation			1		1									
429	Observation			1		1									
430	Observation			1	1										
431	Observation			1		1									
432	Observation			1		1									
433	Observation			1		1									
434	Observation			1		1									
435	Observation			1		1		50		Pairs	Estimate				
436	Observation			1	1										
437	Observation			1		1									
438	Observation			1		1	10			Pairs	Estimate				
439	Observation			1		1	10			Pairs	Estimate				

440	Observation			1		1	1			Pairs	Estimate				
441	Observation			1		1									
442	Observation			1		1	3			Pairs	Estimate				
443	Observation			1		1									
444	Observation			1		1									
445	Observation			1		1									
446	Observation			1		1	10			Pairs	Estimate				
447	Observation			1	1										
448	Observation			1		1									
449	Observation			1		1	10			Pairs	Estimate				
450	Observation			1		1									
451	Observation			1		1									
452	Observation			1	1										
453	Observation			1		1									
453	Observation			1		1									
455	Observation			1		1	10			Pairs	Estimate				
456	Observation			1		1									
457	Observation			1		1									

id	MeanNestDensity (per ha)	MeanNestDensity (per 100 m²)	Cliff	ScreeSlope	ObservedLithology	MeasuredMinAirTemp (°C)	MeasuredMaxAirTemp (°C)	MeasuredMinNestTemp (°C)	DistToCoast (km)	DistToNearest Station (km)	MeanAirTemp (°C)	MeanTotalPrecip (mm)	MeanWindSpeed (ms^{-1})	MeanWindDirection (°)
1									3.81	1.38				
2									143.51	118.66	-10.8	0.6	3.0	51.4
3									147.54	120.29	-10.8	0.6	3.0	50.0
4									145.22	117.73	-10.8	0.6	3.0	50.0
5			Yes	Yes					107.34	1.04	-11.1	0.9	3.8	91.2
6									145.78	39.52	-12.9	1.0	3.5	85.1
7									122.66	31.57	-12.0	1.3	2.3	105.3
8									276.84	67.28	-18.4	0.6	3.3	78.8
9				Yes					293.15	51.97	-20.7	0.6	2.9	83.2

10			Yes	Yes					282.02	37.00	-17.6	0.7	3.0	94.1
11			Yes	Yes					274.21	8.48	-17.8	0.8	2.8	100.3
12			Yes	Yes					280.09	1.15	-19.0	0.8	2.5	107.2
13			Yes	Yes					281.98	0.84	-19.0	0.8	2.5	107.2
14			Yes	Yes					282.42	1.27	-19.0	0.8	2.5	107.2
15			Yes	Yes					284.00	3.04	-19.5	0.8	2.5	108.9
16			Yes	Yes					287.12	6.52	-20.0	0.8	2.5	110.7
17														
18				Yes					98.67	60.27	-9.2	1.8	4.8	122.9
19				Yes					93.33	57.18	-9.1	1.8	4.7	122.9
20			Yes	Yes					112.62	24.93	-10.1	1.6	4.6	128.7
21			Yes	Yes					109.47	29.00	-10.0	1.6	4.5	129.3
22			Yes	Yes					111.45	27.70	-10.0	1.6	4.5	129.3
23									230.00	102.88	-15.8	0.6	3.5	111.2
24			Yes						221.20	40.01	-17.8	0.5	3.3	134.4
25					Heterogeneous migmatite metamorphic				219.89	19.74	-21.9	0.4	3.1	131.5
26					Heterogeneous migmatite metamorphic / layered micaceous gneiss metamorphic				203.27	3.72	-18.6	0.4	3.2	127.0
27					Heterogeneous migmatite metamorphic				199.22	1.75	-18.6	0.4	3.2	127.0
28					Heterogeneous migmatite metamorphic				202.60	2.45	-18.6	0.4	3.2	127.0
29					Heterogeneous migmatite metamorphic				201.95	2.94	-18.9	0.4	3.2	126.5

30									202.98	6.24	-19.1	0.4	3.2	125.9
31					Heterogeneous migmatite metamorphic				201.04	5.69	-19.1	0.4	3.2	125.9
32					Homogeneous granite migmatite				199.65	11.15	-19.7	0.4	3.2	125.0
33				Yes					190.77	12.43	-17.4	0.4	4.0	115.0
34									190.22	12.77	-17.4	0.4	4.0	115.0
35					Charnockite (intrusive)				200.61	36.63	-23.6	0.4	3.0	123.3
36									191.41	31.06	-21.3	0.5	3.2	126.0
37					Charnockite (intrusive)				182.86	20.17	-19.8	0.6	3.5	130.1
38				Yes	Charnockite (intrusive)			-8	182.62	0.73	-20.8	0.6	3.6	137.2
39									184.01	3.76	-20.9	0.6	3.6	137.6
40					Charnockite (intrusive)				173.71	27.01	-19.3	0.8	3.1	140.5
41				Yes					198.55	132.86	-20.5	0.4	4.9	139.5
42									189.30	124.49	-22.1	0.4	4.0	142.0
43									217.76	139.62	-23.8	0.4	5.3	127.3
44				Yes					159.73	80.83	-17.0	0.6	5.1	134.1
45									81.51	2.99	-9.0	0.9	6.7	120.9
46									1.87	87.96	-7.2	1.0	6.5	112.2
47									1.87	87.96	-7.2	1.0	6.5	112.2
48									6.79	77.37	-7.9	0.9	6.5	112.1
49									143.74	71.30	-16.0	0.7	4.9	136.9
50									146.52	88.58	-17.2	0.9	5.0	138.5
51						-9	-6		186.94	13.19	-19.5	0.4	3.4	135.8
52						-6	-4.5		221.41	42.97	-23.2	0.3	5.5	121.8
53									184.91	57.23	-18.4	0.6	3.6	137.4
54									180.03	58.21	-18.4	0.7	3.7	138.0
55			Yes						1.30	27.28	-6.1	0.7	4.3	63.3
56									0.24	2.41				
57									7.40	81.47				

58									0.56	282.52	-6.1	1.4	5.0	94.4
59									1.85	396.61	-7.0	1.9	6.9	120.9
60									0.73	88.27				
61					Mawson charnockite				0.20	16.11				
62									0.12	14.69				
63	4.2	0.042							0.18	7.76				
64	0.9	0.009							0.13	8.20				
65	2.8	0.028							0.06	7.26				
66	1.9	0.019							0.20	8.58				
67									0.04	4.44				
68									0.04	4.39				
69									0.13	4.21				
70	1.5	0.015							0.45	3.36				
71	2.4	0.024							0.06	3.26				
72	0.6	0.006							0.15	2.71				
73									0.05	3.49				
74									0.04	3.14				
75									0.05	3.54				
76	1.7	0.017							0.07	2.77				
77									0.07	2.70				
78	2.2	0.022							0.54	1.20	-6.7	0.8	7.2	132.1
79	1.5	0.015							0.72	1.24	-6.7	0.8	7.2	132.1
80									0.11	1.52	-6.7	0.8	7.2	132.1
81	1.1	0.011							1.05	1.28	-6.7	0.8	7.2	132.1
82									0.09	2.27	-6.7	0.8	7.2	132.1
83									0.02	2.11	-6.7	0.8	7.2	132.1
84									0.18	2.95	-6.7	0.8	7.2	132.1
85									0.11	2.61	-6.7	0.8	7.2	132.1
86	4.8	0.048							1.15	1.67	-6.7	0.8	7.2	132.1
87	1.8	0.018							0.52	3.64	-6.7	0.8	7.2	132.1
88									0.06	4.01	-6.7	0.8	7.2	132.1
89									0.07	4.20	-6.7	0.8	7.2	132.1
90	7.3	0.073							0.06	4.18	-6.9	0.8	7.1	131.9
91									0.16	6.83	-6.9	0.8	7.1	131.9
92									0.09	9.38				

93	0.3	0.003							0.07	7.90				
94	1	0.01							0.10	7.60				
95									0.02	10.99				
96									0.00	10.80				
97									0.04	11.32				
98									0.04	11.10				
99									0.02	10.81				
100	3.2	0.032							0.14	11.50				
101									0.02	10.51				
102									0.05	10.45				
103	3.4	0.034							0.19	12.79				
104									0.48	30.27				
105									0.42	166.02	-8.0	0.9	7.5	147.5
106									0.31	173.11	-7.9	0.9	7.3	147.3
107	1.3	0.013							30.71	40.38	-12.9	0.8	10.0	143.5
108	1.8	0.018							19.67	29.78	-11.0	0.8	9.2	141.1
109	8.6	0.086	Yes	Yes					15.27	20.51	-10.9	0.8	9.4	141.0
110	2.8	0.028							20.52	25.35	-11.0	0.8	9.3	141.1
111	11.9	0.119							12.97	13.76	-9.7	0.8	8.1	137.1
112			Yes	Yes	Sandstone				235.87	50.19	-12.9	0.5	4.1	210.3
113			Yes	Yes	Sandstone				242.35	49.76	-12.8	0.5	4.4	210.3
114			Yes	Yes	Sandstone				247.59	41.59	-10.7	0.5	4.5	208.2
115			Yes						251.49	45.82	-11.3	0.5	6.1	216.6
116			Yes						248.77	43.70	-11.0	0.5	6.1	215.3
117			Yes						246.07	40.85	-9.8	0.5	5.4	209.6
118									243.81	38.48	-9.8	0.5	5.4	209.6

119			Yes						241.81	37.55	-9.8	0.5	5.5	207.9
120				Yes	Granite	-12	12		434.77	283.05	-17.2	0.1	2.6	99.2
121				Yes					471.27	265.75	-17.2	0.1	5.4	84.3
122	3	0.03		Yes					0.13	1.11	-5.7	0.9	5.4	82.6
123				Yes					1.04	3.92	-5.2	0.8	5.1	81.4
124				Yes					0.20	2.19	-6.1	0.9	5.7	83.6
125				Yes					0.14	3.49	-6.1	0.9	5.7	83.6
126				Yes					0.04	7.17	-5.1	0.8	5.0	81.1
127	4.4	0.044		Yes					0.30	2.97	-6.1	0.9	5.7	83.6
128	4.4	0.044		Yes					0.42	1.27	-6.1	0.9	5.7	83.6
129				Yes					0.13	3.24	-5.7	0.9	5.4	82.6
130	4.4	0.044		Yes					0.10	3.71	-5.7	0.9	5.4	82.6
131				Yes					0.32	4.94	-5.2	0.8	5.1	81.4
132				Yes					0.18	2.55	-6.1	0.9	5.7	83.6
133				Yes					0.10	6.47				
134									0.42	42.33				
135				Yes	Metamorphic			-6	0.03	30.27				
136									0.06	26.59				
137									0.15	11.24				
138				Yes					0.49	9.51	-4.6	0.6	4.7	70.3
139				Yes					0.15	9.84				
140				Yes					0.62	6.45	-4.1	0.6	4.5	66.5
141									1.56	9.06	-4.2	0.6	4.7	67.1
142				Yes					0.25	4.11				

143				Yes					3.20	11.57	-4.6	0.6	5.1	68.9
144				Yes					0.18	2.23				
145				Yes					0.17	2.30				
146				Yes					0.13	3.53				
147				Yes					1.95	11.89	-4.6	0.6	5.2	66.1
148				Yes					0.10	4.58				
149				Yes					0.13	4.46				
150				Yes					0.10	4.32				
151				Yes					0.02	4.95				
152				Yes					0.35	10.49				
153				Yes					0.16	9.72				
154				Yes					0.20	12.26				
155				Yes					0.25	12.41				
156				Yes					0.13	12.04				
157				Yes					0.66	21.25	-4.7	0.6	5.2	66.1
158					Gneiss/ dolerit e				3.41	21.66				
159									0.03	173.00	-5.8	1.3	7.0	102.0
160				Yes	Granite				0.63	4.15				
161			Yes	Yes					87.07	119.98	-8.2	1.6	5.2	130.3
162				Yes					61.43	75.40	-8.2	1.2	5.0	138.1
163				Yes					1.68	16.64	-6.4	0.7	6.0	92.6
164					Granite				0.57	106.31				
165					Granite				0.24	104.13				
166									0.12	16.63				

167									0.94	18.05				
168	9	0.09	Yes						0.23	20.90	-5.8	0.9	4.3	113.2
169	7.4	0.074							0.68	20.90	-5.8	1.0	3.9	106.1
170	9.3	0.093							0.15	21.26	-5.8	1.0	3.9	106.1
171	3.5	0.035							0.31	16.01				
172	5.9	0.059	Yes						0.11	15.45				
173	4.9	0.049							0.43	15.25	-5.2	1.0	3.2	92.0
174	24.1	0.241							0.00	13.33				
175	7.9	0.079							0.20	14.18	-5.2	1.0	3.2	92.0
176	0.4	0.004							0.13	10.11	-5.2	1.0	3.2	92.0
177	2.6	0.026							0.84	5.78				
178	5.1	0.051							0.26	6.39				
179	16.8	0.168	Yes						0.13	7.65				
180	5.7	0.057	Yes						1.27	5.87	-5.5	1.0	3.1	91.4
181	4.4	0.044							0.14	5.23				
182	3	0.03							0.02	6.96				
183	4	0.04							0.20	2.82				
184	1.2	0.012							0.39	0.47				
185	0.8	0.008							0.02	1.23				
186									0.42	0.32				
187									0.42	0.32				
188									0.02	3.68				
189	0.6	0.006							0.85	3.63	-5.5	1.0	3.1	91.4
190									0.29	39.97				

191									0.20	10.03				
192									0.38	6.98				
193									0.02	0.90				
194				Yes					0.10	0.43				
195									0.09	0.81				
196									0.17	1.02				
197									0.17	1.21				
198									0.17	1.26				
199									0.03	5.99				
200									0.32	23.88				
201									0.94	41.76				
202									0.53	123.60	-9.1	1.5	7.8	159.6
203									0.09	124.62	-9.1	1.5	7.8	159.6
204									0.29	159.71				
205									3.67	172.26				
206									0.11	176.73				
207									0.05	176.94				
208									0.16	177.46				
209									0.20	179.12				
210									0.04	178.65				
211									0.27	179.21	-8.3	2.2	7.8	176.0
212									4.56	416.42				
213									0.81	334.15				
214			Yes						6.90	875.38				

215									119.61	163.23	-17.1	0.4	3.1	189.7
216									1.28	411.33				
217									0.35	382.89				
218									2.11	313.83				
219									0.19	299.62	-13.5	1.2	1.1	220.9
220					McMurdo volcanics				17.57	272.80	-10.8	1.0	1.1	223.0
221			Yes						0.15	34.69				
222			Yes						1.23	94.70				
223									80.69	408.44	-12.9	0.6	2.4	109.2
224									90.97	404.28	-12.7	0.6	2.6	102.8
225			Yes						90.09	410.41	-12.9	0.7	3.1	85.4
226									101.40	334.50	-10.7	0.7	2.0	49.0
227				Yes					86.06	308.54	-12.0	1.0	2.2	69.2
228			Yes						40.34	172.28	-11.6	2.6	3.1	107.3
229									128.94	151.29	-20.5	1.6	1.6	128.3
230									54.42	97.18	-10.6	2.1	5.2	106.2
231									5.80	586.69	-9.4	1.6	3.6	125.5
232									58.13	457.13	-12.1	1.7	3.0	143.6
233									59.45	449.82	-12.9	1.6	3.3	139.7
234									55.97	449.97	-13.3	1.7	3.2	140.1
235									54.25	450.06	-13.7	1.8	3.1	140.5
236									46.03	466.71	-10.4	2.0	1.9	146.1
237									42.50	466.90	-10.6	2.1	2.0	147.2

238									37.71	675.28	-8.8	1.2	4.6	76.5
239									53.17	625.11	-9.6	0.8	6.2	54.2
240									187.11	192.52	-15.0	0.3	3.3	51.8
241					Dolerite				185.15	189.91	-15.0	0.3	3.3	51.8
242					Dolerite				185.67	187.43	-15.4	0.3	3.3	60.1
243					Dolerite				187.75	187.33	-15.3	0.3	3.6	60.2
244					Dolerite				191.81	191.77	-15.4	0.3	3.6	61.1
245									191.88	190.93	-15.5	0.3	3.7	62.0
246					Dolerite				187.43	181.66	-15.3	0.3	4.3	58.0
247					Dolerite				199.48	196.35	-15.8	0.3	3.9	60.9
248									318.34	340.32	-19.6	0.2	2.7	59.1
249									422.19	428.66	-21.6	0.3	5.4	68.6
250									267.99	291.55	-15.1	0.2	3.4	89.3
251									271.40	292.18	-14.7	0.3	4.3	92.8
252									82.20	192.28	-10.9	2.7	5.9	155.0
253									28.40	230.85	-9.7	2.3	4.3	160.1
254									30.99	219.24	-9.2	2.2	3.4	162.8
255									43.30	203.95	-8.4	2.0	2.7	158.3
256									119.08	94.88	-6.8	0.8	1.7	202.1
257									18.77	179.75	-6.1	1.9	1.2	77.8
258									116.82	21.33	-8.6	0.9	0.8	246.0
259				Yes					80.50	70.00	-7.3	1.4	1.2	60.3
260									74.35	58.43	-5.1	1.0	1.3	317.1
261									68.92	76.77	-8.0	1.4	1.0	51.8

262									63.97	82.06	-8.0	1.5	1.0	46.7
263									56.31	75.66	-4.4	1.3	1.2	323.3
264									72.84	85.00	-7.1	1.1	3.5	62.0
265			Yes		Sandstone				50.23	81.02	-7.3	1.5	0.9	307.0
266				Yes	Sandstone				44.86	86.35	-7.3	1.5	0.9	307.0
267									43.46	114.25	-7.0	1.4	3.9	25.9
268									0.27	312.98				
269									0.42	152.58	-4.2	3.1	2.0	64.7
270									0.71	148.28				
271									86.75	188.63	-6.8	1.5	0.7	202.7
272									104.19	149.75	-8.3	1.7	1.0	209.3
273									114.09	153.40	-6.8	1.7	0.7	197.7
274									101.77	132.87	-5.3	1.8	0.6	162.7
275									92.95	118.52	-6.0	2.1	0.5	173.8
276									4.26	19.04	-4.6	3.1	1.4	71.2
277									44.08	63.84	-7.3	3.3	0.6	231.4
278									0.51	66.49				
279									0.02	24.86				
280									0.27	10.13	-4.2	2.8	1.5	67.7
281									0.33	8.37				
282			Yes						1.11	19.43				
283									0.07	30.50				
284				Yes					0.54	31.86				
285									0.40	35.90				

286									0.42	21.69				
287									0.36	109.51				
288			Yes						0.23	39.08				
289									1.66	18.44				
290									0.03	19.75				
291									0.96	28.53				
292									7.56	20.43	-5.4	2.9	1.9	56.8
293									0.16	0.44				
294									0.38	20.55	-3.8	3.8	1.3	47.8
295									2.45	6.14	-3.5	3.1	1.8	55.1
296									0.85	57.31	-2.9	6.6	1.1	98.7
297									0.32	87.69				
298									61.72	170.54	-7.5	3.5	0.6	257.5
299									64.26	166.79	-6.8	3.4	0.6	247.3
300									43.00	127.38	-6.9	4.5	1.5	264.8
301									52.82	129.34	-5.1	3.7	1.2	264.4
302									77.07	129.99	-5.5	2.6	1.0	266.7
303					Granite				60.83	118.07	-6.0	3.2	1.3	290.5
304									0.19	50.53	-3.2	6.9	2.3	73.3
305									20.40	84.80	-6.6	2.6	1.3	276.6
306									0.35	19.06				
307			Yes						0.90	7.29				
308									0.07	1.32				
309									3.22	13.07	-2.7	5.1	1.6	84.6

310									0.46	1.12	-5.3	5.0	0.8	108.2
311									0.26	1.69	-5.3	5.0	0.8	108.2
312									0.20	25.91				
313									7.50	28.57	-5.3	5.2	1.1	121.3
314									0.98	20.09				
315									1.37	54.56	-2.9	2.1	1.7	285.8
316									6.41	33.02	-4.1	5.2	0.7	180.3
317									0.93	10.03				
318									12.98	46.10	-6.9	2.1	0.9	267.7
319									0.15	34.67	-3.4	2.2	0.8	252.1
320									0.27	24.87				
321									0.01	4.17				
322									0.58	0.70	-2.9	5.0	1.1	127.8
323									0.39	52.04				
324			Yes						1.77	23.93				
325									1.46	34.90	-1.8	1.8	2.5	261.6
326			Yes	Yes					0.84	42.41				
327									0.04	21.56				
328									0.08	30.28				
329									2.41	25.37				
330									0.15	56.55	-0.9	4.1	2.0	224.5
331									2.48	21.64	-1.0	1.8	3.0	275.5
332				Yes					0.44	25.83				
333									4.62	23.01	-1.7	2.1	3.0	281.4

334									0.73	39.65	-3.4	4.0	1.8	232.7
335									4.61	35.98	-2.0	1.9	3.0	262.5
336			Yes						1.64	3.83				
337									0.87	89.59				
338									3.94	210.70	-0.6	2.2	4.4	264.8
339									2.53	55.87	-2.9	2.5	1.2	292.8
340									0.10	7.74				
341									2.54	66.77				
342									0.43	27.06				
343									0.14	5.77				
344			Yes						1.42	2.36				
345									0.88	1.55				
346				Yes					0.14	7.98				
347									0.77	18.29				
348			Yes						0.64	15.85				
349									1.97	19.85				
350									1.69	21.69				
351									0.04	24.08				
352									0.83	24.97				
353									0.48	24.36				
354									0.00	24.34				
355									0.91	24.82				
356			Yes						0.91	24.82				
357			Yes						0.18	23.43				

358									0.80	21.02				
359									0.37	17.93				
360									0.02	16.78				
361									0.02	16.78				
362									0.50	17.85				
363									1.61	19.93				
364									0.16	16.43				
365									0.38	14.89				
366									0.17	15.03				
367									0.23	13.25				
368									1.54	6.86				
369									1.41	850.36				
370			Yes						7.19	853.41				
371			Yes						1.74	845.57				
372			Yes						14.27	856.06				
373			Yes						3.67	845.13				
374			Yes						1.41	846.52				
375			Yes						0.03	847.96				
376			Yes						0.51	853.44				
377			Yes						0.43	825.61				
378			Yes						1.32	787.74				
379			Yes						9.29	728.40				
380			Yes						1.04	688.82				
381			Yes						53.33	632.28				

382			Yes						0.89	649.00				
383			Yes						63.39	702.35				
384					Sandstone/mudstone/dolerite				5.56	18.77				
385									12.14	10.52				
386									1.90	1.00				
387									0.90	7.40				
388									2.20	4.70				
389									1.22	7.86				
390									3.09	9.55	2.9	4.0	4.8	271.9
391									0.55	13.94	2.9	4.0	4.8	271.9
392									0.78	16.15	2.8	4.0	4.7	271.6
393									3.48	22.99	2.6	4.0	4.4	269.9
394									1.08	26.85				
395									0.56	37.05	2.6	4.0	4.2	273.0
396									0.89	37.98	2.6	4.0	4.2	273.0
397									0.74	34.19	2.5	3.9	4.3	268.6
398									1.51	40.07	2.5	3.8	4.1	266.6
399									0.77	49.30				
400									0.77	49.30				
401									5.14	56.28	1.7	4.4	3.5	265.1
402									1.18	53.28	2.1	3.9	3.5	259.9
403									3.41	51.74	1.7	4.4	3.9	253.2
404									8.33	48.99	1.7	4.4	3.9	253.2

405									1.63	47.50				
406									3.92	46.68	1.7	4.4	3.9	253.2
407									12.63	39.12	0.2	5.6	3.8	257.8
408									1.06	36.96	0.3	6.2	3.5	267.0
409									3.26	30.01				
410									3.31	29.48	-0.4	6.0	2.9	272.2
411									3.17	29.22				
412									10.96	24.48	0.7	5.2	3.9	256.7
413									8.77	21.44	-0.4	5.7	3.2	263.1
414									7.77	20.87	1.2	4.9	3.8	257.7
415									1.19	23.26				
416									0.54	26.75				
417									9.93	13.91	-1.5	5.3	2.4	268.6
418									2.61	29.52				
419									2.86	1.53	-0.2	4.6	2.9	261.5
420									0.20	5.96				
421									2.20	2.05	-0.2	4.6	2.9	261.5
422									3.13	31.88	-0.6	5.5	2.7	280.6
423									1.27	8.94				
424									1.64	8.91				
425									4.92	30.88	-0.2	5.3	2.7	280.3
426									9.87	25.96	-0.1	4.8	2.6	276.6
427									3.07	39.16	-0.3	5.5	3.0	285.1
428									0.79	11.96				

429									1.47	11.46				
430									0.31	12.78				
431									3.30	13.76				
432									2.91	16.87	0.6	4.1	2.4	267.5
433									11.36	29.25	-0.1	4.8	2.6	276.6
434									1.32	57.34	0.2	5.4	3.7	286.9
435									2.11	63.98	0.9	4.7	4.5	283.1
436									1.51	21.00				
437									3.55	22.88	1.1	3.9	2.4	267.3
438									4.29	25.85	1.1	3.9	2.4	267.3
439									0.50	29.09	1.1	3.9	2.4	267.3
440									0.32	69.49	0.9	4.7	4.5	283.1
441									1.02	67.62	0.9	4.7	4.5	283.1
442									0.29	76.26				
443									0.78	76.66				
444									2.81	69.78	1.1	4.5	4.4	281.4
445									2.64	42.22	1.2	3.9	2.5	271.8
446									5.05	40.40	1.2	3.8	2.6	272.2
447									4.39	41.69	1.2	3.8	2.6	272.2
448									2.14	76.15				
449									7.46	38.94	1.2	3.8	2.6	272.2
450									0.69	74.08	1.3	4.1	4.4	279.2
451									0.79	71.16	1.3	4.1	4.4	279.2
452									0.29	74.62	1.3	4.1	4.4	279.2

453									0.77	78.13				
453									0.56	78.04				
455									0.60	76.74				
456									1.31	74.47				
457									4.18	80.56				

id	Lithology	DistTo 15Nov (km)	DistTo 50Nov (km)	DistTo 15Feb (km)	DistTo 50Feb (km)	Area700 Nov (km²)	Area1500 Nov (km²)	Area700 Feb (km²)	Area1500 Feb (km²)	Notes
1										
2	Intrusive igneous	1417.84	346.71	169.35	157.25	10,729	101,583	118,208	265,313	Nests are well hidden cavities beneath boulders and in cavities in rock.
3	Unconsolidated sediment	1420.22	348.09	173.02	161.04	10,729	100,646	117,833	265,208	
4	Intrusive igneous	1418.16	347.91	171.34	159.36	10,729	101,479	117,854	265,208	
5	Volcanic igenous	1345.59	357.67	139.33	124.84	13,313	130,167	110,479	264,000	Nests on both scree slopes and vertical cliffs, "particularly above the blue-ice area at the western part of the nunatak". "Snow Petrels breed in precipices up to 400 m high, impossible to reach"
6	Unconsolidated sediment	1372.42	370.01	174.48	161.48	12,854	112,833	108,438	261,167	No nests found
7	Volcanic igenous	1367.55	358.39	152.00	139.52	12,438	117,729	112,292	263,979	
8	Intrusive igneous	1502.06	421.61	301.26	282.45	10,479	76,479	94,667	251,042	
9	Low-medium grade metamorphic	1498.82	431.79	315.46	299.37	10,542	78,063	92,646	249,667	"This site was obviously kept free of snow by the prevailing wind" p 4. "200 miles from the nearest ice front"
10	Intrusive igneous	1484.07	423.08	302.28	289.36	10,626	80,917	95,958	251,000	
11	Intrusive igneous	1465.97	427.08	302.43	294.41	11,083	84,708	95,854	250,729	"the variation in nest site location was high. Nest sites were found in north- and south-facing slopes, as well as on vertical cliffs and scree slopes, with high nest densities even in low parts of the slopes, close to the ice"
12	Low-medium grade metamorphic	1466.93	431.61	308.00	299.88	11,208	84,042	94,646	250,188	"the variation in nest site location was high. Nest sites were found in north- and south-facing slopes, as well as on vertical cliffs and scree slopes, with high nest densities even in low parts of the

										slopes, close to the ice"
13	Intrusive igneous	1468.30	432.56	309.88	301.81	11,208	83,750	94,646	250,125	"the variation in nest site location was high. Nest sites were found in north- and south-facing slopes, as well as on vertical cliffs and scree slopes, with high nest densities even in low parts of the slopes, close to the ice"
14	Intrusive igneous	1468.57	432.80	310.31	302.25	11,208	83,646	94,500	249,958	"the variation in nest site location was high. Nest sites were found in north- and south-facing slopes, as well as on vertical cliffs and scree slopes, with high nest densities even in low parts of the slopes, close to the ice"
15	Low-medium grade metamorphic	1468.73	434.07	311.79	303.69	11,292	83,500	94,229	249,646	"the variation in nest site location was high. Nest sites were found in north- and south-facing slopes, as well as on vertical cliffs and scree slopes, with high nest densities even in low parts of the slopes, close to the ice"
16	Intrusive igneous	1469.75	436.22	314.76	306.64	11,292	83,521	93,438	249,417	"the variation in nest site location was high. Nest sites were found in north- and south-facing slopes, as well as on vertical cliffs and scree slopes, with high nest densities even in low parts of the slopes, close to the ice"
17										
18	Unknown or unclassified	1193.22	394.56	154.85	127.92	23,354	189,250	61,271	231,750	
19	Unknown or unclassified	1190.16	392.08	154.27	127.74	23,688	187,063	60,917	230,479	
20	Intrusive igneous	1204.82	398.44	175.36	147.88	23,563	170,042	58,542	228,271	338 Breeding pairs estimated. "No nest sites were found on loose scree slopes where rocks were less than 500 mm in diameter"
21	Intrusive igneous	1202.66	397.32	172.44	145.07	23,604	171,750	58,438	228,667	85 breeding pairs estimated. "No nest sites were found on loose scree slopes where rocks were less than 500 mm in diameter"
22	Intrusive igneous	1204.19	398.32	174.26	147.07	23,583	170,896	58,625	228,813	86 breeding pairs estimated. "No nest sites were found on loose scree slopes where rocks were less than 500 mm in diameter"

23	High grade metamorphic	1273.10	449.72	277.48	253.77	20,458	113,375	51,234	221,146	
24	Intrusive igneous	1261.21	445.76	268.46	252.90	21,146	112,833	49,939	213,583	"Birds entering cavities in the cliff face"
25	Intrusive igneous	1266.00	449.00	267.63	252.61	20,667	107,438	48,146	209,938	Next to Antarctic Petrels
26	High grade metamorphic	1252.76	438.93	250.94	236.10	21,583	112,125	48,667	209,417	
27	High grade metamorphic	1249.74	436.62	247.02	232.25	21,750	112,625	48,479	208,188	
28	Unconsolidated sediment	1252.62	438.80	250.54	235.76	21,542	112,083	48,417	208,313	
29	High grade metamorphic	1252.42	438.68	250.16	235.44	21,542	111,938	48,313	208,167	Next to Antarctic Petrels and South Polar Skuas
30	High grade metamorphic	1253.53	439.66	251.54	236.89	21,438	110,896	48,271	208,104	
31	High grade metamorphic	1252.03	438.52	249.64	235.01	21,521	111,813	48,375	208,042	Next to Antarctic Petrels and South Polar Skuas
32	High grade metamorphic	1251.25	438.29	248.87	234.42	21,479	110,646	48,000	207,479	Next to Antarctic Petrels and South Polar Skuas
33	Intrusive igneous	1244.24	432.79	239.82	225.42	21,896	113,813	48,188	207,333	
34	Intrusive igneous	1243.81	432.46	239.27	224.88	21,938	113,979	48,188	207,333	
35	High grade metamorphic	1248.87	442.35	253.50	240.31	20,542	104,958	45,979	203,417	Next to Antarctic Petrels and South Polar Skuas
36	High grade metamorphic	1241.63	436.87	244.39	231.21	21,146	107,500	45,979	202,750	
37	High grade metamorphic	1233.47	432.01	235.84	222.50	21,458	110,542	45,938	201,250	Next to Antarctic Petrels
38	Unconsolidated sediment	1227.67	431.62	233.82	220.14	21,524	109,813	45,188	199,021	"Nested under large stone blocks on scree slopes within Antarctic petrel colony". "Highest breeding density was found close to the NE side of the mountain"
39	High grade metamorphic	1228.19	432.63	235.48	221.77	21,427	109,667	44,938	198,646	
40	High grade metamorphic	1216.97	425.99	227.16	213.06	22,314	112,271	44,208	196,104	Next to Antarctic Petrels and South Polar Skuas
41	Intrusive igneous	1213.52	424.34	254.98	239.62	19,922	104,021	39,542	187,125	Within hollows, SNPE sitting 10-50cm back from nest openings
42	Unconsolidated sediment	1196.84	411.57	241.23	224.08	20,438	110,042	39,500	181,646	
43	Low-medium grade metamorphic	1211.96	428.19	265.38	246.30	18,604	101,792	38,563	179,396	
44	Low-medium grade metamorphic	1168.97	391.42	212.50	191.16	20,958	126,583	39,354	172,875	"Nesting sites were found under boulders in moraines and in cavities in bedrock"
45	High grade metamorphic	1115.18	339.58	135.41	111.80	25,458	182,396	40,750	165,125	
46		1056.48	282.23	53.22	27.13	32,146	266,688	41,021	155,458	
47		1056.48	282.23	53.22	27.13	32,146	266,688	41,021	155,458	
48		1062.90	288.88	63.40	37.92	31,396	257,271	41,125	156,438	
49	Intrusive igneous	1153.39	382.65	201.93	180.48	21,042	139,167	39,521	167,521	
50	Intrusive igneous	1147.53	383.66	208.49	186.72	20,188	142,417	39,218	162,750	Numerous colonies; "The birds prefer to breed in cavities under

										or between large boulders"
51	Intrusive igneous	1107.04	377.30	263.91	227.18	9,604	182,146	44,021	125,542	
52	High grade metamorphic	1132.55	406.63	300.34	261.83	9,317	169,146	43,188	126,375	
53	Unconsolidated sediment	1092.82	375.27	272.50	228.81	9,074	205,438	45,375	123,896	
54	High grade metamorphic	1088.30	371.14	268.14	224.32	9,061	210,417	45,333	123,750	
55	High grade metamorphic	883.18	469.75	150.71	113.20	17,438	546,396	54,479	110,479	
56	Unconsolidated sediment	864.83	458.90	125.86	90.79	18,813	549,354	55,104	110,000	
57	High grade metamorphic	786.69	401.96	90.39	48.44	64,167	714,292	54,229	121,938	
58	High grade metamorphic	660.09	242.44	27.26	9.01	161,500	777,875	49,813	122,125	"Their low circling flight, particularly above the rocky slopes of the Antarctic Petrel colony on the western massif, suggestedthe presence of nests higher up the slope".
59	High grade metamorphic	617.91	183.02	25.12	10.59	215,188	805,354	48,229	124,896	Multiple colonies
60	High grade metamorphic	636.35	204.90	59.30	34.54	154,958	834,271	50,500	133,313	
61	Intrusive igneous	607.45	155.48	50.57	29.51	161,021	837,604	49,063	134,188	
62	Intrusive igneous	606.67	154.46	50.39	29.57	161,542	837,271	49,063	133,583	
63	Intrusive igneous	600.92	148.22	47.53	26.99	166,021	839,563	49,771	134,167	
64	Intrusive igneous	603.80	149.65	51.97	31.51	162,063	836,938	49,771	134,167	
65	Intrusive igneous	600.92	148.02	47.90	27.34	165,771	839,521	49,771	134,167	
66	Intrusive igneous	604.39	149.61	53.42	33.06	162,063	838,979	49,771	134,167	
67	Intrusive igneous	599.79	146.12	48.48	27.97	166,417	839,042	49,167	134,167	
68	Intrusive igneous	599.69	146.03	48.40	27.88	166,417	839,042	49,167	134,167	
69	Intrusive igneous	599.98	146.15	48.89	28.39	166,417	839,042	49,167	134,167	
70	Intrusive igneous	600.36	145.83	50.27	29.88	164,063	838,500	49,167	134,167	
71	Intrusive igneous	598.25	144.45	47.69	27.20	166,875	838,479	49,188	134,063	"Higher occupancy of cavities with flat nest bowls, and most breeding occurred on flat nest bowls that contained loose substrate (gravel or sand)". Most breeding nests had single, narrow entrances.
72	Intrusive igneous	599.98	145.30	50.28	29.91	164,771	838,500	49,188	134,167	
73	Intrusive igneous	597.95	144.24	47.34	26.84	167,146	838,563	49,354	134,063	
74	Intrusive igneous	597.78	143.94	47.43	26.95	167,271	838,333	49,604	134,063	
75	Intrusive igneous	597.47	143.76	47.03	26.52	167,521	838,354	49,604	134,063	
76	Intrusive igneous	597.87	143.91	47.70	27.23	167,271	838,333	49,604	134,063	
77	Intrusive igneous	597.66	143.66	47.61	27.15	167,333	838,354	49,750	134,063	
78	Intrusive igneous	598.26	143.72	48.85	28.47	167,333	838,167	49,750	134,063	

79	Intrusive igneous	598.85	143.63	50.29	30.01	165,083	837,729	49,750	134,063	
80	Intrusive igneous	597.32	142.76	48.21	27.83	167,333	838,208	49,750	134,063	
81	Intrusive igneous	598.47	143.07	50.29	30.05	165,375	837,708	49,750	134,063	
82	Intrusive igneous	596.63	142.08	47.71	27.33	167,563	838,313	49,750	134,250	
83	Intrusive igneous	596.65	141.97	47.90	27.55	167,438	838,146	49,750	134,250	
84	Intrusive igneous	596.18	141.74	47.23	26.84	168,354	838,313	49,750	134,250	
85	Intrusive igneous	596.31	141.71	47.55	27.19	167,771	838,229	49,750	134,500	
86	Intrusive igneous	598.09	142.51	50.30	30.08	165,375	838,021	49,708	134,500	
87	Intrusive igneous	595.41	140.47	47.43	27.13	168,229	838,250	49,708	134,000	
88	Intrusive igneous	595.17	140.03	47.54	27.26	168,083	838,646	49,708	134,000	
89	Intrusive igneous	595.02	139.96	47.32	27.03	168,083	838,792	49,708	134,000	
90	Intrusive igneous	595.04	139.91	47.44	27.16	168,083	838,646	49,708	134,000	
91	Intrusive igneous	593.17	138.69	45.16	24.79	170,417	838,792	49,875	134,000	
92	Intrusive igneous	591.48	137.51	43.26	22.82	172,042	838,958	49,875	134,000	
93	Intrusive igneous	592.38	137.91	44.61	24.23	171,292	838,646	49,875	134,000	
94	Intrusive igneous	592.57	137.99	44.89	24.53	171,292	838,646	49,875	134,000	
95	Intrusive igneous	590.28	136.33	42.39	21.96	172,354	838,542	49,375	133,854	
96	Intrusive igneous	590.39	136.37	42.57	22.14	172,229	838,375	49,375	133,854	
97	Intrusive igneous	590.07	136.18	42.13	21.70	172,354	838,542	49,375	133,854	
98	Intrusive igneous	590.19	136.23	42.34	21.91	172,354	838,542	49,375	133,854	
99	Intrusive igneous	590.37	136.29	42.62	22.19	172,229	838,375	49,375	133,854	
100	Intrusive igneous	589.92	136.01	42.05	21.63	172,354	838,542	49,250	133,854	
101	Intrusive igneous	590.46	135.96	43.25	22.87	172,146	838,188	49,250	133,854	
102	Intrusive igneous	590.48	135.87	43.40	23.04	172,000	838,125	49,250	133,854	
103	Intrusive igneous	588.79	134.24	42.10	21.73	172,000	840,063	49,250	133,854	
104		576.04	119.28	36.78	16.69	181,229	840,896	50,333	134,563	
105	High grade metamorphic	514.20	29.61	21.66	15.17	177,083	831,792	55,146	137,125	
106	High grade metamorphic	509.24	26.93	22.85	16.84	176,938	832,188	55,063	137,563	
107	High grade metamorphic	626.37	166.96	79.73	60.22	140,083	831,896	49,063	134,354	
108	High grade metamorphic	619.43	161.65	70.47	50.38	147,729	835,458	49,063	134,354	
109	Intrusive igneous	610.01	150.57	64.97	45.68	154,583	834,500	49,313	134,167	

110	Intrusive igneous	611.76	150.64	68.79	49.98	150,917	833,938	49,667	134,167	
111	Intrusive igneous	599.34	139.12	57.59	38.47	161,000	836,896	49,208	134,000	
112	Intrusive igneous	674.22	289.07	283.39	271.52	62,396	763,667	40,875	140,729	
113	High grade metamorphic	679.16	296.13	290.01	278.15	61,396	762,000	40,208	140,729	
114	High grade metamorphic	681.20	304.00	295.93	283.94	61,875	754,667	40,063	140,646	
115	High grade metamorphic	689.34	318.58	308.74	297.11	60,896	747,229	38,271	140,646	
116		687.73	317.86	307.41	295.98	61,521	749,063	39,104	140,896	
117		685.30	315.44	304.77	293.35	61,625	749,563	39,188	140,667	
118	Unconsolidated sediment	683.29	313.46	302.59	291.19	61,667	750,313	39,271	140,938	
119	Unconsolidated sediment	682.60	313.96	302.40	291.24	61,667	748,854	39,271	140,938	
120	High grade metamorphic	875.10	570.16	507.80	501.43	28,104	517,500	10,592	136,125	Precambrian rocks and Cambrian granites; furthest inland colony; scree slopes are most suitable habitats.
121	High grade metamorphic	906.01	609.60	541.12	534.96	15,438	465,146	4,841	134,417	No nesting confirmed, but suitable nesting habitats (scree slopes) exist. "Observations of higher numbers of snow petrels at the extreme southern point of the Mawson Escarpment strongly suggest the presence of a breeding colony in that area"
122	High grade metamorphic	447.25	100.58	4.07	4.15	99,188	761,083	58,521	147,542	"Nest in areas of eroded bedrock, in crevices, under boulders and in rock falls"
123	High grade metamorphic	448.62	101.89	4.04	4.63	99,188	761,208	58,188	147,250	
124	High grade metamorphic	445.76	98.92	3.75	3.94	99,292	761,000	58,583	147,833	"Nest in areas of eroded bedrock, in crevices, under boulders and in rock falls"
125	High grade metamorphic	444.72	97.83	3.18	3.27	99,458	761,354	58,771	147,833	"Nest in areas of eroded bedrock, in crevices, under boulders and in rock falls"
126	High grade metamorphic	448.76	101.62	4.85	5.31	100,229	761,813	58,625	147,542	"Nest in areas of eroded bedrock, in crevices, under boulders and in rock falls"
127	High grade metamorphic	444.50	97.38	4.68	5.16	101,667	761,688	58,792	147,833	"Nest in areas of eroded bedrock, in crevices, under

										boulders and in rock falls"
128	High grade metamorphic	443.22	96.13	3.08	3.32	101,042	762,000	58,771	147,771	"Nest in areas of eroded bedrock, in crevices, under boulders and in rock falls"
129	High grade metamorphic	444.08	96.69	6.38	7.13	102,063	761,167	58,604	147,542	"Nest in areas of eroded bedrock, in crevices, under boulders and in rock falls"
130	High grade metamorphic	443.66	96.24	6.24	6.97	102,063	761,750	58,792	147,542	"Nest in areas of eroded bedrock, in crevices, under boulders and in rock falls"
131	High grade metamorphic	444.26	96.57	8.03	9.70	102,063	763,167	59,042	147,271	"Nest in areas of eroded bedrock, in crevices, under boulders and in rock falls"
132	High grade metamorphic	440.62	92.83	6.02	6.93	103,021	763,229	58,771	147,396	"Nest in areas of eroded bedrock, in crevices, under boulders and in rock falls"
133	High grade metamorphic	441.87	93.90	8.61	9.83	103,042	763,396	58,604	147,542	"Nest in areas of eroded bedrock, in crevices, under boulders and in rock falls"
134	High grade metamorphic	409.45	57.49	24.32	26.82	119,854	768,438	60,292	147,313	
135	High grade metamorphic	382.62	33.78	5.65	9.14	132,979	771,063	61,295	146,813	SNPE nesting colonies are not constrained by h.a.s.l, inter-nest distance, or slope angle, but instead by the availability of boulders and crevices for nesting. There is a huge variation in these three parameters. "Nests occur on flat ground as well as steep slopes…nest from barely above the high tide mark to the tops of cliffs, and nests may be solitary or in clusters".
136	High grade metamorphic	379.55	30.99	2.64	6.13	135,042	770,271	61,251	146,958	
137	Unknown or unclassified	368.91	27.42	6.28	9.76	143,500	773,646	61,481	146,771	
138	High grade metamorphic	364.90	24.40	2.10	1.38	143,833	773,500	61,958	146,354	
139	High grade metamorphic	367.82	27.70	7.09	10.57	144,625	775,021	61,481	146,771	
140	Unconsolidated sediment	364.65	23.57	1.83	5.31	145,833	774,083	61,771	146,208	"Probably nests throughout much of the western part"
141	Unconsolidated sediment	361.87	25.32	4.70	1.23	147,208	775,792	61,958	145,500	

142	Unknown or unclassified	362.26	26.13	7.01	10.49	149,229	776,229	61,897	146,146	
143	High grade metamorphic	355.36	25.95	7.96	4.48	152,938	775,646	62,042	145,938	"Fair numbers in the area approximately south and east of Club Lake"
144	Unknown or unclassified	360.04	24.02	4.92	8.40	150,521	776,021	61,813	146,208	
145	High grade metamorphic	359.48	23.52	4.42	7.89	150,688	776,021	61,813	146,208	
146	Unknown or unclassified	359.88	24.78	6.04	9.52	150,521	776,479	61,813	146,146	
147	Unconsolidated sediment	354.14	25.32	7.57	4.10	153,417	775,646	62,042	145,938	"Abundant"
148	Unknown or unclassified	359.67	25.33	6.88	10.36	150,521	776,333	61,813	146,146	
149	Unknown or unclassified	359.10	24.75	6.27	9.75	151,000	776,708	61,813	146,146	
150	Unknown or unclassified	357.93	23.17	4.47	7.95	152,229	776,000	62,042	146,208	
151	High grade metamorphic	356.90	21.71	2.85	6.33	152,625	776,604	61,958	146,208	
152	High grade metamorphic	353.26	22.22	4.07	0.60	153,271	776,417	61,958	145,667	
153	High grade metamorphic	353.22	19.91	1.21	2.26	155,167	777,458	61,958	145,479	
154	High grade metamorphic	351.57	21.53	3.74	0.27	155,521	776,729	62,292	145,667	
155	High grade metamorphic	351.38	21.26	3.47	0.09	155,521	776,729	62,292	145,667	
156	Unconsolidated sediment	351.46	19.19	0.67	2.80	155,646	778,021	61,958	145,479	Snow petrels are "sparse throughout"
157	Intrusive igneous	345.60	23.62	7.81	5.35	158,063	778,000	62,604	145,604	"Fair numbers, nesting at moderate density"
158	Unknown or unclassified	344.54	18.40	1.96	4.41	163,104	779,167	62,688	145,667	
159	Volcanic igenous	323.49	160.24	75.43	47.30	237,063	751,896	75,958	147,646	
160	Intrusive igneous	217.28	30.24	13.53	8.50	205,292	718,854	78,104	148,500	Nests commonly had 2+ entrances; space inside nests varied; also a considerable number of non-breeding birds.
161	High grade metamorphic	247.45	121.16	128.95	119.15	190,833	658,313	69,417	153,396	
162	Intrusive igneous	272.14	148.06	152.82	136.20	197,500	644,750	68,792	153,271	
163	High grade metamorphic	312.37	159.11	137.30	101.81	208,688	619,250	69,854	151,479	70% of nests in crevices/cracks, 30% under/between large boulders. "The birds seem to select for nest

										sites, only those rocks which are the least susceptible to weathering"
164	High grade metamorphic	372.13	12.84	55.93	9.49	188,604	534,083	67,417	152,250	
165	High grade metamorphic	369.42	9.41	52.42	5.89	189,083	534,021	67,854	152,104	
166	High grade metamorphic	319.31	14.97	36.21	16.26	189,250	521,313	66,750	149,917	
167	High grade metamorphic	318.30	16.71	37.03	18.26	189,292	521,271	66,750	149,917	
168	High grade metamorphic	335.96	14.76	45.60	13.50	182,458	521,125	65,000	150,750	
169	High grade metamorphic	335.90	15.65	46.32	14.33	182,292	520,917	64,979	150,625	
170	Intrusive igneous	335.82	16.85	47.20	15.44	182,229	520,208	64,979	150,375	
171	High grade metamorphic	331.89	8.09	40.01	6.87	185,229	520,250	66,313	150,417	
172	High grade metamorphic	331.87	8.98	40.71	7.70	184,021	520,063	65,000	150,333	
173	Intrusive igneous	331.85	10.48	41.86	9.09	183,083	520,292	64,979	150,479	
174	High grade metamorphic	330.55	8.15	39.99	6.78	183,917	520,458	64,875	150,479	
175	High grade metamorphic	330.52	10.26	41.51	8.77	182,896	519,542	64,979	150,167	
176	High grade metamorphic	328.04	6.22	38.24	4.74	184,313	519,583	64,979	150,167	
177	High grade metamorphic	325.69	1.56	34.64	1.28	184,792	518,688	65,250	149,896	
178	High grade metamorphic	325.67	0.61	33.80	1.50	185,563	518,979	66,063	149,979	
179	High grade metamorphic	325.66	0.74	33.14	2.01	185,667	520,396	66,292	150,063	Most nests oriented towards prevailing winds; some nesting sites were more exposed, suitable to Cape pigeon.
180	High grade metamorphic	325.70	1.85	34.86	1.18	184,396	518,313	64,979	149,792	"Nests are made in any rocky area with suitable crevices under or between the rocks".
181	High grade metamorphic	324.55	1.68	33.11	3.07	185,896	518,979	66,292	149,979	
182	High grade metamorphic	324.56	2.58	33.18	3.90	186,833	521,042	66,292	150,063	
183	High grade metamorphic	323.46	2.80	33.29	4.00	185,458	518,854	65,625	149,896	
184	High grade metamorphic	322.37	2.04	32.87	3.42	185,875	518,313	65,250	149,792	

185	High grade metamorphic	322.38	2.76	33.08	4.12	185,979	518,313	65,250	149,792	
186	High grade metamorphic	322.37	1.44	32.66	2.75	185,417	517,958	65,250	149,792	Less than half the occupied nest sites were used for breeding.
187	High grade metamorphic	322.37	1.44	32.66	2.75	185,417	517,958	65,250	149,792	
188	High grade metamorphic	320.24	2.28	32.24	4.10	187,125	517,958	65,250	149,750	
189	High grade metamorphic	320.48	1.45	31.94	2.83	186,979	517,833	65,250	149,750	
190	High grade metamorphic	305.22	19.59	31.26	5.72	190,167	509,188	64,604	148,729	
191	High grade metamorphic	297.79	77.86	23.07	9.00	205,750	465,646	65,583	201,021	
192	High grade metamorphic	296.32	75.22	20.72	10.40	206,229	466,979	64,646	201,292	
193	Low-medium grade metamorphic	295.38	71.85	20.44	11.95	206,000	467,938	64,583	201,646	
194	High grade metamorphic	295.33	72.01	20.47	11.97	206,000	467,938	64,583	201,646	Colonies range from dense to loosely aggregated. "Snow petrels nest in cracks or under boulders situated in rocky areas"
195	Low-medium grade metamorphic	295.05	71.80	20.73	12.34	206,188	467,938	64,583	201,646	
196	Low-medium grade metamorphic	295.13	71.74	20.66	12.25	206,188	467,938	64,583	201,646	
197	Low-medium grade metamorphic	294.83	71.66	20.92	12.61	206,188	467,708	64,583	201,667	
198	High grade metamorphic	294.54	71.68	21.17	12.94	206,188	467,708	64,583	201,667	
199	High grade metamorphic	290.89	71.38	24.25	17.07	206,708	464,854	64,583	201,146	
200	High grade metamorphic	288.33	62.69	18.82	9.18	207,563	466,771	64,708	202,333	
201	Low-medium grade metamorphic	281.18	56.25	20.73	8.44	207,417	467,438	64,688	202,375	
202	Intrusive igneous	259.64	37.45	25.86	7.85	209,104	475,250	67,938	202,917	
203	Intrusive igneous	262.15	40.58	29.26	11.29	208,792	475,354	67,938	203,021	
204	Low-medium grade metamorphic	233.68	33.20	30.21	12.10	214,146	470,104	69,750	200,688	
205	High grade metamorphic	240.32	25.74	25.95	4.94	212,000	473,167	70,042	200,750	
206	Low-medium grade metamorphic	235.81	25.32	25.36	8.59	213,396	473,479	70,250	200,771	

207	Low-medium grade metamorphic	233.04	25.50	25.58	9.61	213,979	471,729	70,250	200,542	
208	Low-medium grade metamorphic	235.56	25.47	25.71	9.12	213,313	473,667	70,250	200,792	
209	Low-medium grade metamorphic	239.22	24.56	24.99	7.34	212,708	473,708	70,771	201,042	
210	Intrusive igneous	233.79	25.79	26.36	10.43	213,729	472,646	70,708	200,729	
211	High grade metamorphic	236.37	25.82	26.49	9.97	213,208	474,042	70,771	201,021	
212	Sedimentary	393.63	142.93	177.03	114.23	181,354	509,688	96,938	227,792	
213	Volcanic igenous									
214	Volcanic igenous									Limited suitable terrain for petrel breeding.
215	High grade metamorphic	769.04	433.35	226.70	189.37	43,104	525,979	98,250	306,771	
216	Unconsolidated sediment	690.28	426.25	25.15	29.96	68,438	533,500	120,771	329,000	
217	Sedimentary	695.63	396.28	11.25	5.13	70,542	529,729	124,104	330,646	
218	Volcanic igenous	703.37	325.05	17.73	4.70	74,896	518,333	127,354	333,438	
219	Sedimentary	706.70	315.36	29.32	18.23	74,958	515,563	126,208	333,479	
220	Intrusive igneous	712.95	295.60	43.52	34.84	75,188	511,875	125,083	333,042	
221	Volcanic igenous	774.52	108.95	28.73	10.06	79,917	448,333	87,688	328,979	
222	Volcanic igenous	816.05	65.69	27.63	24.24	84,104	246,938	65,792	333,833	
223	Intrusive igneous	974.35	118.21	106.39	79.11	58,628	187,563	143,542	389,688	
224	Intrusive igneous	975.48	127.85	116.01	89.22	57,438	186,792	142,917	389,729	Nests on gentle slopes.
225	Intrusive igneous	974.99	129.76	117.50	91.03	55,063	191,792	144,688	390,125	Nesting above an extensive Antarctic petrel colony
226	Intrusive igneous	944.11	265.80	214.91	150.47	27,313	290,458	158,792	396,146	
227	Volcanic igenous	939.50	270.86	200.07	137.98	26,021	321,479	166,021	396,792	"Protected nooks under rocks on a talus slope".
228	Volcanic igenous	877.49	296.89	189.92	134.52	20,417	390,125	172,250	398,208	
229	Volcanic igenous	744.38	250.54	179.52	157.86	29,271	396,396	161,500	398,000	
230	Volcanic igenous	698.15	163.67	83.65	62.91	30,250	450,042	174,208	393,250	

231	Intrusive igneous	277.55	30.14	25.66	22.33	41,104	374,646	150,771	362,833	
232	Volcanic igenous	337.99	121.94	122.30	110.71	34,208	353,896	123,667	360,958	
233	Volcanic igenous	344.24	128.63	129.13	116.88	34,000	352,875	122,333	361,208	
234	Volcanic igenous	343.73	127.72	128.56	115.53	33,958	352,771	121,875	361,354	
235	Volcanic igenous	343.50	127.30	128.31	114.89	33,958	352,354	121,875	361,208	
236	High grade metamorphic	328.72	110.75	111.94	98.77	34,667	353,167	123,833	358,333	
237	High grade metamorphic	328.37	109.94	111.54	97.43	34,500	354,250	123,042	358,396	
238	Volcanic igenous	314.91	112.56	76.41	58.95	68,396	363,188	128,250	305,958	
239	Volcanic igenous	342.73	136.82	103.01	80.99	49,854	355,208	120,604	309,958	
240	Intrusive igneous	1566.65	589.55	371.49	285.06	6,917	28,271	59,438	226,042	
241	Intrusive igneous	1565.44	586.54	368.22	281.90	6,917	28,354	60,271	226,125	
242	Intrusive igneous	1565.47	577.38	360.05	275.02	6,917	28,083	61,938	226,313	
243	Intrusive igneous	1565.83	570.99	355.12	271.18	7,042	28,292	62,833	226,896	"Nests were mainly limited to cracks and ledges in the dolerite"
244	Intrusive igneous	1568.53	573.97	359.03	275.33	6,958	27,313	61,833	225,417	
245	Intrusive igneous	1568.11	570.85	356.30	273.03	7,021	27,563	62,688	225,875	
246	Intrusive igneous	1562.25	552.38	338.29	256.52	7,083	28,979	66,542	228,667	
247	Intrusive igneous	1571.49	566.11	354.45	273.04	7,000	27,146	62,958	225,417	"colony was situated in and among blocks of weathered dolerite on top of the outcrop"; "nests were mainly limited to cracks and ledges in the dolerite"
248	High grade metamorphic	1608.68	731.67	527.85	440.82	5,354	21,146	33,542	203,729	
249	High grade metamorphic	1681.60	737.09	563.82	495.46	4,521	19,500	21,292	198,938	
250	High grade metamorphic	1582.78	698.38	486.84	396.59	5,604	23,958	41,146	211,354	
251	Sedimentary	1592.23	692.10	482.60	394.48	5,583	23,438	41,708	210,771	
252	Volcanic igenous	551.92	191.11	146.06	100.56	31,083	312,500	77,646	321,750	

253	Volcanic igenous	508.92	147.46	99.54	53.00	42,375	316,146	80,625	318,458	
254	Volcanic igenous	513.81	155.88	106.64	64.55	42,083	314,542	80,750	320,958	
255	Volcanic igenous	523.94	168.23	118.14	79.67	39,271	314,438	80,021	323,875	
256	Sedimentary	501.67	233.42	163.07	132.85	55,750	330,271	73,563	349,583	
257	Volcanic igenous	405.87	148.00	76.05	52.55	88,646	334,292	79,417	327,375	
258	Low-medium grade metamorphic	453.45	268.05	201.11	175.78	80,354	335,479	72,458	345,813	
259	Low-medium grade metamorphic	421.27	250.00	176.43	146.67	96,146	337,979	73,771	339,917	Abundant lichens around the nest site. Netsing in close proximity, governed by the availability of nest sites.
260	Sedimentary	436.23	282.30	197.85	169.45	92,542	335,125	71,396	344,833	
261	Low-medium grade metamorphic	416.67	252.41	175.20	145.28	98,813	337,521	72,708	338,917	
262	Low-medium grade metamorphic	413.27	251.50	172.99	143.07	99,375	337,750	72,604	338,688	
263	Sedimentary	424.70	277.52	186.17	155.53	96,146	335,021	71,583	344,021	
264	Intrusive igneous	441.81	304.71	202.50	172.35	90,229	332,417	70,271	348,021	
265	Sedimentary	418.90	271.24	180.36	149.20	99,500	336,188	71,354	341,292	
266	Sedimentary	416.03	271.34	177.22	145.52	100,542	335,875	71,417	341,229	
267	Intrusive igneous	419.16	291.01	172.32	140.97	98,500	333,500	70,042	343,604	
268	Low-medium grade metamorphic	277.33	160.77	41.16	26.41	135,792	341,229	74,625	293,021	
269	Volcanic igenous	339.26	221.77	65.74	39.90	119,396	333,083	67,604	324,792	
270	Volcanic igenous	334.59	217.41	62.09	37.80	119,438	332,542	67,563	323,396	
271	Sedimentary	370.84	222.99	184.18	169.83	93,021	334,875	67,604	333,667	
272	High grade metamorphic	351.57	216.83	149.24	134.50	99,646	336,583	65,563	327,938	
273	Sedimentary	345.05	209.90	157.10	144.45	98,750	335,729	65,313	327,479	
274	Low-medium grade metamorphic	334.36	206.44	138.07	126.08	100,396	336,729	64,125	324,125	
275	Low-medium grade metamorphic	326.00	203.03	125.15	113.94	103,063	336,646	63,833	322,354	

276	Unconsolidated sediment	264.10	153.62	31.24	21.32	115,021	334,021	58,958	308,083	
277	Intrusive igneous	275.93	172.70	81.61	73.98	110,021	333,688	59,917	308,750	
278	Volcanic igenous	291.79	177.97	27.71	9.16	116,188	334,229	60,896	317,208	
279	Intrusive igneous	265.80	152.24	18.63	5.93	117,292	334,292	60,146	308,833	
280	Unconsolidated sediment	256.90	147.57	27.92	19.37	115,917	334,125	58,833	306,146	
281	High grade metamorphic	255.56	145.99	24.79	16.14	115,833	334,208	58,521	306,417	
282	Intrusive igneous	233.77	129.89	22.25	17.40	117,521	334,021	57,208	300,271	
283	Intrusive igneous	225.03	122.40	19.10	14.99	118,729	334,104	56,750	297,854	
284	Unconsolidated sediment	229.62	130.51	36.11	32.09	116,354	333,938	56,625	297,771	
285	Intrusive igneous	228.18	130.36	39.36	35.47	116,708	333,833	56,333	297,208	
286	Intrusive igneous	204.52	102.01	0.34	3.73	122,521	334,313	55,833	291,688	
287	Volcanic igenous	161.67	89.66	20.43	14.14	116,083	327,958	48,458	273,583	
288	Intrusive igneous	223.52	125.86	35.39	31.64	117,438	334,083	56,208	295,396	
289	Intrusive igneous	204.00	102.57	7.40	2.42	120,354	334,104	55,167	291,250	
290	Intrusive igneous	203.38	103.22	11.23	5.03	120,063	333,833	55,458	290,604	
291	Volcanic igenous	204.13	106.90	20.73	12.99	118,979	333,417	55,167	290,729	
292	Volcanic igenous	191.90	95.53	21.50	18.05	122,854	333,875	54,458	286,917	
293	Intrusive igneous	193.25	95.04	14.94	9.05	121,417	333,917	54,271	287,604	
294	Volcanic igenous	197.82	99.77	14.50	3.62	119,625	333,292	54,771	288,896	
295	Intrusive igneous	189.99	93.51	19.43	12.69	121,396	333,646	54,125	285,646	
296	Intrusive igneous	171.16	82.99	24.62	11.34	119,750	330,146	51,021	276,396	
297	Volcanic igenous	164.97	81.88	11.04	2.42	117,479	327,917	49,542	274,042	
298	Intrusive igneous	183.32	131.02	95.83	91.51	108,563	328,521	50,646	286,583	
299	Intrusive igneous	180.80	129.63	97.27	93.06	108,333	328,458	50,813	286,354	

300	Intrusive igneous	152.26	108.57	77.99	72.99	108,896	328,167	50,063	279,979	
301	Intrusive igneous	152.87	112.47	85.75	80.67	108,167	328,792	51,146	282,167	
302	Intrusive igneous	144.40	109.04	102.43	98.90	106,750	329,500	53,229	285,188	
303	High grade metamorphic	140.49	108.15	87.65	83.13	107,521	328,958	52,000	282,292	
304	Volcanic igenous	93.16	43.60	12.37	8.27	108,542	325,417	45,354	266,479	
305		99.66	87.04	86.61	82.96	108,104	329,417	54,563	275,438	
306	Volcanic igenous	66.10	29.46	16.01	13.12	107,917	324,917	45,292	263,021	
307	Intrusive igneous	55.64	20.14	9.98	7.32	107,708	324,271	44,750	260,771	
308	Volcanic igenous	53.56	14.89	2.08	0.66	107,979	324,000	44,104	259,604	
309	Volcanic igenous	51.60	20.51	15.24	11.75	107,917	323,979	45,667	260,917	
310	Volcanic igenous	30.45	18.97	20.45	16.82	107,354	324,938	49,563	259,083	
311	Volcanic igenous	29.21	18.15	19.98	16.21	107,521	324,813	49,458	258,750	
312	Volcanic igenous	12.66	5.11	8.35	4.86	107,521	323,792	50,000	254,354	
313	Volcanic igenous	21.85	13.66	16.00	13.44	107,042	322,542	45,542	249,688	
314	Intrusive igneous	8.30	5.80	3.48	5.96	106,938	322,646	47,313	248,625	
315	Volcanic igenous	76.74	45.18	44.46	22.41	113,938	334,958	71,958	272,479	
316	Volcanic igenous	13.76	10.64	13.03	10.56	106,854	321,896	48,896	244,646	
317	Sedimentary	50.07	22.81	22.39	9.76	115,396	336,063	74,125	268,375	
318	Volcanic igenous	62.04	41.70	44.78	32.28	113,604	333,729	69,042	264,667	
319	Sedimentary	58.24	34.83	39.00	26.23	112,563	331,458	66,688	258,646	
320	Volcanic igenous	51.72	30.28	35.54	24.97	112,083	330,208	64,792	252,417	
321	Volcanic igenous	8.77	6.33	8.84	6.36	108,021	324,750	54,354	249,167	No nests found, but suspected breeding.
322	Intrusive igneous	12.17	9.89	12.39	9.91	108,083	325,250	54,583	248,854	"Located at the bottom of a cavity on a coastal stack"; 15 SNPEs were non-breeding visitors.

323	Volcanic igenous	5.61	7.85	5.45	7.91	106,083	322,208	48,750	242,271	
324	Volcanic igenous	51.73	28.84	34.46	23.17	111,917	330,542	64,875	253,375	
325	Volcanic igenous	26.77	8.37	9.47	4.53	113,917	332,542	69,396	255,000	
326	Volcanic igenous	26.37	11.62	12.90	9.83	113,854	332,854	69,917	254,333	page 159, Wednesday 5th December. One nest was under an overhanging rock. "The nest is a mere hollow in the rocky ground"
327	Volcanic igenous	50.27	28.03	33.42	22.61	111,813	330,167	64,688	251,125	
328	Volcanic igenous	24.26	13.18	14.44	12.06	113,438	332,208	68,333	252,229	
329	Volcanic igenous	23.49	8.80	12.80	5.11	112,688	330,563	66,375	245,479	
330	Volcanic igenous									
331	Volcanic igenous	20.21	13.99	11.57	15.45	114,792	332,250	70,438	244,479	
332	Volcanic igenous	26.33	13.38	11.24	8.90	116,521	333,292	74,625	246,792	
333	Volcanic igenous	21.11	10.26	13.51	8.14	113,021	330,500	67,000	242,292	
334	Low-medium grade metamorphic	19.32	13.76	17.12	13.60	109,854	326,229	60,104	236,375	
335	Low-medium grade metamorphic	24.78	16.01	18.17	15.71	114,813	331,375	70,958	233,875	
336	Volcanic igenous									Neighbouring Cape pigeons
337	Volcanic igenous	71.15	82.97	79.42	83.12	105,792	316,729	55,729	197,333	
338	Low-medium grade metamorphic									
339	Sedimentary	74.86	71.71	69.14	63.07	110,604	329,917	63,292	265,688	
340	Volcanic igenous	34.60	15.10	19.82	9.65	112,125	330,646	65,146	246,813	
341	High grade metamorphic									
342	High grade metamorphic									
343	High grade metamorphic									
344	High grade metamorphic									
345	High grade metamorphic									

346	High grade metamorphic									
347	High grade metamorphic									
348	High grade metamorphic									
349	High grade metamorphic									
350	High grade metamorphic									
351	High grade metamorphic									
352	High grade metamorphic									
353	Sedimentary									
354	Sedimentary									
355	Sedimentary									
356	Sedimentary									
357	Sedimentary									
358	High grade metamorphic									
359	High grade metamorphic									
360	Sedimentary									
361	Sedimentary									
362	High grade metamorphic									
363	High grade metamorphic									
364	High grade metamorphic									
365	High grade metamorphic									
366	High grade metamorphic									
367	High grade metamorphic									
368	High grade metamorphic									
369	Intrusive igneous									

370	Intrusive igneous									"Nests were sparsely scattered on cliffs, sometimes adjacent to Antarctic Fulmars and Cape Petrels". Nests are ubiquitous around the edge of the island.
371	Intrusive igneous									Nests are ubiquitous around the edge of the island.
372	Intrusive igneous									"Many nests were present on ledges within the active volcanic crater of Bellingshausen Island", suggestive of low level predation by Skuas
373	Intrusive igneous									
374	Intrusive igneous									
375	Intrusive igneous									Nesting amongest loose colonies of Antarctic Fulmars and Cape Petrels
376	Intrusive igneous									
377	Intrusive igneous									Nests sympatrically with Antarctic fulmars.
378	Intrusive igneous									Nests close to cape petrels.
379	Intrusive igneous									
380	Intrusive igneous									Adjacent to Antarctic Fulmars
381	Intrusive igneous									
382	Intrusive igneous									Adjacent to Cape Petrels
383	Intrusive igneous									
384	Sedimentary									Northern limit of SNPE breeding range. Breed on high inland cliffs.
385	Sedimentary									
386	Sedimentary									
387	Sedimentary									
388	Sedimentary									
389	Sedimentary									
390	Sedimentary									

391	Sedimentary									
392	Sedimentary									
393	Sedimentary									
394	Sedimentary									
395	Sedimentary									
396	Sedimentary									
397	Sedimentary									
398	Sedimentary									
399	Sedimentary									
400	Sedimentary									
401	Sedimentary									
402	Sedimentary									
403	Sedimentary									
404	Sedimentary									
405	Volcanic igenous									
406	Sedimentary									
407	Sedimentary									
408	Sedimentary									
409	Sedimentary									
410	Sedimentary									
411	Sedimentary									
412	Sedimentary									
413	Sedimentary									
414	Sedimentary									

415	Sedimentary									
416	Sedimentary									
417	Sedimentary									
418	Sedimentary									
419	Sedimentary									
420	Sedimentary									
421	Sedimentary									
422	Volcanic igenous									
423	Sedimentary									
424	Sedimentary									
425	Sedimentary									
426	Sedimentary									
427	Volcanic igenous									
428	Sedimentary									
429	Sedimentary									
430	Sedimentary									
431	Sedimentary									
432	Sedimentary									
433	Sedimentary									
434	Volcanic igenous									
435	Volcanic igenous									
436	Sedimentary									
437	Sedimentary									
438	Sedimentary									

439	Sedimentary									
440	Volcanic igenous									
441	Volcanic igenous									
442	Volcanic igenous									
443	Volcanic igenous									
444	Volcanic igenous									
445	Sedimentary									
446	Sedimentary									
447	Sedimentary									
448	Intrusive igneous									
449	Sedimentary									
450	Volcanic igenous									
451	Intrusive igneous									
452	Volcanic igenous									
453	Volcanic igenous									
453	Volcanic igenous									
455	Sedimentary									
456	Sedimentary									
457	Intrusive igneous									

Appendix B: Snow petrel paper

In this paper manuscript, Figures 1 through 7 correspond to thesis Figures 6 through 12, respectively. “Table 1” in the paper manuscript is also “Table 1” in the thesis.

Title: The breeding distribution and habitat use of the snow petrel (*Pagodroma nivea*), the world’s most southerly breeding vertebrate

Aim: To quantify the known global breeding distribution and habitat characteristics of snow petrels.

Location: Antarctica, Southern Ocean, maritime and subantarctic islands

Time period: Up to present day

Major taxa studied: Snow petrel (*Pagodroma nivea*)

Methods: We compiled a new database of published and unpublished records of known snow petrel breeding sites. We quantified local environmental conditions by appending indices of climate and substrate at these sites, and at the regional scale by appending sea-ice conditions within accessible foraging areas between 1992-2021.

Results: Snow petrels are reported at 456 breeding sites across Antarctica and subantarctic islands. Population estimates available for 222 sites totalled a minimum of ~77,400 known breeding pairs, although with so many missing data, the true breeding population will be much higher. Breeding sites are close to the coast (median = 1.15 km) and research stations (median = 26 km). The median distance to the sea ice edge is 430 km in November (breeding season sea-ice maximum). Locally, most breeding pairs are located in cavities on high-grade metamorphic rocks. The median of the average summer temperatures at breeding sites is -6.9°C; the most extreme (low) temperatures are at the most inland sites, and the highest temperatures at their northern breeding limit.

Main conclusions: Inventorying the known breeding sites has enabled characterisation of breeding habitat for the global distribution. Breeding location and cavity selection is likely controlled most importantly by the availability of suitable breeding substrate within sustainable distance of suitable foraging habitat. Within this range, cavities may then be selected based on local conditions such as cavity size and aspect. Our database will allow formal analyses of habitat selection, and provides a baseline against which to monitor future changes in the distribution of snow petrels in response to climate change.

Keywords:

Breeding distribution, climate, habitat, lithology, sea-ice conditions, snow petrel

1. Introduction

Globally, seabirds are one of the most threatened marine taxonomic groups (Sydeman et al., 2012; Dias et al., 2019). However, knowledge of their spatial distribution and population sizes are incomplete (Rodríguez et al., 2019). This gap is exacerbated in polar regions where many seabird breeding sites are poorly quantified, particularly in remote, inaccessible locations. Satellite remote sensing in Antarctica has enabled the discovery and estimation of population sizes for colonies of several surface-nesting species: Adélie penguins *Pygoscelis adeliae*, emperor penguins *Aptenodytes forsteri*, chinstrap penguins *P. antarcticus* and Antarctic petrels *Thalassoica antarctica* (Schwaller et al., 1989; Fretwell & Trathan, 2009; Fretwell et al., 2012; Schwaller et al., 2013; Lynch & LaRue, 2014; Fretwell et al., 2015; Schwaller et al., 2018; Román et al., 2022). However, knowledge of the circumpolar distributions of smaller cavity-nesting or burrowing seabirds remains largely reliant on direct observations (Southwell et al., 2011; Barbraud et al., 2018). Our focus here is on defining the breeding distribution of the most southerly breeding vertebrate, the snow petrel

Pagodroma nivea, which was last reviewed almost three decades ago (Croxall et al., 1995). Since then, scientific research has intensified on the continent and several targeted surveys have been undertaken (Barbraud et al., 1999; Convey et al., 1999; Olivier et al., 2004; Pande et al., 2020). As a result, it is now timely to provide an updated review of the known circumpolar snow petrel breeding distribution.

Snow petrels are a high-trophic-level seabird endemic to Antarctica with a northern breeding limit in South Georgia (Croxall et al., 1995). They have one of the highest affinities for pack ice of all Antarctic seabirds, feeding predominantly on fish, krill, and squid in proportions that vary dependent on foraging location (Ainley & Jacobs, 1981; Ainley et al., 1984; Ridoux & Offredo, 1989). When foraging at sea, snow petrels are largely confined to the Marginal Ice Zone [MIZ] and in particular, intermediate sea-ice concentrations of 12.5-50% (Zink, 1981; Ainley et al., 1984; 1998). Foraging ranges during the breeding season are limited by the central-place constraint (Delord et al., 2016), and variability in sea-ice conditions within foraging areas used by snow petrels, both prior to and during the breeding season, affects annual adult survival, colony size, and breeding phenology (Barbraud et al., 2000; Barbraud & Weimerskirch, 2001; Jenouvrier et al., 2005; Sauser et al., 2021b).

Snow petrels are cavity nesters, requiring ice-free areas for breeding (Walton, 1984). The lithology and geomorphology at breeding sites is thus important in determining cavity presence. Nesting cavities occur in cliff faces, on scree slopes, and under boulders on flat and sloping ground. Specific characteristics including slope, aspect, number of entrances, and nest bowl slope are variable. However, nests with single, narrow entrances are more frequently used, and hatching success and chick survival are greatest when nest bowls are flat (Jouventin & Bried, 2001; Einoder et al., 2014). Local meteorological conditions can affect access to nests or cause breeding failure (Sydeman et al., 2012), and it has been suggested that the interplay between nest aspect and local wind direction is critical in providing suitable snow-free cavities (Olivier & Wotherspoon, 2006). However, the relationship is not consistent; in the Windmill Islands, most snow petrel nesting cavities are oriented towards strong prevailing winds (Cowan, 1981), whereas in the Bunger Hills and Dronning Maud Land they are typically oriented for protection from prevailing katabatic winds (Wand & Hermichen, 2005). Variability in local climatic conditions during the breeding season, including timing, intensity and duration of precipitation, wind speed, direction and duration, and local air temperatures, affect snow petrel breeding phenology and demography (Chastel et al., 1993; Sauser et al., 2021a; 2021b). Baseline knowledge of conditions in the foraging and breeding habitats of snow petrels is therefore required for predicting how populations are likely to respond to future environmental changes at sea and on land.

In the only comprehensive review to date, snow petrels were confirmed as breeding at 195 sites across Antarctica and subantarctic islands, and suspected to breed at another 103 localities (Croxall et al., 1995). From available population data, this yielded a minimum known total breeding population of 63,000 pairs (Croxall et al., 1995). Typically, a large proportion (> 50%) of petrel populations is represented by non-breeders (juveniles, immatures, and non-breeding adults) (Phillips et al., 2017; Carneiro et al., 2020), and based on regional at-sea counts (Ainley et al., 1984; Cooper & Woehler, 1994), a total population size of several million birds was estimated (Croxall et al., 1995). However, regional breeding populations are often much smaller than at-sea densities would suggest. For example, at-sea estimations suggest there are 1.97 million snow petrels in the Ross Sea area, but in this region only 14 breeding sites were recorded, totalling ~5300 breeding pairs (Ainley et al., 1984; Croxall et al., 1995), suggesting many breeding sites may remain undetected.

The primary aim of this study was to quantify the known global breeding distribution and habitat use of snow petrels, as any relationships between lithology and cavity availability, or foraging habitat use and the circumpolar distribution have not yet been quantified. To do so, we first collated records of breeding locations, including population estimates when available. Our secondary aims were to (1) characterise the local scale environmental conditions at breeding sites (specifically lithology and climate variables including

temperature, precipitation and wind speed) and distance from the coast, and (2) define the maximum and mean foraging ranges from breeding sites, and characterise regional sea-ice conditions accessible within these foraging ranges. All data are presented in an accompanying open access database, which we hope will facilitate ongoing research and conservation.

2. Methods

2.1 Database compilation

To determine the known breeding distribution, an intensive search of the published literature and archived field reports was conducted, and all identified breeding sites were incorporated into a database with the following information: site name and decimal coordinates; site aspect, elevation and local lithology; and when survey data were available, nest density. Snow petrel nest densities range from highly dispersed (0.3 nests per ha) to relatively dense aggregations (24.1 nests per ha) (Olivier et al., 2004; Olivier & Wotherspoon, 2008), and uncalculated densities may be higher. However, even the maximum densities do not reach the high densities of colonies of closely related colonial breeders such as the Antarctic petrel (Mehlum et al., 1988; Schwaller et al., 2018). Therefore, it is difficult to define the spatial extent of a snow petrel colony, and to avoid ambiguity, we use the term 'breeding site' instead of 'colony', where a breeding site is defined as a locality with individual coordinates where breeding is likely or confirmed (based on observations).

Archived field reports, field notebooks, and maps from 1945 onwards at the British Antarctic Survey were searched to extract relevant spatial data, including from locations provided by Croxall et al. (1995). We also contacted seabird biologists with field knowledge of the Antarctic region, and included their unpublished observations.

Where quantitative data (e.g., coordinates, estimates of population size) had been observed and reported multiple times for a specific breeding site, the latest data was included in the database. Additional fields included breeding site identification [IDs] and Antarctic Conservation Biogeographic Region / Benthic Biogeographic Region (Terauds & Lee, 2016; Convey et al., 2014). For breeding sites between 30°E and 150°E, fields of 'Spatial sub-group' and 'Site_ID(s)' were added to conform with the spatial reference system of Southwell et al. (2021). At each locality, we distinguished whether breeding was confirmed or unconfirmed. For breeding to be confirmed, observations of active nests and the presence of eggs or chicks had to be reported. Otherwise, where nests were suspected but not found (e.g., Moss Island (González-Zevallos et al., 2013), or breeding was either not mentioned or reported to be likely or possible (e.g., Stinear Peninsula (Pande et al., 2020)), breeding was recorded as unconfirmed. Sites where breeding was checked for (i.e. during dedicated surveys) but did not occur were recorded as absences.

2.2 Local environmental conditions

To describe breeding habitat use at the local scale, climate and lithology at the terrestrial breeding sites were quantified.

Climate reanalysis data for the period 1992-2021 were obtained from the ERA5-Land monthly averaged dataset, Copernicus (Muñoz Sabater, 2019), including: 2m surface temperature, total precipitation, and 10m wind speed and direction. Seasonal 30-year averages and summary statistics for each variable were then calculated for each breeding site. The breeding season was defined as November-March.

Lithological data were extracted from the SCAR GeoMAP shapefile, comprising the known geology of all Antarctic bedrock and surficial deposits (Cox et al., 2023a). Breeding site lithologies were subsequently grouped into 8 categories for analysis, according to the simple lithological description in Cox et al. (2023b). In order to determine if habitat use reflected availability, the relative frequency distribution of lithology at breeding sites was compared to that within all exposed rock polygons.

2.3 Regional sea-ice conditions

To characterise the foraging habitat available to snow petrels at each breeding site, we assumed a mean and maximum summer foraging range of 700 km and 1500 km respectively (Delord et al., 2016; Durham University, unpub. data).

Passive microwave sea-ice data for the years 1992-2021 were acquired from the National Snow and Ice Data Centre (NSIDC). Sea-ice conditions were based on 30-year averages in November and February – chosen as the points in the breeding season when sea-ice extent [SIE] is at its maximum and minimum, respectively. In November, most breeding snow petrels return to breeding sites and eggs are laid, and most remain at breeding sites in February during the post-brood chick-rearing period. We focused on the low sea-ice concentration [SIC] MIZ most commonly used by breeding snow petrels for foraging. For November and February, we calculated the contours at the outer ice edge with 15% SIC (Olivier et al., 2005) and at 50% SIC, as the highest at-sea densities of snow petrels are recorded at the sea-ice edge and with SICs of up to 50% (Zink, 1981). We also generated the associated rasters of SIC. We calculated the distance from breeding sites to the 15 and 50% SIC contours for these months in 1992-2021, then calculated the average over the 30 years. Finally, we estimated the foraging area within the mean and maximum foraging ranges of each breeding site, using buffers of 700 and 1500 km from breeding sites, by counting the number of pixels between 15-50% SIC for the relevant months between 1992 and 2021, and transforming to an area by multiplying by the area of a single pixel (625 km^2). For all sea ice metrics, results were plotted by frequency, and summarised by calculating the median, interquartile range [IQR], and range. All analyses were carried out in QGIS and Rstudio.

3. Results

3.1 Spatial distribution and size of breeding sites

Our database represents a considerable expansion in knowledge of the global breeding distribution (Figure 1) since Croxall et al. (1995). We list 456 confirmed and suspected (snow petrels observed but breeding unconfirmed) breeding sites. Of these, 158 are newly identified, principally in Dronning Maud Land (28 new sites), the Prince Charles Mountains (11 new inland, 43 new coastal sites), and Adélie Land (19 new sites). Additionally, surveys in localities such as the Larsemann Hills (Pande et al., 2020) have enabled separation of a single breeding site in Croxall et al. (1995) into multiple sites in our database. Of the 456 known sites, breeding was confirmed at 267 (59%), and unconfirmed (but suspected, based on observations) at the remaining 189. Most breeding sites (74%) are located around the Antarctic continent, and 120 (26%) on islands (Bouvet Island, Balleny Islands, South Orkney Islands, South Sandwich Islands, South Georgia). However, when considering the total population estimate, just 51% of known breeding pairs are on the continent – noting that population estimates are only available for 55% of continental breeding sites, and that the estimate of 20,000 breeding pairs on Laurie Island (South Orkney Islands) constitutes a large proportion of the known breeding population.

The median distance of breeding sites from the coastline (based on Gerrish et al., 2023) was 1.15 km (IQR = 0.23 to 42.75 km, range = 0.00 to 471.27 km, n = 456). Prior to 1995, the furthest known inland breeding sites were in the Tottanfjella, Dronning Maud Land, over 300 km from the coast (Bowra et al., 1966). Although most known breeding sites are very close to the coast (Figure 2a), a small breeding site exists 440 km inland at Greenall Glacier, Mawson Escarpment, and an unconfirmed breeding site at Rimington Bluff (470 km inland) in the inland Prince Charles Mountain (Goldsworthy & Thomson, 2000). The site at Greenall Glacier increases the distance inland at which snow petrels are known to breed by 140 km.

The number of breeding pairs is extremely variable among sites (median = 50, IQR = 10 to 171, range = 1 to 20,000, n = 222; Figure 2b). At some, single breeding pairs were recorded (e.g., Orvinfjella region, Dronning Maud Land; Dragons Teeth Cliffs, Prince Charles Mountains; Mount Haskel, north-west Antarctic Peninsula). In contrast, 4,575 breeding pairs were estimated on Browning Peninsula, South Windmill Islands (Olivier et

al., 2004), and 20,000 breeding pairs on Laurie Island, South Orkney Islands (Clarke, 1906; Croxall et al., 1995). However, the number of breeding pairs is only known (counts or estimates) at 222 sites (49%). Together, this indicates a minimum total breeding population estimate of ~77,400 pairs. Where population sizes are known, 69% of breeding sites contain ≤ 100 pairs.

Most known breeding sites are relatively close to research stations (median distance = 25.96 km, IQR = 8.53 to 81.76 km, range = 0.32 to 875.38 km; Figure 3), with 406 breeding sites (86%) < 200 km from the nearest station, and 297 (65%) < 50 km from the nearest station. However, much exposed rock (a requirement for nesting) is available beyond 50 km from stations where considerably fewer sites are reported, and unknown breeding sites may exist.

3.2 Local environmental conditions

There was extensive variation in environmental conditions at breeding sites (Figure 4; Table 1), with a median temperature of -6.9°C (IQR = -12.8 to -4.2°C, range = -23.8 to 2.9°C, n = 247), total precipitation of 1.0 mm (IQR = 0.7 to 3.1 mm, range = 0.1 to 6.9 mm) and seasonal wind speed of 3.5 ms^{-1} (IQR = 2.5 to 4.9 ms^{-1}, range = 0.5 to 10.0 ms^{-1}). The mildest climatic conditions are experienced at South Georgia (the northern breeding limit), where mean seasonal temperatures and total precipitation were > 0°C and > 3.0 mm, respectively, but mean wind speeds were similar to the median for all sites. On the Antarctic Peninsula, mean seasonal surface temperatures vary between -10 and 0°C, and total precipitation between 0.5 and 7.0 mm, with warmer and wetter conditions closer to the west coast. The lowest, most extreme mean seasonal temperatures are experienced at inland Antarctic breeding sites, varying between -23.8 and -4.0°C, whereas mean seasonal wind speeds are highest at sites in coastal East Antarctica.

The most available lithology by frequency in Antarctica is intrusive igneous (27%), followed by sedimentary (21%) and high-grade metamorphic rock (18%) (Figure 5a). Breeding sites are found most often on intrusive igneous rock (28%) and high-grade metamorphic rock (26%). Fewer sites are on sedimentary rock (17%) despite its relatively high availability (Figure 5a). For the 222 breeding sites with population estimates, the number of breeding pairs on high-grade metamorphic rock (> 45,000 pairs) outnumbers the total pairs on intrusive igneous rock (< 17,000 pairs) or any other lithology.

3.3 Regional sea-ice conditions

Sea-ice conditions in foraging areas accessible to breeding snow petrels differed between regions and during the breeding months (Figure 6). Breeding sites on Bouvet Island, the South Shetland Islands, South Orkney Islands, South Sandwich Islands, and South Georgia, are at or beyond the 30-year average November ice edge contour (Figure 6a). The likely foraging habitat is therefore very different to sites with accessible foraging areas within the MIZ. We have therefore quantified foraging-habitat use only for breeding sites where the birds likely feed within the MIZ (n = 333).

In November, when SIE is at its maximum during the breeding season, the median distance from breeding sites to the ice edge is 430 km (IQR = 295 to 694 km, range = 6 to 1682 km), and to the 50% SIC contour is 136 km (IQR = 30 to 282 km, range = 1 to 737 km) (Figure 7a, 7b). These are generally within the mean foraging range (~700 km) and well within the maximum foraging range (1500 km). The 15-50% SIC zone lies beyond the mean foraging range only for inland breeding sites in Dronning Maud Land, the Transantarctic Mountains, and Marie Byrd Land. The November 50% SIC contour only reached the coast adjacent to coastal breeding sites east and west of Amery Ice Shelf, Adélie Land, and north of the Ross Ice Shelf (Figure 6a). Within the assumed mean foraging range, the median area of sea ice between 15 and 50% SIC in November is 113,000 km^2 (IQR = 42,400 to 167,000 km^2, range = 4,520 to 237,000 km^2). Within the maximum foraging range, the median foraging area is 396,000 km^2 (IQR = 325,000 to 762,000 km^2, range = 19,500 to 841,000 km^2).

Between November and February, the ice edge retreats towards the continent by hundreds of km (mean = 472 km, standard deviation = 344 km, range = -8 to 1248 km). The greatest retreat is north of Dronning Maud Land (> 1000 km). By February, the most extensive and highest concentration remaining sea ice (> 90% SIC) is in the Weddell and Bellingshausen Seas, and adjacent to the coast of North Victoria Land; these are all areas with no or relatively few known snow petrel breeding sites (Figure 6b). The median distance from breeding sites to the February ice edge is 47 km (IQR = 21 to 163 km, range = 0.3 to 564 km), and to the 50% SIC contour is 27 km (IQR = 10 to 136 km, range = 0.1 to 535 km) (Figure 7c, 7d). Within the assumed mean foraging range, the median area of sea ice between 15 and 50% SIC in February is 60,900 km^2 (IQR = 46,700 to 67,600 km^2, range = 4,840 to 174,000 km^2), and within the maximum foraging range, the median area of 15-50 % SIC is 201,000 km^2 (IQR = 146,000 to 265,000 km^2, range = 110,000 to 398,000 km^2).

4. Discussion

4.1 Geographic distribution

More snow petrel breeding sites are known within East Antarctica (69 breeding sites, between 76°E and 112°E), and the north-west Antarctic Peninsula (61 breeding sites, between 61°S and 69°S) than in other regions (Figure 1). From available population estimates, East Antarctica also holds the highest numbers of breeding pairs (at least 21,160), followed by the South Orkney Islands (at least 20,129 pairs, including 20,000 on Laurie Island) (Clarke, 1906). As a loosely colonial cavity-nesting species, defining the extent of a snow petrel breeding site and colony is difficult, and many population sizes may be underestimated. However, the population estimate for Laurie Island probably represents multiple colonies (Coria et al., 2011).

The breeding distribution in relation to distance to the coast suggests that the furthest inland breeding site at Greenall Glacier (440 km inland) is an outlier compared with the 323 breeding sites that are ≤ 10 km from the coast. However, the distance from breeding sites to the MIZ, their main foraging habitat, is more biologically relevant. At “Skiltvakta” in the Shackleton Range (Transantarctic Mountains), breeding is unconfirmed, but this is 1680 km and 740 km from the ice edge and 50% SIC contour, respectively, in November. Therefore this site, relative to accessible foraging habitat, is more remote. In total, 64 breeding sites in the Transantarctic Mountains and Dronning Maud Land are > 1000 km from the November sea ice edge.

4.2 Regional absences

Our review of known breeding sites highlights that there are extensive regions of exposed bedrock where nesting has not been recorded. These gaps could be due to lack of search effort or true absences. Notably, no sites have been recorded on the eastern Antarctic Peninsula south of 69°05’S, adjacent to the western edge of the Weddell Sea (Figure 1). This contrasts with the rest of the Antarctic Peninsula, a region of relatively high seabird abundance (Schrimpf et al., 2020), with at least 89 snow petrel breeding sites and minimum of 1264 breeding pairs. Similarly, only 8 breeding sites are known in Victoria Land, one of continental Antarctica’s biggest ice-free regions. With a large proportion of exposed low-elevation coastal bedrock (Kim et al., 2015), the number of breeding sites here is thus unlikely to be limited by bedrock availability. Furthermore, the disparity between the estimated number of breeding pairs from land-based observations in Victoria Land and adjacent islands (~5300 pairs; this study) and the estimate of 1.97 million snow petrels in the Ross Sea region based on densities recorded at sea (Ainley et al., 1984), seems likely to indicate there are numerous unknown breeding sites in this area.

Our results show there is a systematic decrease in the number of breeding sites in areas of bedrock with distance from the nearest research station, demonstrating a geographical bias in knowledge and survey effort that is clearly related to human presence, likely due to logistical constraints (Figure 3). Though research stations are also predominantly located at coastal sites with exposed rock, snow petrels are

confirmed to breed up to 440 km inland. Thus, the lack of breeding sites further from stations (and further inland) where bedrock remains available (Figure 3), suggests it is highly likely that these more distant areas are under-sampled, and that many remote sites remain undiscovered. This would explain obvious gaps in the circumpolar breeding distribution in North and South Victoria Land, where exposed bedrock is readily available and at-sea density distributions suggest there are millions of snow petrels, but only 8 breeding sites are known.

From several surveys, snow petrel absence sites have been inferred with a varying degree of certainty. In East Antarctica, 5 small unnamed islands within the Davis Islands, 10 sites within the Larsemann Hills, and 6 sites within the Haswell Archipelago were surveyed and no evidence of breeding was detected (Melick et al., 1996; Pande et al., 2020; Golubev, 2022). Similarly, snow petrels apparently do not breed at Jutulrora and Straumsvola in Dronning Maud Land (Ryan & Watkins, 1988), nor Vesleskarvet (Steele & Hiller, 1997). In Adélie Land, surveys found no evidence of breeding at 9 sites along the coast and 3 sites on inland mountains (Barbraud et al., 1999). A partial survey of Southern Masson in the Framnes Mountains (inland Prince Charles Mountains) also found no snow petrel nests (Olivier & Wotherspoon, 2008). These sites with no evidence of breeding are close to regions where snow petrels do breed (e.g., 12 known breeding sites in the Larsemann Hills, summing to > 470 breeding pairs). Hence the distribution of confirmed absences is insufficient to explain any large regional gaps in Figure 1. The proximity of presences and absences suggests that regional sea-ice conditions are likely to be the same, so that distance to suitable foraging habitat is unlikely to be a limiting factor that would explain why breeding does not take place (Ainley et al., 1984). Instead, it is possible these local absences reflect nesting-habitat availability or preferences, as follows.

4.3 Potential environmental limits on breeding distribution

The selection of a suitable nest site is a critical decision for any bird (Stauffer & Best, 1982). As central-place foragers breeding on land and foraging at sea, snow petrels face a distance-dependent cost of accessing food, and seabird populations in general are regulated by bottom-up processes and food availability (Wakefield et al., 2014; Sauser et al., 2021b). Breeding sites may therefore be chosen based on the quality and proximity of foraging habitat (Bolton et al., 2019), as well as the suitability of local nest sites (Li & Martin, 1991; Lõhmus & Remm, 2005). Ainley et al. (1984) hypothesised that the snow petrel breeding distribution is affected by the existence of accessible pack ice during the breeding season. Our results support this hypothesis, given the distribution of distances from breeding sites to 15% SIC and 50% SIC in November (medians of 430 and 136 km, respectively). As such, the persistence of high SIC in the western Weddell Sea, which is highly variable in extent but survives summer melt (Figure 6b; Turner et al., 2020), could explain the lack of breeding sites on the eastern Antarctic Peninsula.

At a local scale, snow petrels are constrained to pre-existing cavities provided by the substrate (Ramos et al., 1997). They are therefore subject to intraspecific, as well as interspecific competition for these resources with other seabirds that have a similar habitat preference (Lõhmus & Remm, 2005; Wiebe, 2011). The availability of suitable cavities is inherently linked to rock type, jointing, and weathering. Our results demonstrate that snow petrels breed most frequently in cavities in high-grade metamorphic and intrusive igneous rocks (Figure 5a). Estimated breeding population sizes are highest on high-grade metamorphic rocks, despite the higher availability of igneous intrusive and sedimentary rocks (Figure 5), suggesting that metamorphic rocks are more likely to incorporate suitable cavities. Additionally, specific selection of lithologies by snow petrels at a local scale is implied at multiple localities. At Edisto Inlet in Cape Hallett, no suitable cavities were observed on the eastern cliffs composed of volcanic rocks, whereas over 6 miles of the western cliffs, composed of fine-grained metamorphic rock, were occupied extensively by snow petrel nests (Maher, 1962). Frequent strong winds and precipitation at this locality during the 1960/61 austral summer resulted in nesting cavities being buried by snow (Maher, 1962). Therefore, it is unlikely that nests on the western cliffs were selected due to favourable aspect, but that there were no suitable cavities in the eastern volcanic cliffs. By contrast, in the northern Prince Charles Mountains, relatively few snow petrels

nest in the high-grade metamorphic rock (Precambrian basement gneisses), despite it being the dominant exposed bedrock in the region. Instead, the majority of known sites are in the Amery group sandstones, where suitable cavities form through salt wedging (Heatwole et al., 1991). Furthermore, Verkulich & Hiller (1994) suggest that snow petrels in the Bunger Hills select mainly metamorphic and igneous rocks for nesting, since they are least susceptible to weathering, but also highlight the importance of aspect for protection against strong winds and snow accumulation. Therefore, we hypothesise that lithology, specifically the availability of high-grade metamorphic and intrusive igneous rocks, is an important local-scale control on snow petrel nesting-habitat selection, given its association with both cavity availability and durability.

In the predominantly high-grade metamorphic mountains of Dronning Maud Land (Cox et al., 2023a), cavity availability is unlikely to be limiting the breeding distribution. Here, observations report most breeding sites face north, which may provide shelter from katabatic winds and therefore a more favourable microclimate (Bowra et al., 1966; Mehlum et al., 1988; Ryan & Watkins, 1989; Johansson & Thor, 2004). Nests with a favourable aspect have higher breeding success (Olivier et al., 2005). Therefore, where the availability of cavities is not limited, interplay between nest aspect and local climate may determine nest site selection (Olivier & Wotherspoon, 2006)**.**

Based on these results, breeding location and cavity selection by snow petrels is likely to be driven by a hierarchy of regional and local environmental conditions, most importantly limited by suitable breeding substrate availability (bare rock) within a sustainable distance of suitable foraging habitat (MIZ) (Ainley et al., 1984). At locations within the foraging range of suitable foraging habitat, snow petrels may then select specific cavities based on availability (related to lithology), and local conditions such as cavity size (for predation protection) and aspect (Olivier & Wotherspoon, 2006). Therefore, models of habitat selection that incorporate both distance to the MIZ and the availability of exposed high-grade metamorphic rock could be used to estimate the breeding distribution of snow petrels throughout their range.

4.4 Past and future breeding distribution

Radiocarbon dates from snow petrel stomach-oil deposits – thick, layered accumulations outside nests – demonstrate discontinuous but persistent occupation of breeding sites throughout Dronning Maud Land, East Antarctica, the Shackleton Range and Prince Charles Mountains, since before the Last Glacial Maximum [LGM] and throughout the Holocene (Hiller et al., 1988; Thor & Low, 2011; Berg et al., 2019a; 2019b; McClymont et al., 2022). Conditions at these breeding sites and in foraging areas must have remained favourable during this period to facilitate nesting. However, the reconstructed LGM summer sea ice edge was located beyond the modern foraging range, so it has been proposed that coastal polynyas within the sea ice, or at ice-shelf fronts, must have provided suitable foraging habitat (Thatje et al., 2008; McClymont et al., 2022). Although these ice-free areas may have supported large population sizes during the LGM (Carrea et al., 2019), such populations are hypothesised to have been reproductively isolated, resulting in the evolution of two morphologically distinct snow petrel subspecies (Jouventin & Viot, 1985; Henri & Schön, 2017; Carrea et al., 2019). During our review of breeding records, presence of the lesser (*P.n. nivea*) vs greater (*P.n. confuse/major*) snow petrel was rarely distinguished, so their relative breeding distributions remain poorly quantified. A summary of the distribution of most known forms is given in Hobbs (2019), though that compilation omits known lesser snow petrels breeding on Cockburn Island (Cowan, 1981).

Snow petrels respond to environmental factors operating both at breeding sites and in foraging areas, and, as high-trophic-level predators, their breeding and foraging success are potentially valuable indicators of ecosystem health (Sydeman et al., 2012; González-Zevallos et al., 2013). Climate-driven changes in either breeding or foraging habitats could drive changes in the snow petrel breeding distribution. Most commonly, the effects of climate on seabirds are indirect and bottom-up, driven by spatiotemporal changes in prey distributions resulting from climate-driven changes in the pelagic environment (González-Zevallos et al., 2013). Seabird distributions in the future could be limited or expand in association with changes in prey

availability or meteorological conditions at breeding sites, which are likely to be regionally specific (Gonzalez et al., 2023). Snow petrel population size is hypothesised to be negatively affected by a reduction in SIE (Jenouvrier et al., 2005). Winter sea ice is necessary to maintain Antarctic krill *Euphausia superba* and so its extent and duration affects abundance and food supply for snow petrels during the following summer (Loeb et al., 1997). Greater than average winter SIE thus improves the survival and breeding performance of snow petrels (Barbraud et al., 2000; Barbraud & Weimerskirch, 2001; Jenouvrier et al., 2005). Summer SIE also affects their breeding success, which is depressed if November SIE is lower, whilst fledgling body condition is higher when the November SIE is greater than average (Barbraud & Weimerskirch, 2001). Despite the surprising stability overall of Antarctic SIE over the past decades, recent years have experienced major declines and record minima in both winter and summer SIE, and the trend of more extreme lows is predicted to continue (Fogt et al., 2022; Raphael & Handcock, 2022). Dependence of snow petrels on the proximity of the MIZ suggests that with the projected southwards retreat of SIE, they will lose substantial areas of foraging habitat. The small snow petrel population size at their northern limit on South Georgia (~ 3000 breeding pairs) is suggested to result from limited sea ice nearby during the breeding season (Ainley et al., 1984). Regional variability in future sea-ice trends (Purich & Doddridge, 2023) may result in abandonment of breeding sites in some regions as foraging habitat becomes unsuitable, resulting in a southwards contraction of the breeding distribution.

In contrast, new exposed coastal-breeding habitats may emerge as the climate warms. A high proportion (71%) of known snow petrel breeding sites are ≤ 10 km from the coast. As such, increased availability of ice-free rock may increase the options for snow petrels to expand in these areas, although they may also face competition for this habitat from other seabirds.

Direct climate effects (extreme weather events) can also impact seabird distributions and breeding success at a local scale. Nesting cavities shelter snow petrels to some extent from extreme weather, but the timing and duration of local snow accumulation nevertheless influences breeding success (Croxall et al., 2002; Einoder et al., 2014), breeding probability (Chastel et al., 1993), hatching success (Olivier et al., 2005), and fledging probability (Sauser et al., 2021b). Increased or prolonged snowfall can affect nest accessibility, and a simultaneous increase in local temperatures increases the risk of flooding (Chastel et al., 1993). Extreme storm activity (severe winds and high precipitation) in Dronning Maud Land during the 2021/22 austral summer caused near-complete breeding failure and mass mortality of snow petrels and conspecifics across multiple breeding sites extending over > 700 km (Descamps et al., 2023). Mass mortality events can have major lasting effects on long-lived seabirds which are slow to reproduce (Mitchell et al., 2020), with the distributions of some (e.g., black-legged kittiwakes *Rissa tridactyla*) known to change as a result of poor breeding performance in particular areas (Boulinier et al., 2008). However, the only long-term demographic studies of snow petrels are at the Pointe Géologie Archipelago (Adélie Land) and Reeve Hill, Casey Station (East Antarctica) (Figure 1). Most long-term studies conclude intraspecific differences between sexes and neighbouring breeding sites in responses to local weather effects and larger scale climatic patterns (Sauser et al., 2021a). Therefore, longer-term impacts of extreme breeding season weather, such as intensive storms, on the snow petrel breeding distribution remain uncertain. By quantifying average climatic conditions at breeding sites, we provide important baseline data against which future distributional shifts can be assessed. Our study highlights the need for much more widespread long-term monitoring of snow petrel colonies, including at least population trends and breeding success, and ideally, long-term demographic studies. In addition, tracking studies and the development of species distribution models of habitat suitability in foraging areas would help in predicting the future distribution of snow petrels in relation to climate driven change.